

A JOURNAL OF THE MACEDONIAN ASSOCIATION OF STRUCTURAL ENGINEERS NO. 9 / 2010
СПИСАНИЕ НА ДРУШТВОТО НА ГРАДЕЖНИТЕ КОНСТРУКТОРИ НА МАКЕДОНИЈА БР. 9 / 2010

STRUCTURAL ENGINEER
ГРАДЕЖЕН КОНСТРУКТОР

CONTENTS



Editor in Chief:
Prof. d-r Golubka Necevska
Cvetanovska

President of MASE
Prof. Goran Markovski

Editorial Board:

Prof. d-r Gustavo Ayala, Mexico
Prof. d-r Sande Atanasovski, Macedonia
Prof. d-r Elena Vasseva, Bulgaria
Prof. d-r Djordje Vuksanovic, Serbia
Prof. d-r Mihail Garevski, Macedonia
Prof. d-r Vladimir Gocevski, Canada
Prof. d-r Kiril Gramatikov, Macedonia
Prof. d-r Zoran Desovski, Macedonia
Prof. d-r Sofia Diniz, Brazil
Prof. d-r Elena Dumova Jovanoska, Macedonia
Prof. d-r Roko Zarnic, Slovenia
Prof. d-r Peter Mark, Germany
Prof. d-r Federico Mazzolani, Italy
Prof. d-r Aurelio Muttoni, Switzerland
Prof. d-r Tihomir Nikolovski, Macedonia
Prof. d-r Zdravko Petkov Bonev, Bulgaria
Prof. d-r Niko Pojani, Albania
Prof. d-r Jure Radic, Croatia
Prof. d-r Vlatka Rajcic, Croatia
Prof. d-r Forcim Softa, Albania
Prof. d-r Mladen Ulicevic, Monte Negro
Prof. d-r Matej Fischinger, Slovenia
Prof. d-r Ruediger Hoeffer, Germany
Prof. d-r Veronika Sendova, Macedonia
Prof. d-r Petar Cvetanovski, Macedonia
Angel Mark Sereci, USA

Cover Design:
Assoc. prof. Mitko Hadzi-Pulja

Technical preparation:
Zoran Simonovski

Printing:
Geneks, Kochani

Number of copies: 100

The MASE journal Structural Engineer is distributed to all its registered members at no charge.

e-mail: mase@gf.ukim.edu.mk

web site: <http://www.mase.org.mk>

ISBN 9989-9785-3-0 (No.9)

A preferential tax rate of 5 % is paid for the magazine Building designer against the Law for VAT, paragraph 1, point 8

STRUCTURAL ENGINEER

JOURNAL OF THE MACEDONIAN ASSOCIATION OF STRUCTURAL ENGINEERS

No. 9/2010

FOREWORD BY THE EDITOR

567 **IN-PLANE SHEAR BEHAVIOUR OF UNREINFORCED MASONRY WALLS**
Sergej CURILOV, Elena DUMOVA-JOVANOSKA

576 **CONTRIBUTION OF SEISMIC STRENGTHENING OF MONUMENTS TO THEIR BLAST RESISTANCE**
Goran JEKIC, Veronika SENDOVA, Ljubomir TASKOV

584 **PERFECTLY MATCHED LAYERS - AN ABSORBING BOUNDARY CONDITION FOR ELASTIC WAVE PROPAGATION**
Josif JOSIFOVSKI, Vasil VITANOV, Oto von ESTORFF

592 **SEISMIC STABILITY OF THE OLD BRIDGE IN MOSTAR**
Mladen KUSTURA, Lidija KRSTEVSKA, Mladen GLIBIC, Ljubomir TASKOV

599 **STIFFNESS CHARACTERISTICS MODELLING OF RC FRAME STRUCTURES ACCORDING TO EUROCODE 8**
Ljupco LAZAROV, Koce TODOROV

608 **HAVE WE FORGOTTEN SKOPJE 1963 EARTHQUAKE?**
Goran MARKOVSKI

615 **EARTHQUAKE-INDUCED LANDSLIDES - GIS METHODOLOGY FOR ZONATION**
Julijana CVETANOVSKA, Vlatko SESOV

624 **ANALYTICAL INVESTIGATIONS OF SEISMIC BEHAVIOUR OF RC FRAME BUILDINGS WITH MASONRY INFILL**
Roberta APOSTOLSKA, Golubka NECEVSKA CVETANOVSKA, Julijana CVETANOVSKA

FOREWORD BY THE EDITOR

Dear colleagues,

This is the latest issue of the scientific-professional journal "Structural Engineer" published by the Macedonian Association of Structural Engineers (MASE) as the most active association within the frames of the Macedonian Federation of Structural Engineers. In the elapsed period, the regular publication of this journal was accompanied by many difficulties of different nature, but we believe that we have always, since the publication of the first issue, succeeded in attracting your professional attention by selection of interesting (from our point of view) scientific and professional papers, first of all, in the field of structural engineering and civil engineering in general.

With the publication of this issue, we would like to remind you of the beginnings of this journal back to 1995 as well as the achievements and the efforts put by our colleagues in making this journal reputable and pleasing to be read by the wider professional public in the Republic of Macedonia and beyond. We are particularly indebted to Prof. Dr. Sande Atanasovski and Prof. Dr. Tihomir Nikolovski who have so far been editors-in-chief, all those who have so far been members of the editorial board and all authors of papers published in the preceding issues of this journal.

Our editor-in-chief and the new editorial board consisting of 20 members from 13 countries worldwide (Mexico, Bulgaria, Serbia, Canada, Brasilia, Germany, Italy, Switzerland, Albania, Montenegro, Croatia, Slovenia and Macedonia) have seriously taken the task of enabling continuation of this journal and preservation of its high quality and attractiveness and have accepted the challenge of making this journal grow into a reputable international scientific journal that will extensively arouse the interest of the scientific and professional public in reading and publishing scientific and professional papers.

This issue is dedicated to the 14th European Conference on Earthquake Engineering organized by the Macedonian Association for Earthquake Engineering (MAEE) and held in Ohrid in the period August 30 to September 3, 2010. This conference attended by more than 900 participants can be rightfully considered the biggest event in the field of earthquake engineering, construction and science that has ever taken place in the Republic of Macedonia.

Presented in this issue are selected papers that were presented at this Conference which, in our opinion, will arouse the interest of the scientific and professional public in the Republic of Macedonia and beyond.

In the next issues, you can expect new, topical contents.

Editor-in-Chief

Prof. Dr. Golubka Necevska - Cvetanovska



IN-PLANE SHEAR BEHAVIOUR OF UNREINFORCED MASONRY WALLS

S. Churilov, E. Dumova-Jovanoska

*University "Ss. Cyril and Methodius"
Faculty of Civil Engineering
Skopje, Macedonia*

ABSTRACT

This paper presents the experimental testing and results of unreinforced masonry panels in order to obtain their behaviour under cycling loading. This study is part from an ongoing research programme. Mechanical properties of the constituent materials for masonry were tested and a database of characteristic properties was created. Several series of unreinforced masonry walls were constructed from solid clay bricks and lime mortar and tested under constant vertical load and cyclic horizontal loads. Later, strengthened masonry walls with reinforced-concrete coating will be tested using the same geometry and boundary conditions. The purpose of the experimental investigations is to obtain the force-displacement curves, analyze the behaviour of masonry walls and establish design formulas for simple calculation of wall capacities for unreinforced and strengthened masonry walls. The results of the experiments will highlight the properties, advantages and limitations of the applied strengthening method.

Keywords: masonry, shear, unreinforced, in-plane, cyclic

1. INTRODUCTION

In many seismically active regions around the world unreinforced masonry buildings represent a significant portion of the building stock. There is a large building stock of low-rise residential unreinforced masonry buildings in Macedonia and Balkan region. Their vulnerability is caused by the failure of unreinforced masonry shear walls due to the in-plane or out-of plane seismic loading. Large quantities of masonry structures do not satisfy the latest code provisions and therefore application of strengthening methods is necessary. This paper presents a part from an ongoing research for experimental and analytical investigation of strengthening and retrofit method applied to residential masonry buildings in Macedonia with a special attention on cost expenses, method for application and time for implementation.

Macedonia is one of the most active seismic

places in Balkan Peninsula, see Fig. 1. It lies in the south part of the Eurasian plate where three tectonic plates, African, Asian and European meet. It is mostly the work of African plate sliding beneath Eurasian plate that caused the geographic formation which we see today, and it is also the reason why there are frequent earthquake tremors in the region. The friction between the plates has brought about a number of fault lines which run across Macedonia approximately along the course of river beds. The one under Kochani along the river Bregalnica contributed to the 1904 earthquake, and the Skopje fault line along the river Vardar contributed to the 1963 earthquake which destroyed most of the city (Evans, 2007).

Various techniques have been employed to strengthen and retrofit existing unreinforced masonry buildings. The conventional techniques such as post-tensioning and adding

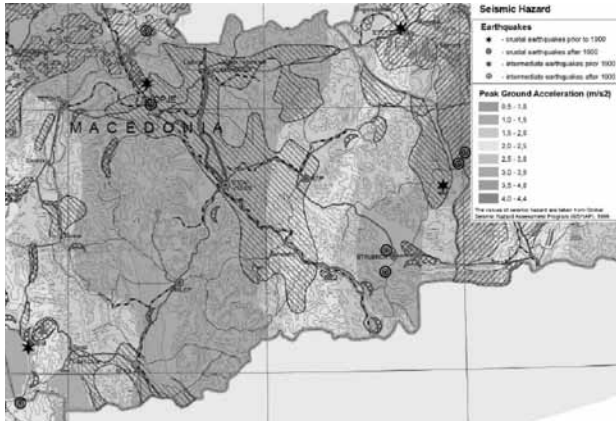


Figure 1. Seismic hazard map of Macedonia

steel reinforcements present complications in their application due to excessive time required for application, disruption of operations, corrosion of the steel and difficulties in handling of materials.

In recent years, FRP materials have emerged as a promising alternative retrofit solution, with their light-weight, high strength, non-corrosive and electromagnetically inert properties, quick and easy application and with significant cost drops since their introduction in the early 1990s.

One of the most used traditional techniques for strengthening existing residential masonry buildings in Macedonia by improving its lateral resistance and energy dissipation capacity of the system is application of reinforced-concrete coating (jacket) on one or both sides of the walls.

2. EXPERIMENTAL TESTS ON MASONRY ELEMENTS

In the present experimental study the testing of mechanical properties of bricks, mortar and masonry is performed according MKS codes and EN methods for testing. Three types of solid clay bricks, one type of hollow clay bricks and two mortar grades were tested to obtain mechanical properties. Three types of newly produced bricks from different manufacturers: 'Elenica' (A-solid), 'Prilep' (B-solid) and 'KIK' (C-hollow) were used and one type was 50-60 years old brick extracted from existing low-rise masonry building ('D'-solid). All bricks



Figure 2. Earthquake damage on masonry building

have usual dimensions for this type of masonry elements with length, thickness and height of 250x120x65 mm. Hand made lime (LM) and cement mortar (CM) samples were tested with the following cement:lime:sand grades by volume: LM=0:1:3; CM=1:0:3.

2.1 Properties of bricks

In order to understand the mechanical behaviour of a given material or structure, it is fundamental to perform experimental tests on it. In this way, it is possible to characterize its behaviour from the undamaged state through to peak and post-peak state. The properties of bricks were obtained by experimental testing according MKS B.D8.011:1987 standard. Table 1 summarizes the obtained results.

The results show that series A and C deviate in small amount from the prescribed dimensions, while series B shows greater deviation. Series B shows greater surface unevenness and corner roundness in comparison with the other two series which leads to slightly lower unit weight. Series C results in lowest unit weight due to presence of holes through the unit. All brick types showed no visible failure after 5 cycles of freezing/unfreezing on temperatures ranging from -200C to +200C.

In order to obtain compressive and tensile strength, compression and tensile flexural tests were performed. According to this code compression tests were carried out on a series of 5 brick

Table 1. Physical properties of bricks

Series	Length [mm]	Width [mm]	Height [mm]	Weight in dry state [g]	Weight in saturated state [g]	Water absorption [%]	Weight after freezing [g]	Unit weight [kg/m ³]
A	250,3	120,1	64,4	3721,0	4138,4	11,2	3719,9	1922,6
B	241,1	120,9	64,5	3227,2	3692,7	14,4	3219,3	1719,9
C	253,9	124,4	65,6	2565,4	2919,4	13,8	2556,9	1239,7

sandwich specimen made from 2 bricks glued with thin layer of cement mash, as shown in Fig. 3. Servo-controlled 'Interfels' testing machine with load capacity of 3000 kN was used to test all brick specimens. Table 2 presents the obtained compressive strength with respect to brick type.

For comparison of the obtained values for compressive strength another set of tests on cube samples with dimensions 50x50x50 mm extracted from the actual bricks was performed. The results from these tests presented in Table 3 showed higher values ranging from 1.5 to 2.3 times for each series.

Table 4 and Figure 4 present obtained values for brick tensile flexural strength and experimental failure mechanisms. Tensile strength was tested on a series of single bricks supported by steel roller bearings, simple beam system. Load was applied gradually through steel rod on top of the bricks acting like concentrated load.

2.2 Properties of mortars

Parallel to the research done on the mechanical behaviour of solid clay specimens, this Section introduces a complementary experiment carried out on lime and cement mortar samples. The mortar types adopted in the tests were

**Figure 3. Compression tests and failure mechanisms of solid clay bricks****Table 2. Compressive strength of bricks according MKS standard**

Series	Compressive strength [MPa]						
2A1	9,9	2B1	3,1	2C1	/ (error in test)	2D1	9,9
2A2	13,1	2B2	4,3	2C2	7,7	2D2	3,5
2A3	7,3	2B3	2,6	2C3	6,9	2D3	6,6
2A4	12,0	2B4	4,6	2C4	6,4	2D4	6,1
2A5	11,9	2B5	5,5	2C5	4,7	2D5	4,4
Mean	10,8	Mean	4,0	Mean	6,4	Mean	6,1

Table 3. Compressive strength of bricks on cube samples

Series	Compressive strength [MPa]	Series	Compressive strength [MPa]	Series	Compressive strength [MPa]
A12	20,3	B11	7,1	D1	18,7
A13	17,8	B12	9,4	D2	22,9
A22	16,2	B22	8,2	D3	16,3
A23	17,8	B23	11,0	D6	6,9
A32	13,9	B32	8,7	D7	6,7
A33	12,2	B33	11,5	D8	6,5
Mean	16,4	Mean	9,3	Mean	13,0

Table 4. Tensile strength of bricks

Series	Tensile strength [MPa]						
A1	3,6	B1	1,6	C1	0,6	D1	3,0
A2	2,2	B2	1,6	C2	0,9	D2	2,9
A3	3,0	B3	1,5	C3	0,9	D3	2,4
A4	2,8	B4	1,6	C4	1,0	D4	1,4
A5	2,1	B5	0,9	C5	1,0	D5	4,6
A6	2,8	B6	1,7				
A7	2,1						
Mean	2,7	Mean	1,5	Mean	0,9	Mean	2,9

**Figure 4. Tensile flexural tests and failure mechanism of solid clay bricks****Figure 5. Experimental tests and failure mechanisms of mortar samples**

considered to reflect the most commonly used bonding material in existing buildings, lime mortars, and to compare it with the properties of 'stronger' cement mortars. These tests were done according MKS U.M8.002:1968 standard on a 28 days aged samples with dimensions 40x40x160 mm.

2.3 Compressive strength of masonry

Masonry compressive strength was tested on one wallet (UMWC-1) with dimensions 120x120x25 cm and three wallets (UMWC-2) with dimensions 52x32x12.5 cm build from solid clay bricks from series A and lime mortar with grading 0:1:3.

The wallet UMWC-1 was precompressed with load from the self-weight of the top RC beam.

Load application was by manual with monotonic increasing of displacement increments while data acquisition was automatic. The test set-up and results are presented in Fig. 6. Maximum vertical force measured was 705,6 kN at a displacement of 18,7 mm, which yields masonry compressive strength of 2,35 MPa. Initial modulus of elasticity is 200 MPa, while secant modulus is 50 MPa.

Wallets denoted as UMWC-2 were tested in axial compression according EN 1052-1:1998. Load application and data acquisition was automatic by 'Interfels' testing machine. Figure 7 and Table 6 present wallet sample, failure mechanisms and obtained compressive strength.

Table 5. Properties of mortar

Cement mortar				Lime mortar					
Sample		Unit weight [kg/m³]	Tensile strength [MPa]	Compressive strength [MPa]	Sample		Unit weight [kg/m³]	Tensile strength [MPa]	Compressive strength [MPa]
1	1	2127,0	5,2	20,2	1	1	1385,3	0,08	0,5
	2			18,3		2			0,5
2	3	1986,5	5,2	19,5	2	3	1367,0	0,10	0,6
	4			18,6		4			0,5
3	5	2132,5	6,0	36,7	3	5	1391,9	0,19	0,6
	6			26,6		6			0,7
4	7	2012,8	5,0	24,7	4	7	1367,7	0,10	0,5
	8			26,8		8			0,5
5	9	2090,6	6,0	21,4	5	9	1409,0	0,08	0,5
	10			19,6		10			0,6
6	11	2074,2	5,5	25,1	6	11	1380,0	0,05	0,5
	12			25,6		12			0,6
7	13	2140,2	5,7	26,4	Mean вредност		1383,5	0,10	0,6
	14			26,8					
8	15	2139,8	8,5	37,1					
	16			35,7					
9	17	2083,3	6,7	37,6					
	18			37,8					
Mean вредност		2087,4	6,0	26,9					

Using the equation 3.2 proposed in EN 1996-1-1:2005, determination of characteristic compressive strength of masonry for clay bricks of Group 1, $f_k=0,55 \cdot f_{b0} \cdot 0,7 \cdot f_{m0} \cdot 0,3$, with normalized mean compressive strength of bricks from series A, Table 3 ($d=0,81$), and compressive strength of lime mortar given in Table 5, one can obtain masonry compressive strength $f_k=2,35$ MPa. If the normalized mean compressive strength of bricks from series A is taken from Table 2, then $f_k=1,76$ MPa. When the compressive strength of bricks is not normalized with d , then characteristic compressive strength of masonry is calculated as 2,73 MPa and 2,04 MPa, respectively.

2.4 Shear strength of masonry triplets

Clay bricks from series A and lime mortar were used to prepare nine masonry triplets. The shear strength of masonry triplets was obtained as described in EN 1052-3:2002. Two load cells were used to carry out the shear tests, see Fig. 8. One load cell was used for monitoring the shear force and the other for monitoring compressive force acting perpendicular to the shear force. First, the desired compressive force was applied to the triplet and maintained constant during the test, while shear force was increased until the masonry triplet rupture occurred. Three pre-compressive stresses were adopted, as proposed in EN 1052-3, namely 0,2 MPa, 0,6 MPa and 1,0 MPa. The shear stresses obtained

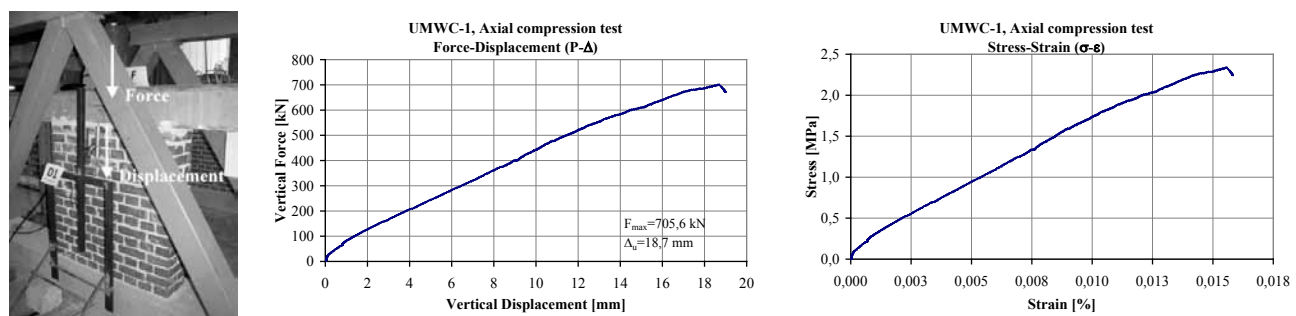


Figure 6. Compression test on wallet UMWC-1

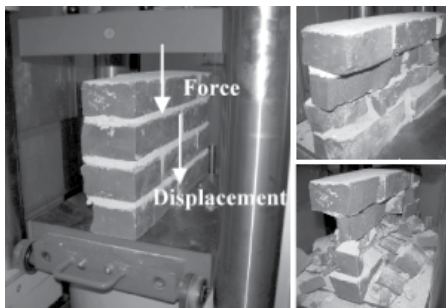


Figure 7. Compression test on wallets UMWC-2

with the conducted tests are presented in Fig. 8. It also presents the linear regression as proposed in the standard. Triplets shear failure occurred mainly at mortar bed joints with predominant type of fracture A.1 as indicated in the standard.

3. EXPERIMENTAL TESTS ON MASONRY WALLS

Many tests on masonry samples or small masonry walls have been performed, very often using diagonal compression loading to provide combined shear and compression load. To develop a suitable test set-up it is essential to know how the shear stress is generated and distributed (Marzahn, 1998). The elastic theory, although strictly applicable to homogeneous material can be used for uncracked masonry with certain reservations. The theory expresses that the shear stresses reach their maximum at a square element without pre-stressing at the centroidal axis, and the shear stresses generate principal stresses. The

principal stresses, one compressive and the other tensile, are inclined by 45° to the longitudinal axis and the bed joint, respectively. Their values are equal to the shear stresses, see Fig. 9. It is assumed that the failure will occur if the principal tensile stress reaches the diagonal tensile strength of masonry covering both the sliding failure in bed joints and the cracking of units.

Similar to this arrangement a rectangular shaped wall is formed with a length of 2,6 m, and height of 1,8 m thus reaching the limitations of the testing frame. First, vertical loading is applied and kept constant during testing and then horizontal displacement increments are cyclically applied on the top RC beam. Displacements are measured in several points using displacement transducers. The experimental setup is shown in Fig. 11. Several tests were carried out to evaluate the shear resistance of unreinforced masonry walls. In this paper only results of two tests are presented, see Fig. 12.

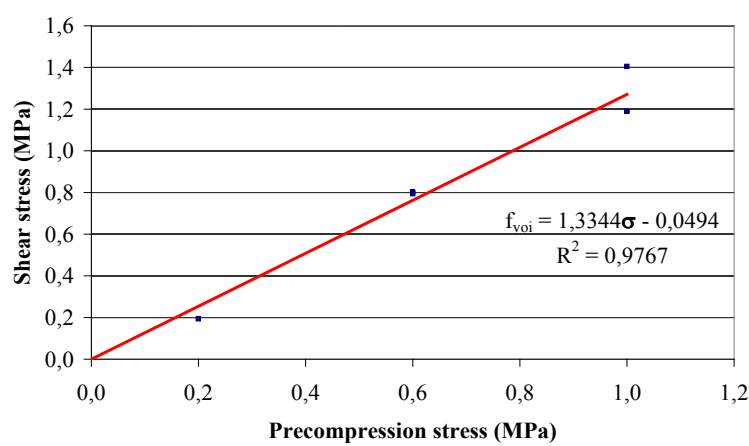
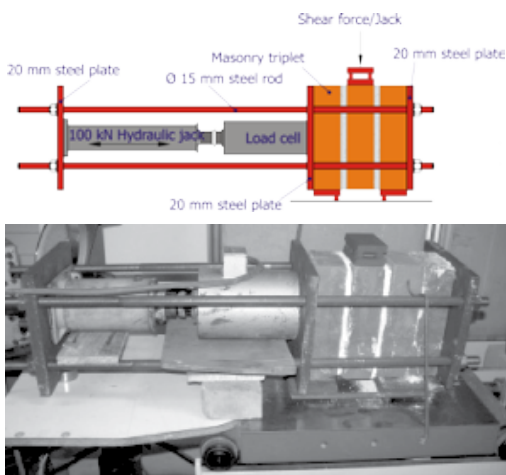


Figure 8. Compression test on wallets UMWC-2

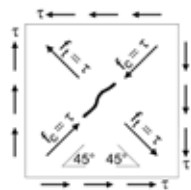


Figure 9. Homogenous element subjected to pure shear

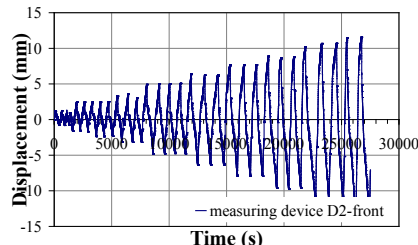


Figure 10. Displacement history

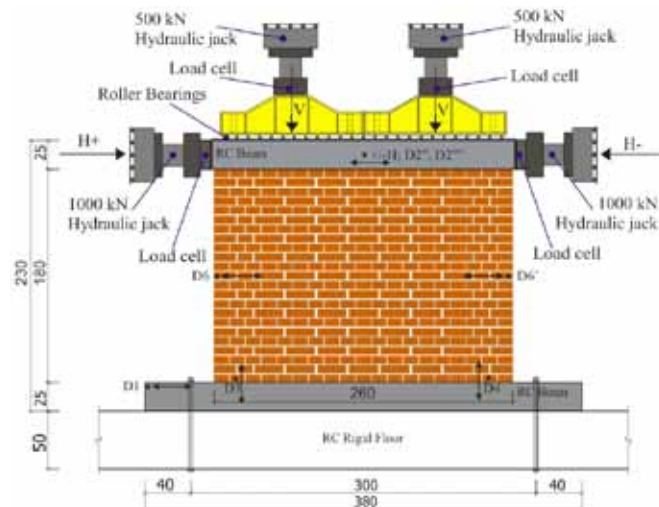


Figure 11. Test set-up for shear tests of masonry walls

Unreinforced masonry walls from solid clay bricks (series A) and lime mortar with dimensions 260x180x25 cm (UMW1) and 150x180x25 cm (UMW2) were constructed and tested with vertical precompression stress of 1,0 MPa. UMW1 reached maximum resistance of 213,2 kN at corresponding displacement of 6,74 mm and ultimate displacement of 12,2 mm. For wall UMW2 maximum obtained resistance was 99,13 kN at displacement of 7,35 mm and ultimate displacement of 17,24 mm. From Figure 12 it is possible to observe a global behaviour characterized by energy dissipation and some ductile behaviour. UMW2 showed greater ductility than UMW1 with expected lower maximum resistance and slowly decreasing softening branch as presented by hysteresis envelopes.

Both walls failed with combination of shear and compression failure with head and bed joint failure and brick failure, as shown in Fig. 13.

3.1 Masonry resistance to lateral loads

When a masonry building is subjected to a ground motion, the resisting elements may have three different failure modes in their plane: sliding shear, diagonal shear cracking and flexure. Sliding shear failure mode usually occurs for a low level of axial load and poor quality mortar, causing the sliding of an upper part of the wall on one of the horizontal joints. As reported by Tomažević (1999), it usually happens in the upper floors of buildings, where vertical loading acting on the wall is low but accelerations are high because of the shape of the seismic response of a masonry building. The sliding shear resistance is given by Eq. (1).

$$H_{sl} = L \cdot t \cdot (f_{vo} + \mu \cdot \sigma_0) \quad (1)$$

where L is the length of the wall, t is the thickness, f_{vo} is the initial shear strength under zero

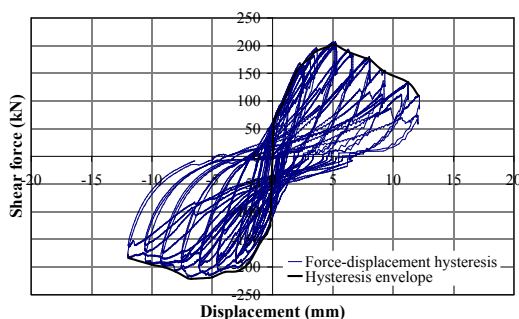
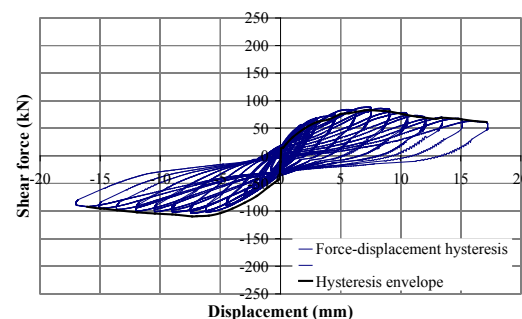


Figure 12. Typical lateral displacement-lateral resistance hysteresis loops for walls UMW1 and UMW2



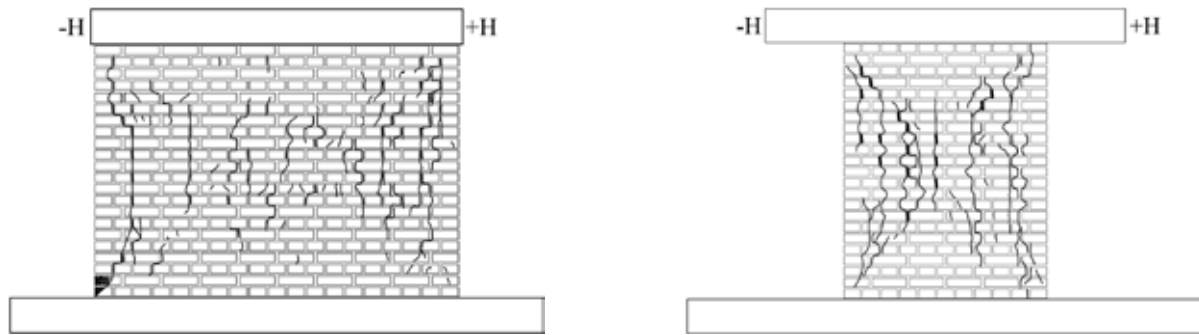


Figure 13. Observed failure mechanisms and crack propagation for walls UMW1 and UMW2

compressive strength, μ is the contribution of compression stresses (usually 0,1-0,4), σ_0 is the compression stress perpendicular to shear. Diagonal shear cracking is the common masonry failure mode under seismic loads and happens for a combination of vertical and horizontal loads where the principal tensile stresses developed in the wall due to this action exceed the tensile strength of masonry. The formulation of the maximum lateral resistance of a wall falling in diagonal shear cracking is presented by Eq. (2).

$$H_{sd} = A \cdot \frac{f_t}{b} \cdot \sqrt{\frac{\sigma_0}{f_t} + 1}, \quad b = \frac{h}{L} \quad (1,1 \leq b \leq 1,5) \quad (2)$$

where A is the horizontal cross-section area of the wall, f_t is the tensile strength of masonry, b is the shear stress distribution factor, depending on the geometry of the wall and N/H_{max} ratio.

Flexural resistance of unreinforced masonry is conditioned by crushing of the compressive part. Considering the behaviour of masonry subjected to uniaxial compression similar to that of concrete, with a similar shape of an equivalent rectangular stress block, the flexural resistance can be calculated by using Eq. (3).

$$H_{fl} = \frac{\frac{\sigma_0 \cdot t \cdot L^2}{2} \cdot \left(1 - \frac{\sigma_0}{f}\right)}{\alpha \cdot h} \quad (3)$$

where f is the compressive strength of masonry and a is coefficient which defines position of the

moment inflection point along the height of the wall. If the design capacity is correlated with design actions then in Eq. (3) design value of compression stress σ_d , characteristic value of compressive strength of masonry f_k and partial safety factor for masonry γ_m should be considered.

Equations (1), (2) and (3) are used to predict the maximum load and failure modes of walls UMW1 and UMW2 for uncracked wall section. Adopted compressive strength is given in Table 6, while tensile strength is taken as 0,05·compressive strength and compression stress perpendicular to shear is 1,0 MPa. The results from those calculations are compared with experimentally obtained values and shown in Table 7 and Fig. 14.

4. CONCLUSION

This paper presents a research into experimental investigation of the behaviour of in-plane loaded unreinforced masonry panels and the results of the experiments carried out. Although this research is currently in progress, this study demonstrates the behaviour of unstrengthened URM walls under cyclic loads, shows damage propagation and failure mechanisms, horizontal load-displacement hysteresis behaviour and diagrams, identification of the characteristic limit states, stiffness degradation and energy dissipation. Furthermore, the investigations will be enlarged with experimental testing of strengthened masonry panels with RC jacketing to compare with the behaviour of plain masonry walls.

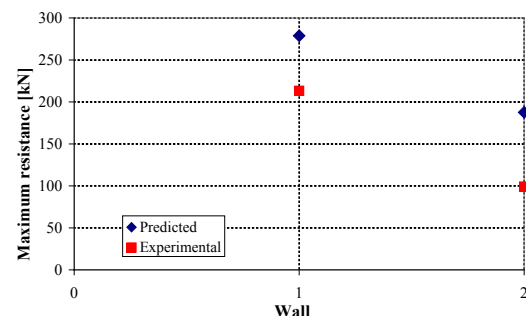
Table 7. Predicted and experimental maximum resistance

Failure/Resistance	Predicted		Experimental	
	UMW1	UMW2	UMW1	UMW2
Sliding shear [kN]	266,50	263,75		
Diagonal shear [kN]	278,83	187,54	213,2	99,13
Flexure failure [kN]	688,52	291,30		

Dominant failure mode is marked in grey cells.

Difference in prediction vs. experimental results:

UMW1 – 30,6 %; UMW2 – 89,2 %

**Figure 14. Predicted vs. Experimental results**

ACKNOWLEDGMENTS

The authors acknowledge factory for clay bricks and blocks "Elenica", Strumica for supplying solid clay bricks used in the tests, University "Ss. Cyril and Methodius", Faculty of Civil Engineering-Skopje for help in preparation and

execution of laboratory tests, "ADING" AD for supplying admixtures for test set-up, Factory "Karpos" for providing RC beams and University "Ss. Cyril and Methodius", Faculty of Mechanical Engineering for contribution in data acquisition during experimental tests.

REFERENCES

- Evans, T. (2007). Macedonia: The Bradt Travel Guide, Edition: 2, illustrated. Published by Bradt Travel Guides.
- MKS B.D8.011 (1987). Testing methods of clay bricks, blocks and slabs.
- MKS U.M8.002 (1968). Mortars for masonry and plastering. Testing methods.
- CEN-EN 1052-1 (1998). Methods of tests for masonry - Part 1: Determination of compressive strength.
- CEN-EN 1996-1-1 (2005). Eurocode 6 - Design of masonry structures - Part 1-1:General rules for reinforced and unreinforced masonry structures.
- CEN-EN 1052-3 (2002). Methods of test for masonry - Part 3:Determination of initial shear strength.
- Marzahn, G. (1998). The Shear Strength of Dry-Stacked Masonry Walls. LACER No. 3, 247-262.
- Tomažević, M. (1999). Earthquake-Resistant Design of Masonry Buildings, Series on Innovation in Structures and Construction, Vol. 1, Imperial College Press, London.
- Tomažević, M., Klemenc, I., Lutman, M., (2000). Strengthening of existing stone-masonry houses: lessons learned from the earthquake of Bovec of April 12, 1998, European Earthquake Engineering, 1, 13-22.



CONTRIBUTION OF SEISMIC STRENGTHENING OF MONUMENTS TO THEIR BLAST RESISTANCE

G. Jekic, V. Shendova & L. Tashkov

Institute of Earthquake Engineering and Engineering Seismology - IZIIS

University Ss. Cyril and Methodius, Skopje, Macedonia

ABSTRACT:

St. Athanasius Church in Leshok was destroyed as a result of a bomb attack on 21 August, 2001. One year later, the European Agency for Reconstruction and the Ministry of Culture of the Republic of Macedonia decided to begin a restoration of the church. The Institute of Earthquake Engineering and Engineering Seismology, IZIIS, Skopje prepared the Main Project for reconstruction. The project for restoration consisted of repair and strengthening of the damaged church narthex and complete reconstruction and seismic strengthening of the ruined naos, in compliance with the adopted seismic safety concept. This paper deals with the effectiveness of the adopted concept for seismic strengthening of the restored church regarding its blast resistance. The analysis of blast resistance consisted of re-enactment of the event that led to destruction and simulation of possible scenarios of blast effect upon the church, with different quantities of explosive charge acting from three different locations.

Keywords: historic monuments, reconstruction, seismic strengthening, explosion, blast resistance

1. INTRODUCTION

The St. Athanasius church is a part of the monastery complex "St. Mother of God", situated near the village of Leshok, 8 km north-east from Tetovo, in Republic of Macedonia. The complex is 700 years old and represents an invaluable historical and cultural value. Since 1957 it has been under the Law on Protection of Cultural Monuments.

From structural aspect, the church represents a three-conched structure with an elongated narthex on the west side and bell towers. The walls are constructed of stone masonry in lime mortar. The vaults, the tambours and the domes are constructed of brick masonry. The dome and the tambour rested on the massive circular from the inside and polygonal from the outside apses – conches via a system of spherical triangles – pendentives. The tambour was octagonal

from the outside and circular from the inside. This church was an active, spiritual temple of the Macedonian Orthodox Church.

The church was exposed to strong detonation from a bomb attack on 21 August, 2001, during the armed conflict in the Republic of Macedonia. As a result of the attack, it was almost completely destroyed. The vaulted structure surmounting the gallery was destroyed, while only the timber beams of the floor structure remained with visible deformation of the wood. In the part of the two preserved bell towers, there were visible large cracks with a width greater than 2 cm along the height of the bearing walls, in the staircase area, the walls of the tambours and the domes, (Fig.1).

In June, 2002, the European Agency for Reconstruction and the Ministry of Culture of the Republic of Macedonia took an initiative for



Figure 1. Remains of the St Athanasius church after the detonation



Figure 2. St Athanasius church after the reconstruction

reconstruction and restoration of the church to its authentic shape. The architectural and archaeological investigations were entrusted to the National Conservation Centre, while the Main Project on the restoration was elaborated by IZIIS, Skopje.

2. RESTORATION OF THE ST. ATHANASIUS CHURCH

In accordance with the legislative regulations of the Republic of Macedonia, the monuments are categorized as structures of extraordinary importance, for which it is necessary to evaluate their existing seismic stability in the process of their protection, and, if necessary, take measures for their conservation, restoration, repair and seismic strengthening. Such repair and strengthening should enable an economically justified and technically consistent seismic protection through providing of the necessary bearing capacity and deformability for an acceptable level of damage in case of future earthquakes.

From structural aspects, there have been two approaches taken in the attempt to renovate and reconstruct the structure of St. Athanasius church again. Based on the performed detailed analysis of the structure, two solutions have been prepared: (i) a solution for repair and strengthening of the *existing damaged part* of the monastic church and (ii) a solution for

seismic strengthening of the *demolished part* of the church to be reconstructed. It was generally concluded that such designed repair and seismic strengthening of the St. Athanasius church satisfied the prescribed requirements and criteria for such type of historic structures. In fact, although damaged by a blast, the church of St. Athanasius was strengthened in accordance with the regulations providing resistance to future earthquakes.

3. ANALYSIS OF BLAST RESISTANCE OF RECONSTRUCTED CHURCH OF ST. ATHANASIUS

3.1.1. Introductory notes

Depending on the location of an explosion and the area of the exposed surface, an explosion can be classified as:

- local explosion
- distant explosion

This classification has been made considering that the simplified methods for blast loading allow assuming of maximal reflected pressure, acting on the directly exposed surface if the angle of incidence α is smaller than 45° . The term "local explosion" means that the blast wave acts under an angle of incidence greater than 45° in some parts of the exposed surface. It requires zoning of the surface, depending on the angle of

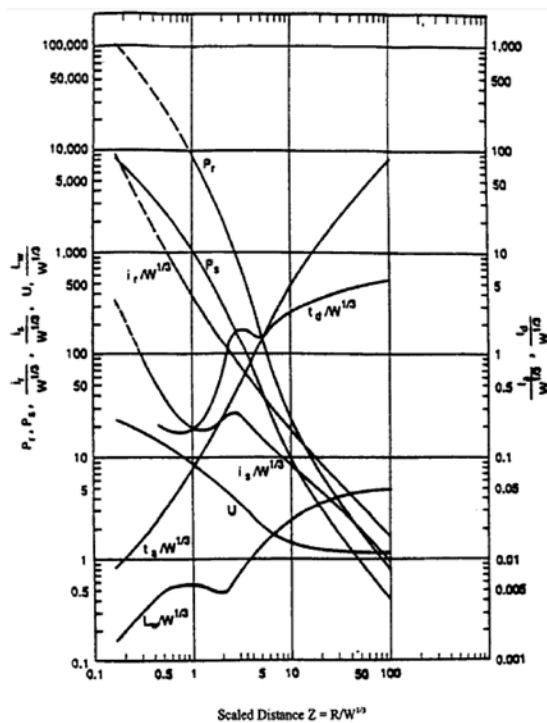


Figure 3. Positive Phase Airblast for Hemispherical TNT Detonation on the Surface at Sea Level
(U.S. Departments of the Army, Navy and Air Force 1990)

incidence and distance of a particular zone from the explosion centre. Distant explosion presupposes sufficient distance from the explosion center so that the exposed surface can be considered as a single zone of the blast influence, all under maximal reflected pressure, since the blast wave acts under an angle of incidence smaller than 45° in any part of the exposed surface. The blast wave parameters in the analysis

are obtained using the graph for hemispherical TNT detonation on the surface at sea level, (Fig. 3). All the parameters are given as function of the scaled distance $Z=R/W^{1/3}$ where R is the distance from the explosion in ft and W is the mass of TNT in lb.

3.2. Methods of analysis

In the Macedonian technical regulations and those of many other countries, there is no article that treats protection of structures of cultural and historical heritage against explosions. However, it is useful to know how the applied concept of restoration and seismic strengthening of structures of monuments is effective in increasing their resistance to explosions. For that purpose, an analysis of the blast resistance of the restored church was performed for the purpose of estimating the effectiveness of the adopted concept for seismic strengthening of monuments in improving their blast resistance.

3.2.1. Re-enacting the occurred explosion and defining the collapse mechanism

The details about the event that caused the destruction of St. Athanasius church remain unknown. However, based on the documentation from the scene immediately after the blast, several key assumptions have been adopted:

- the location of the explosion can be assumed,

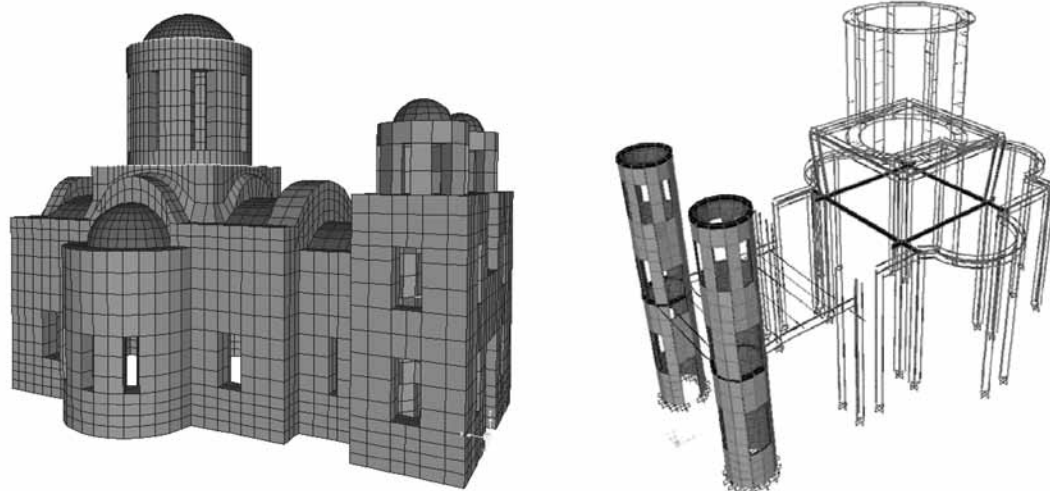


Figure 4. SAP2000 3-D model of the St Athanasius church and the strengthening elements

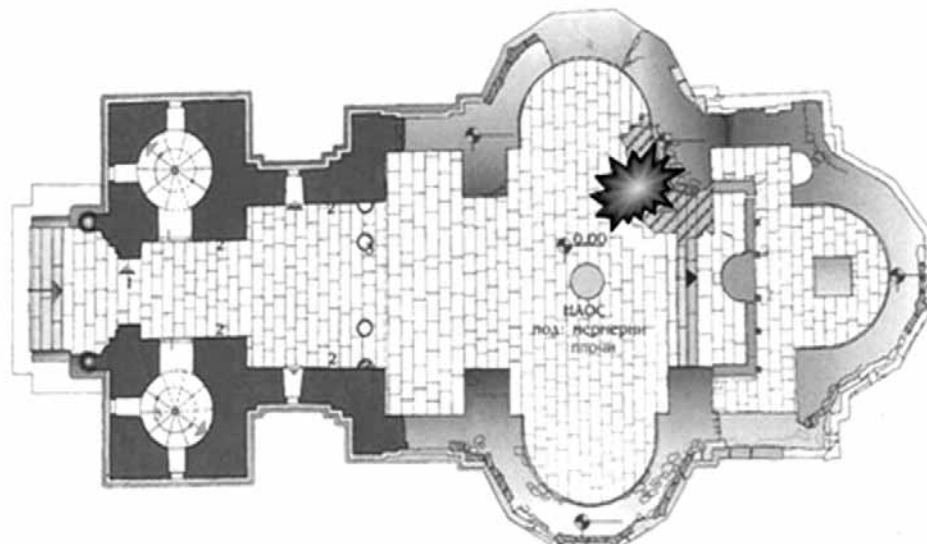


Figure 5. Location of the explosion

considering the extent of the destruction of the ground immediately after the explosion and the debris found (the blast resulted in appearance of a hole in the ground of about 1.2 m in diameter, (Fig. 5);

- the quantity of used explosives can be assumed, taking into account the presence of unexploded container in which the explosive was placed (plastic bottle, 1 liter in volume); the type of used explosives is still unknown;
- the collapse mechanism can be assumed, considering the location of the debris of the collapsed part of the church.

According to the documentation from the scene immediately after the blast, the material from the collapsed part of the church wasn't blown over the immediate surroundings, but concentrated at the point where the structure existed, (Fig. 1), which confirms the assumption that it suffered collapse due to inability to withstand its own weight. The location of the debris indicates that the destruction of the structure was not due to the intensity of the overpressure caused by the blast wave, but was a result of local stability loss (Fig. 6) resulting in progressive collapse of the entire facility in a few seconds.

The local loss of bearing material led to redistribution of the stresses from the self weight

load into other parts of the bearing wall, exceeding their ultimate stresses, causing further collapse and further unfavorable distribution of stresses. This chain reaction resulted in progressive collapse of the structure of the church (Fig. 6).

3.2.2. Analysis of blast resistance of St. Athanasius church from effects of near explosion

The present analysis considers simulation of explosion of 10, 15 and 20 kg TNT from 6 m distance from the explosion center, (Fig. 7).

Depending on the distance from the centre of the explosion and the angle of incidence (α) of the blast wave, zoning of the front wall has been made. Each zone has different magnitude of reflected pressure with different duration. The side wall is a special zone, loaded according to the principles adopted for loading the side walls. The load functions are time dependent, with duration of 1.0 second, divided into 10,000 time steps. In order to simplify the process of loading the front wall, the side wall and the roof, a referent time function of loading has been adopted for every considered quantity of explosive. The referent time function is the time function of the most exposed zone – the one with an angle of incidence between 0° and 45° and distance from the ex-

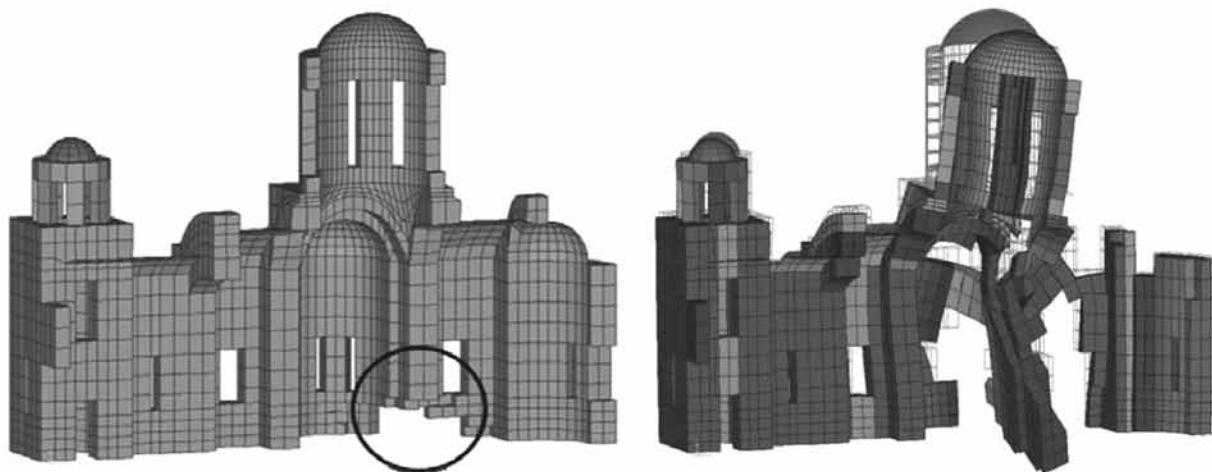


Figure 6. Removing elements with stress over ft and the collapse of the church

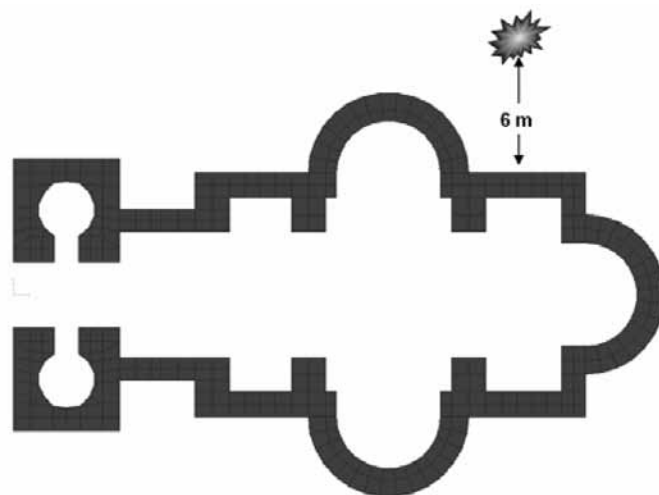


Figure 7. Location of the simulated near explosion

plosion center $R=6$ m. The reflected pressure on each zone separately, in the calculation of loads, has been scaled with reduction coefficient "k", which is defined as to allow for loading the corresponding zone with the reference time function, thereby to meet the real impulse which acts on that zone, (Fig. 8). Analyses in SAP2000 and comparisons of results have been carried out to determine the effect of seismic strengthening on linear force-displacement relationship of the masonry, as a major structural component of the structure. The effects of strengthening on the stress state of the non-strengthened church (former state) and the strengthened church (current state) are significant.

The stress magnitudes of the critical joint of the north-east column are shown in the graph (Fig. 9) for both states. From the relationship shown, it can be concluded that strain S_{33} is proportionate to the quantity of explosives used - the difference in the S_{33} strain is greater for larger quantities of explosives. The W- S_{33} relationship is not linear, but has an exponential form.

3.2.3. Analysis of blast resistance of St. Athanasius church from effects of distant explosion

The present analysis considers simulation of explosion of 50, 75 and 100 kg TNT from 20 m and 30 m distance from the explosion center, (Fig. 10).

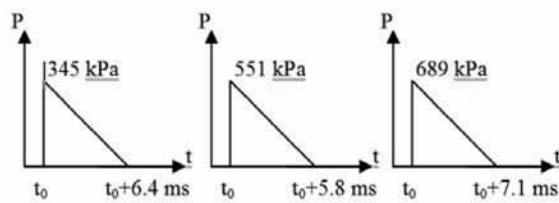


Figure 8. Referent loading function for explosion of 10 kg TNT, 15 kg TNT and 20 kg TNT, respectively, at $R=6$ m

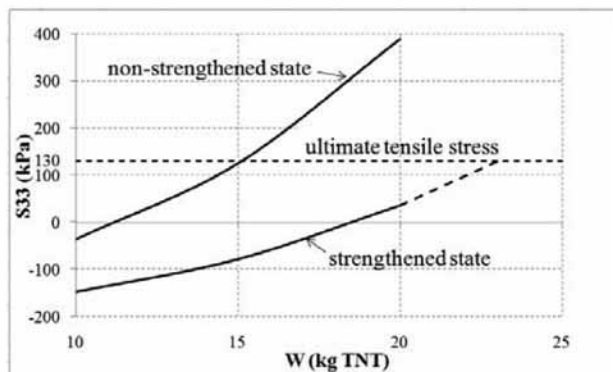


Figure 9. Comparison of the stress magnitudes in a critical joint for near explosion ($R=6$ m)

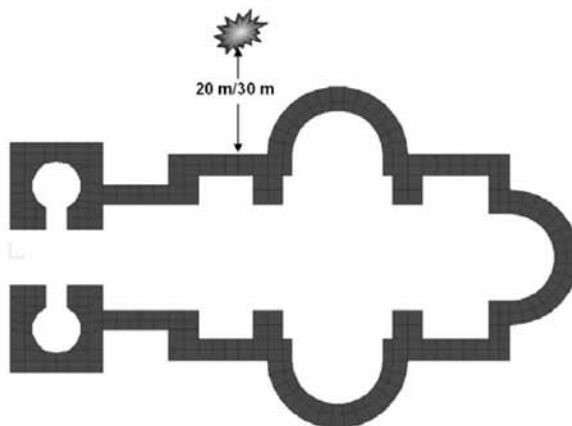


Figure 10. Location of the simulated distant explosion

The analyzed distances and the area of the front wall allow assuming that the whole front wall can be considered as a single zone under maximal reflected pressure, since the blast wave acts with an angle of incidence smaller than 45° on any node of the wall. The whole front wall is under the same magnitude of reflected pressure with the same duration. Just like in the scenario of near explosion, the load functions are time dependent with duration of 1.0 second, divided into 10,000 time steps. In order

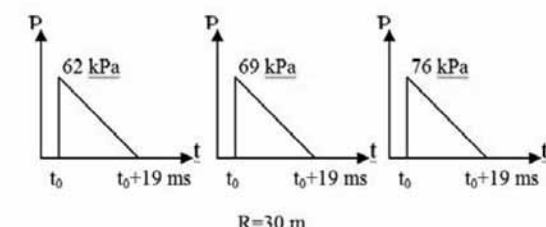
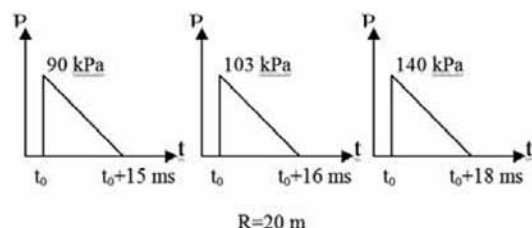


Figure 11. Referent loading function for explosion of 50 kg TNT, 75 kg TNT and 100 kg TNT, respectively, at $R=20$ m and $R=30$ m

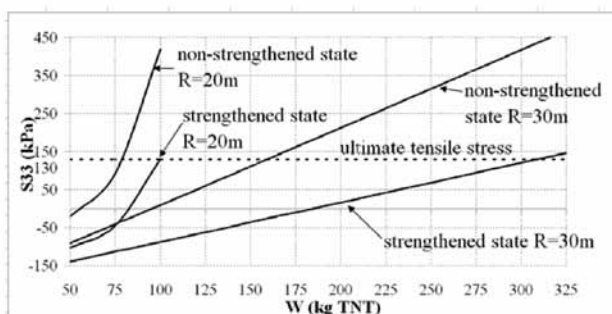


Figure 12. Comparison of the stress magnitudes in a critical joint for distant explosion ($R_1=20$ m, $R_2=30$ m)

to simplify the process of loading the front wall, side wall and roof, a referent time function of loading has been adopted for each considered quantity of explosive at any distance, separately. The referent time function is the time function of the front. The reflected pressure on the side walls and roof in the calculation of loads is scaled by reduction coefficient „ k “, which is defined as to allow for loading the corresponding surface with the referent time function, thereby to meet the real impulse, which acts on that surface, (Fig. 11).

In order to obtain the critical quantity of explosive, an additional scenario with 350 kg TNT acting from distance $R=30$ m has been analyzed.

Analyses in SAP2000 and comparisons of results have been carried out to determine

Table 1. Critical quantity of TNT explosive for the north-east column

R (m)	Non-strengthened		Strengthened	
	20	30	20	30
W _{cr} (kg TNT)	80	160	100	310

the effect of seismic strengthening on linear force-displacement relationship. The effects of strengthening are significant on the stress state of the non-strengthened church (former state) and the strengthened church (current state) just like in the scenarios with near explosions. The stress magnitudes of the critical joint of the north-east column are shown in the graph (Fig. 12) for both states and all the scenarios included in the analysis. In Table 1, the critical quantities of TNT explosive for R=20 m and R=30 m are presented.

It was found that the effectiveness of the strengthening of the structure was more pronounced in the case of a higher value of reflected pressure impulse, as the main parameter of blast loading effect of explosion.

To get a clear insight into the stress state of the whole structure in both cases of explosion (near and distant), it is necessary to make the same comparative analysis of all the model joints.

4. CONCLUSIONS

The applied seismic strengthening of cultural and historical monuments has a limited influence on the resistance of the structures against blast effects. The influence of strengthening depends on the concept of strengthening, the exposure of the frontal surface to explosion, the site of initiation of the explosion and the quantity of the explosives used.

The blast effect depends on the quantity of explosives used and the distance from the site of initiation to the endangered structure. The analysis performed led to the conclusion that the effectiveness of the seismic strengthening

of the structure was more expressed in the case of higher energy value of the blast wave.

The effectiveness of strengthening for blast resistance of the structure can be determined only for a previously defined scenario (known place of initiation of the explosion, known type of explosives and known quantity of the explosive charge).

In order to improve the concept of rehabilitation and seismic strengthening of structures at high risk of exposure to explosions and buildings of special interest or facilities at risk pertaining to secondary hazard, further analysis of possible scenarios is recommended, using the approach for blast loading treated in this paper.

REFERENCES

- American Society of Civil Engineers (ASCE) 1999. *Structural Design for Physical Security*. State of the Practice. Structural Engineering Institute (SEI)
- Jekic G. 2010. *Effectiveness of Seismic Strengthening of Monuments for their Blast Resistance*. Master Thesis. Institute of Earhquake Engineering and Engineering Seismology. University Ss. Cyril and Methodius. Skopje
- Naumoski N. & Balazic J. 2004. *Protection of Buildings from Blast Effects*. A State of the Art Report, Architectural and Engineering Recourses Directorate, Architectural and Engineering Services, Real Property Branch, Public Works and Government Services Canada. Gatineau, Quebec, Canada
- Remenikov A. M. A Review of Methods for Predicting Bomb Blast Effects on Buildings. *Journal of Battlefield Technology*. 2003, 6(3) 5-10. Argos Press Pty Ltd
- Sendova V. *Methodology for Repair and Strengthening of Historical Monuments Damaged due to Man-Made and Natural Disasters*, Institute of Earthquake Engineering and Engineering Seismology – IZIIS, University “SS. Cyril and Methodius”, Skopje
- Sendova V. 2002. *Main Project on the Reconstruction, Seismic Strengthening and Repair of the Structure of the Monastic Church of St. Athanasius*. Report IZIIS 2002-29. Skopje
- Smith P.D. 2007. State of the art in Europe and activity developed within WG3 Impact and Explosion. *Proc. of the International Symposium within the COST C26 “Urban Habitat Constructions under Catastrophic Events*: 274-280. Prague



PERFECTLY MATCHED LAYERS - AN ABSORBING BOUNDARY CONDITION FOR ELASTIC WAVE PROPAGATION

J. Josifovski, V. Vitanov

*University Ss. Cyril and Methodius, Faculty of Civil Engineering,
Skopje, R. Macedonia*

O. von Estorff

*Hamburg University of Technology, Institute of Modelling and Computation,
Hamburg, Germany*

ABSTRACT

The solution of the wave equation for unbounded domains is often of interest in various fields of science and engineering. In particular, the solution of the elastodynamic wave equation for an unbounded domain finds application in simulation of wave propagation and soil-structure interaction.

The present paper deals with the development of a Perfectly Matched Layer as an absorbing boundary condition for time-harmonic elastodynamic problems.

The Perfectly Matched Layer formulation allows a widely used discrete numerical technique such as the finite element method to be employed for investigation of unbounded domains. By enforcing the radiation condition in an unphysical layer positioned adjacent to the bounded domain of interest, one obtains a kind of sponge absorbing the propagating waves of all angles of incidence and frequencies.

To demonstrate the applicability and accuracy of the new approach a fairly simple but representative example is evaluated to reveal the special Perfectly Matched Layer features. The solution is compared to other boundary formulations, such as the viscous-damper boundary.

Keywords: *absorbing boundary condition, perfectly matched layer, propagation of elastic waves.*

1. INTRODUCTION

In geotechnical engineering the investigation of unbounded domains is often of particular interest. A typical example can be found in structural dynamics, where the elastodynamic wave equation of an unbounded domain needs to be solved in order to describe the dynamic interaction between the structure and its underlying soil.

The definition of an unbounded domain requires an enforcement of a radiation condition in any unbounded direction. Irregularities in the geometry of the domain, or in the material, often compel a numerical solution of the problem using different mathematical formulations. According to many researchers and engineers, the finite element method in combination with an efficient artificial boundary,

taking care of the absorption of waves, would be the best choice. The artificial boundary presented in this contribution imposes the necessary radiation condition and ensures that no spurious reflections occur into the domain of interest.

In the past decade quite a few techniques have been developed which solve the problem of the unbounded domains more or less successfully. One of them is the Perfectly Matched Layer (PML) as an absorbing boundary layer, which had turned out to be very promising since it was reported to be rather efficient and accurate.

The Perfectly Matched Layer is working like an absorbing sponge for all propagating waves independent of the incidence angle or frequencies. In general, the PML boundary can be de-

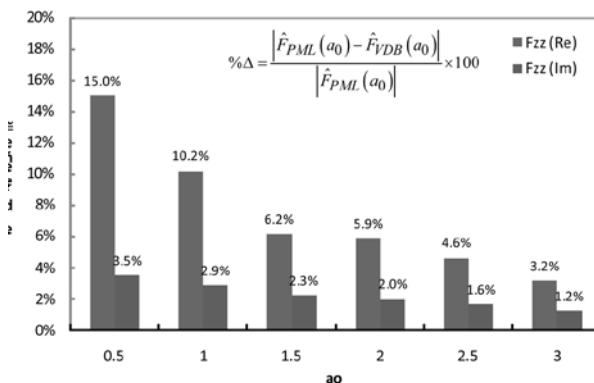


Figure 1. PMM truncation: (a) PMM adjacent to an unbounded domain and (b) PML with a fixed edge

fined with the same material as the one used in the domain of interest but additionally having attenuation characteristics introduced.

The general idea is sketched in Figure 1. If the outgoing wave originated in Ω_{BD} , see Figure 1(a), enters the Ω_{PM}^∞ so-called Perfectly Matched Medium (PMM) where it is attenuated enough in a finite distance. Only then, the Ω_{PM}^∞ can be truncated by a fixed (Dirichlet) boundary without any significant wave reflection, see Figure 1(b).

As a consequence, the displacements of the coupled system $(\Omega_{BD} \cup \Omega_{PM})$ in Ω_{BD} should be almost the same as those of the unbounded elastic domain Ω . Hence, the Perfectly Matched Layer Ω_{PM} , is created from the Perfectly Matched Medium Ω_{PM}^∞ , thus $\Omega_{BD} \cup \Omega_{PM}$ is considered as a replacement of the unbounded elastic domain Ω .

2. GOVERNING EQUATIONS

In the present paper the Perfectly Matched Layer has been derived using a second-order displacement-based finite element formulation. A wave propagation analysis is performed, where the near-field (bounded domain) is discretized with standard isoparametric finite elements, surrounded by a dynamic far-field representing an unphysical domain (or layer) where the absorbing boundary condition is enforced through special types of functions, which are able to damp the outgoing as well as the reflected wave within the layer.

2.1. Elastic medium

Consider a homogeneous isotropic elastic medium subjected to a time-harmonic excitation. The oscillation of the elastic medium will be in the form $\mathbf{u}(x)\exp(i\omega t)$ with ω as circular frequency. The governing equations can be summarized as follows:

Equilibrium equation

$$\sum_j \frac{\partial \sigma_{ij}}{\partial x_j} = -\omega^2 \rho u_i \quad (\text{no summation on } i) \quad (1a)$$

Constitutive relation

$$\sigma_{ij} = \sum_{kl} C_{ijkl} \varepsilon_{kl} \quad (1b)$$

Kinematic relation

$$\varepsilon_{ij} = \frac{1}{2} \left[\frac{\partial u_i}{\partial x_j} + \frac{\partial u_j}{\partial x_i} \right] \quad (1c)$$

where C_{ijkl} is written in terms of the Kronecker delta δ_{ij} such that

$$C_{ijkl} = \left(\kappa - \frac{2}{3} \mu \right) \delta_{ij} \delta_{kl} + \mu (\delta_{ik} \delta_{jl} + \delta_{il} \delta_{jk}) \quad (2)$$

σ_{ij} and ε_{ij} are the components of the stress $\boldsymbol{\sigma}$ and strain $\boldsymbol{\varepsilon}$ tensors, respectively, and C_{ijkl} are the components of the material stiffness tensor \mathbf{C} ; κ is the bulk modulus, μ the shear modulus, and ρ the unit mass density of the medium.

2.2. Perfectly Matched Medium

Consider the governing equations (1) for an elastic medium, where the coordinates x_i will be replaced by stretched coordinates \tilde{x}_i , defined as

$$\tilde{x}_i := \int_0^{x_i} \lambda_i(x_i) dx \quad (3)$$

This procedure of stretching, in particular, is responsible for the physical mapping of the coordinates in the dynamic wave equation. The coordinate-stretching formally implies

$$\frac{\partial}{\partial \tilde{x}_i} = \frac{1}{\lambda_i(x_i)} \frac{\partial}{\partial x_i} \quad (4)$$

where x_i are real coordinates, \tilde{x}_i are complex stretched-coordinates and $\lambda_i(x_i)$ are non-zero, continuous, complex-valued coordinate-stretching function. At the same time this procedure creates a complex formulation for inhomogeneous viscoelastic Perfectly Matched Medium (PMM).

A plane-strain elastodynamic motion of a PMM is defined by introducing (4) into the governing equations (1) as follows:

Equilibrium equation

$$\sum_j \frac{1}{\lambda_j(x_j)} \frac{\partial \sigma_{ij}}{\partial x_j} = -\omega^2 \rho u_i \quad (no summation on i) \quad (5a)$$

Constitutive relation

$$\sigma_{ij} = \sum_{k,l} C_{ijkl} \varepsilon_{kl} \quad (5b)$$

Kinematic relation

$$\varepsilon_{ij} = \frac{1}{2} \left[\frac{1}{\lambda_j(x_j)} \frac{\partial u_i}{\partial x_j} + \frac{1}{\lambda_i(x_i)} \frac{\partial u_j}{\partial x_i} \right] \quad (5c)$$

If such two stretched adjacent media have the same λ_i at their interface, then the matching property will ensure that any propagating wave will pass through the interface without reflection.

Consider the $x_1 - x_2$ plane, with two perfectly matched media defined on the

1. left halfplane

$(= (x_1, x_2) \mid x_1 < 0)$ with $\lambda_i(x_i) = \lambda_i^{lm}(x_i)$, and

2. right halfplane

$(= (x_1, x_2) \mid x_1 \geq 0)$ with $\lambda_i(x_i) = \lambda_i^{rm}(x_i)$.

The wave propagates from the left medium, up-

per index (lm), in x_1 direction, through the PMM interface into right medium, upper index (rm), as depicted in Figure 2.

If $\lambda_1^{lm}(0) = \lambda_1^{rm}(0)$ and $\lambda_2^{lm} = \lambda_2^{rm} = 1$, then the two Perfectly Matched Media can be considered as one PMM, where the continuous λ_1 is defined piecewise on the two half-planes. (In this case λ_2 has not to be considered). The homogeneous isotropic elastic medium governed by the equations (1) is a special case of a PMM where $\lambda_1^{lm} = \lambda_1^{rm} = 1$. The same arguments hold for the wave propagation in x_2 direction.

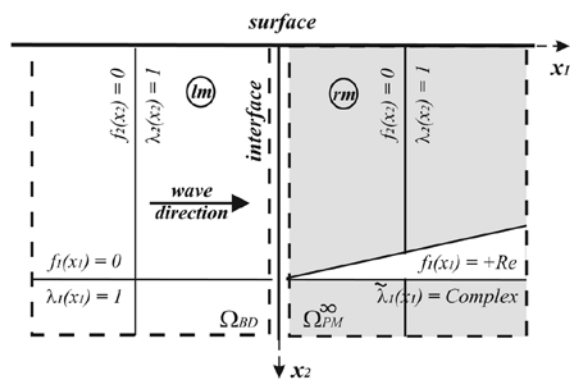


Figure 2. Adjacent PMMs as left (lm) and right (rm) media

2.3. Finite element implementation

Consider a two-dimensional homogeneous isotropic elastic continuum undergoing a time-harmonic plane-strain oscillation. This motion will be described in two rectangular Cartesian coordinate:

1) a x_i system, with respect to a basis $\{e_i\}$, and
 2) a x'_i system, with respect to a basis $\{e'_i\}$, with the two bases related by the rotation matrix \mathbf{Q} , with components $Q_{ij} := e_i \cdot e'_j$. The finite element formulation implementation of the perfectly matched layer condition is related to a rotated coordinate system $\{e'_i\}$ through the definition of $\lambda'_i(x'_i)$ as coordinate-stretching function globally on the computational domain. In this way by replacing x_i by x'_i , the Eqs. (5) are expressed in terms of the coordinates x'_i . Afterwards, the equations with the stretched coordinates are transformed back to the x_i system with respect

to an orthonormal basis $\{e_i\}$, obtaining

Equilibrium equation

$$(\sigma \tilde{\Lambda}) \nabla = -\omega^2 \rho [\lambda_1(x'_1) \lambda_2(x'_2)] \mathbf{u} \quad (6a)$$

Constitutive relation

$$\sigma = \mathbf{C} \varepsilon \quad (6b)$$

Kinematic relation

$$\varepsilon = \frac{1}{2} \left[(\mathbf{u} \nabla^T) \mathbf{\Lambda} + \mathbf{\Lambda}^T (\mathbf{u} \nabla^T)^T \right] \quad (6c)$$

where $\lambda_i(x'_i)$ are the coordinate-stretching functions defining the stretch tensors $\tilde{\Lambda}$ and Λ . The transformation of Eq. (6) to unprimed quantities in the basis $\{e_i\}$ is obtained by

$$\begin{aligned} \sigma &= \begin{bmatrix} \sigma_{11} & \sigma_{12} \\ \sigma_{21} & \sigma_{22} \end{bmatrix} = \mathbf{Q} \sigma' \mathbf{Q}^T, \quad \varepsilon = \begin{bmatrix} \varepsilon_{11} & \varepsilon_{12} \\ \varepsilon_{21} & \varepsilon_{22} \end{bmatrix} = \mathbf{Q} \varepsilon' \mathbf{Q}^T, \\ \mathbf{u} &= \begin{Bmatrix} u_1 \\ u_2 \end{Bmatrix} = \mathbf{Q} \mathbf{u}', \quad \nabla = \begin{Bmatrix} \frac{\partial}{\partial x_1} \\ \frac{\partial}{\partial x_2} \end{Bmatrix} = \mathbf{Q} \nabla' \end{aligned} \quad (7)$$

corresponding to the primed quantities via the usual change-of-basis rules for vector and tensor components.

The weak form of the governing equations Eq. (6) is derived by taking its inner product with an arbitrary weighting function \mathbf{w} and integrating the resultant scalar over the entire computational domain Ω using integration-by-parts and the divergence theorem to obtain

$$\int_{\Omega} \tilde{\varepsilon} : \sigma \, d\Omega - \omega^2 \int_{\Omega} \rho f_m \mathbf{w} \cdot \mathbf{u} \, d\Omega = \int_{\Gamma} \mathbf{w} \cdot \sigma \tilde{\Lambda} \mathbf{n} \, d\Gamma \quad (8)$$

where $\Gamma = \partial\Omega$ is the boundary of Ω and \mathbf{n} is its unit normal; f_m is defined by $f_m := [\lambda_1(x'_1) \lambda_2(x'_2)]$. The symmetry of σ has been used to obtain the first integral on the left hand side, with

$$\tilde{\varepsilon} = \frac{1}{2} [(\nabla \mathbf{w}) \tilde{\Lambda} + \tilde{\Lambda}^T (\nabla \mathbf{w})^T]. \quad (9)$$

Assuming element-wise interpolations of \mathbf{u} and \mathbf{w} in terms of shape functions \mathbf{N} , imposing Eq. (6b) and (6c) point-wise in Eq. (7), and restricting the integrals to the element domain $\Omega = \Omega_e$, gives the stiffness and mass matrices for a PML element. In terms of nodal submatrices, with I and J being the node numbers, these are expressed as

$$\mathbf{k}_{ij}^e = \int_{\Omega_e} \tilde{\mathbf{B}}_I^T \mathbf{D} \mathbf{B}_J \, d\Omega \quad (10)$$

$$\mathbf{m}_{ij}^e = \mathbf{I} \int_{\Omega_e} \rho f_m N_I N_J \, d\Omega \quad (11)$$

where \mathbf{I} is the identity matrix of size (2×2) , and

$$\mathbf{D} := \begin{bmatrix} \kappa + 4\mu/3 & \kappa - 2\mu/3 & \square \\ \kappa - 2\mu/3 & \kappa + 4\mu/3 & \square \\ \square & \square & \mu \end{bmatrix},$$

$$\tilde{\mathbf{B}}_I := \begin{bmatrix} N_{I1}^{(1)} & \cdot \\ \cdot & N_{I2}^{(1)} \\ N_{I2}^{(1)} & N_{I1}^{(1)} \end{bmatrix}, \quad \mathbf{B}_I := \begin{bmatrix} N_{I1}^{(2)} & \cdot \\ \cdot & N_{I2}^{(2)} \\ N_{I2}^{(2)} & N_{I1}^{(2)} \end{bmatrix} \quad (12)$$

with nodal shape functions $N_{ii}^{(1)} := \tilde{\Lambda}_{ij} N_{I,j}$ and $N_{ii}^{(2)} := \Lambda_{ij} N_{I,j}$, described using $\tilde{\Lambda} = \mathbf{Q} \tilde{\Lambda}' \mathbf{Q}^T$ and $\Lambda = \mathbf{Q} \Lambda' \mathbf{Q}^T$, known as the *left* and *right stretch tensors*, respectively:

$$\tilde{\Lambda}' := \begin{bmatrix} \lambda_2(x'_2) & \square \\ \square & \lambda_1(x'_1) \end{bmatrix} \text{ and } \Lambda' := \begin{bmatrix} \lambda_2(x'_2) & \square \\ \square & \lambda_1(x'_1) \end{bmatrix} \quad (13)$$

hence diagonal with respect to the basis $\{e'_i\}$, i.e. *characteristic basis* of the PMM. The Eqs. (8) and (9), the functions λ_i in $\tilde{\mathbf{B}}$, \mathbf{B} and in f_m are defined globally on the computational domain, not element-wise. Note the evidence of coordinate-stretching in the FE matrices, where the stretch tensors $\tilde{\Lambda}$ and Λ are incorporated in the nodal compatibility matrices $\tilde{\mathbf{B}}_I$ and \mathbf{B}_I , not in the material matrix \mathbf{D} . Thus, the system matrices for the Ω are symmetric complex-valued and frequency-dependent which have to be computed anew for each frequency. The coordi-

nate-stretching procedure performs ‘mapping’ of a typical element in the layer such that it extends towards ‘infinity’. This is obtained in two steps illustratively presented in Figure 3.

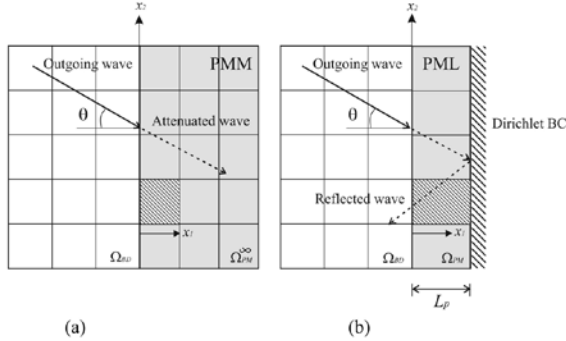


Figure 3 Finite element mapping of the unbounded domain

The PML element is first stretched to discretize unbounded domain as in Figure 3(a), then it is truncated (with Dirichlet condition) to a Perfectly Matched Layer element with a depth L_p , see Figure 3(b). These elements are positioned adjacent to those discretizing the bounded domain.

3. INVESTIGATIONS

To estimate the performance of the proposed PML formulation it will be compared to other methods by means of a foundation vibration analysis. Consider a rigid surface massless strip-foundation over a half-space, excited by a vertical harmonic displacement with unit amplitude $u_0 = 1$ and excitation frequency ω , see Figure 4.

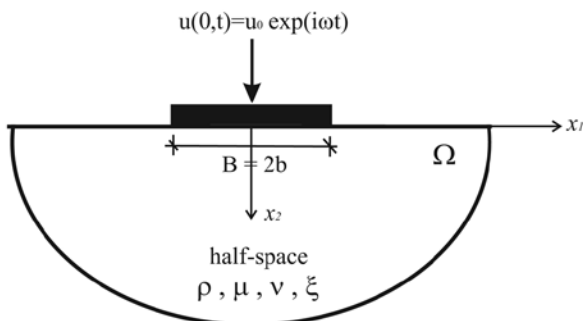


Figure 4 Surface strip-foundation over a half-space excited by vertical oscillations

The foundation dimensions are: width $B = 3m$ and height $h_f = 1.2m$. The soil half-space is defined as linear isotropic viscoelastic mate-

rial with a shear wave velocity of $c_s = 92.2m/s$, a unit mass density of $\rho = 2000kg/m^3$, a Poisson’s ratio of $\nu = 0.3$ and damping coefficient of $\zeta = 0.05$.

In the present analyses, two parallel finite element models are discretized, one using viscous-damper as boundary (VDB) and the other a PML as absorbing condition, both are shown in Figure 5. The VDB finite element model depicted in Figure 5(a) is discretized by 56×46 isoparametric quadrilateral elements (with dimensions $a = b = B/6 = 0.25m$.

Hence, the viscous-damper boundary condition is enforced at the edge of the model. The PML finite element model differs conceptually because it defines a bounded domain Ω_{BD} discretized by 28×19 isoparametric quadrilateral elements, adjacent to which an absorbing layer Ω_{PM} is positioned as shown in Figure 5(b). This PML with depth $L_p = 3.5m$ enlarges mesh to a 30×20 with additional $n_p = 68$ elements. It should be noted both finite element models discretized an identical region which positions the boundary condition at distance $L = 7m$ from the source of excitation.

The analysis quantitatively compares both methodologies by looking at the dimensionless response functions related through a compliance matrix $\mathbf{F}^\infty(a_0)$ as follows:

$$\mathbf{u} = \mathbf{F}^\infty(a_0) \mathbf{P} \quad (14)$$

$$\begin{Bmatrix} u_2 \\ u_1 \\ bu_{r12} \end{Bmatrix} = \begin{bmatrix} F_{22}(a_0) & 0 & 0 \\ 0 & F_{11}(a_0) & F_{1r12}(a_0) \\ 0 & F_{1r12}(a_0) & F_{r12}(a_0) \end{bmatrix} \begin{Bmatrix} P_2 \\ P_1 \\ M_{r12}/b \end{Bmatrix} \quad (15)$$

The conversion is done by normalization of the physical parameters the transformation from dimensional variables to their dimensionless equivalent variables “ \wedge ” through the relation:

$$\hat{F}_{ii} = \mu \cdot F_{ii} \quad (16)$$

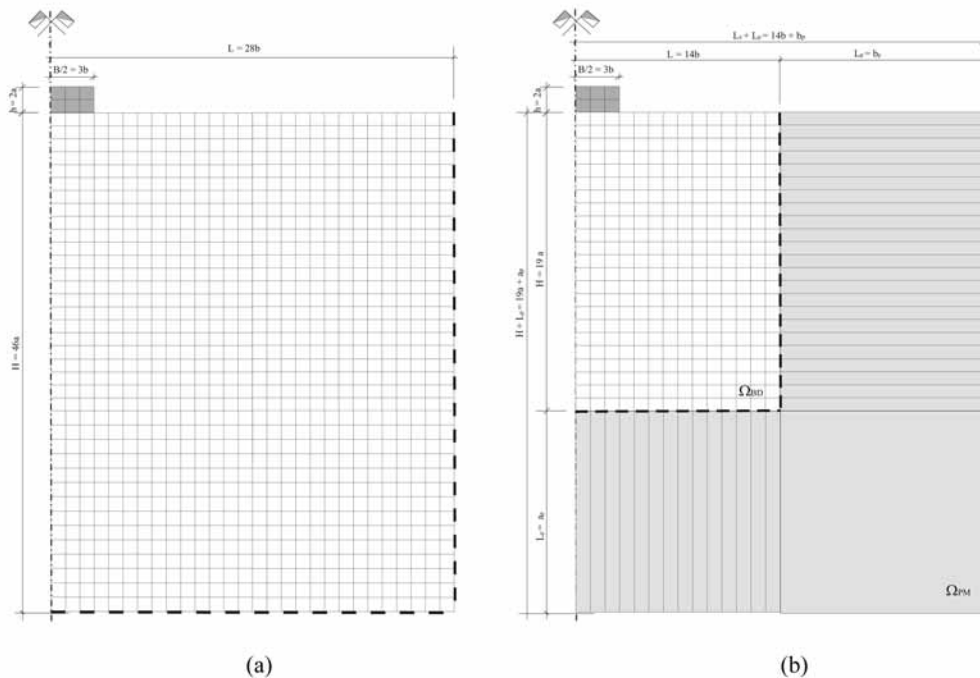


Figure 5. Finite element model of strip-foundation over elastic half-space with (a) VDB and (b) PML condition

For pure translation degrees ($i=1,2$) all dependent from the dimensionless frequency $a_0 = (\omega \cdot b)/c_s$ with b (half of the foundation width) as a characteristic dimension. The complex compliance

$\hat{F}_{22}(a_0) = \hat{F}_{22}^{\text{Re}}(a_0) + i\hat{F}_{22}^{\text{Im}}(a_0)$ of the foundation vertical degree with real (Re) and imaginary (Im) part is presented in Figure 6, respectively.

Although an exceptional matching of the curves can be observed in both parts of the complex function, there is also a small deviation especially for lower frequencies. The PML as a rigorous condition is considered to produce exact solutions, in contrast to the VDB which is an approximate condition. To complete the picture, a relative amplitude difference Δ with respect to the PML method is illustratively presented in Figure 7.

From the cumulative diagram it is obvious that at the lower excitation frequencies the relative difference is more pronounced decreasing with the increasing frequency. The qualitative side of the analysis shows that the VDB model produces 15% error in lower frequency range for $a_0 \leq 0.5$ and around 10% at $a_0 = 1.0$. This could be ar-

gued with the fact that at lower frequencies the viscous-damper boundary condition has restrictions with respect to the angle of wave incidence which may lead to some stability problems. Thus, the viscous-damper condition should be positioned at distances greater than $L = 7\text{ m}$ from the source of the oscillation to obtain the same accuracy as in the case of the PML. Another aspect of the comparative analyses is presented in Table 1. The ratio t/N of the elapsed calculation time t and the related number of elements N defines the computation time per element.

Table 1 Comparison of PML and VDB with respect to computation time per element

Method	t (min)	N (/)	t/N (s)
PML	13.4	600	1.34
VDB	24.8	2576	0.58

Since the PML attenuation is defined on the global computational domain, not element-wise, the model can be discretized with fewer elements which reduce the computational time significantly. In this analysis the spatial discretization in the VDB model needs 4.3 times more elements than the PML. In fact, although PML is computationally more expen-

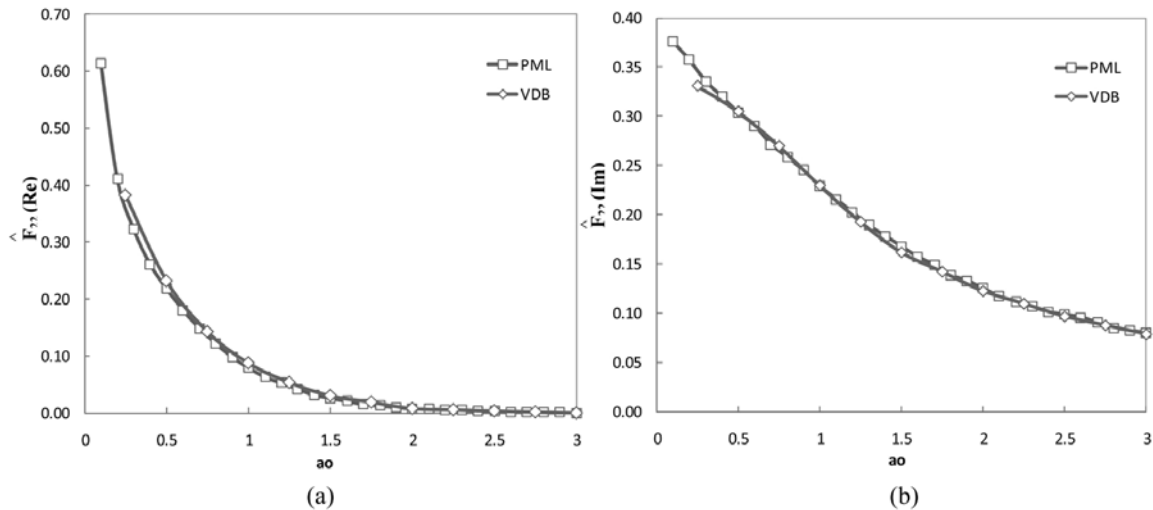


Figure 6. Comparison of the compliance function of a surface foundation over half-space with

$$(a) \hat{F}_{22}^{\text{Re}}(a_0) \text{ and (b)} -\hat{F}_{22}^{\text{Im}}(a_0)$$

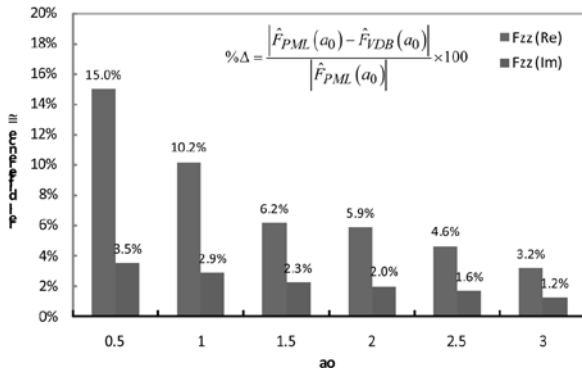


Figure 7 Relative differences in compliance functions for a rigid surface foundation on half-space

sive due to its complex formulation, it still remains more efficient because fewer elements are needed for the same level of accuracy. In the current study the time gain was 46 percent.

Finally, it can be summarized that the Perfectly Matched Layer formulation not only takes less computation time but also produces better results with fewer elements making it an efficient method and preferable as a boundary condition in solution of elastodynamic problems.

4. CONCLUSIONS

The formulation and application of a Perfectly Matched Layer in definition of unbounded domains for elastodynamics has been presented. Its adsorption capability was found to be very

convincing, even in the case of a rather small PML thickness and even for relatively low frequencies. In fact, the results have shown that the PML absorption remains equally efficient at wavelengths far larger than the PML thickness. As a consequence, the PML thickness can be kept minimal even for studies involving low frequencies, and no rescaling of the model size is required. The recommended value of the PML thickness is defined through the ratio $\lambda_{\max}/L_p \leq 10$ which will ensure an accurate solution.

The performance of the PML condition has been compared with another dynamic boundary method. The results show that the PML does not only take less computational time but also produces better accuracy with fewer elements. This suggests that the bounded domain may be restricted to the region of interest in order to lower the computational cost. This constitutes the major advantage of the PML with respect to the other methods classifying it as very efficient and preferable choice in the solution of elastodynamic problems.

The current contribution brings a formulation of the PML condition derived in the frequency domain. It is recommended that for further research the PML condition should be derived di-

rectly in the time domain, which will eventually enable the investigation of a nonlinear behaviour inside the bounded soil region. Moreover, the PML offers an efficient modelling alternative for the simulation of wave propagation in unbounded domains not only for elastodynamic problems but also in other fields of engineering, such as, for instance, acoustics.

REFERENCES

- Bèrenger, J.-P. (1994). A perfectly matched layer for the absorption of electromagnetic waves, *J. Comput. Phys.* 114, 185–200.
- Basu, U. and Chopra, A.K. (2003). Perfectly matched layers for time-harmonic elastodynamics of unbounded domains. Theory and finite-element implementation, *Comput. Methods Appl. Mech. Engrg.* 192, 1337–1375.
- Harari, I. and Albocher, U. (2006). Studies of FE/PML for exterior problems of time-harmonic elastic waves, *Comput. Methods Appl. Mech. Engrg.* 195, 3854–3879.

ACKNOWLEDGMENT

The financial support of the first author by the DAAD (Deutscher Akademischer Austausch Dienst) through the SEEFORM (South Eastern European Ph.D. Formation in Engineering) program is gratefully acknowledged.



SEISMIC STABILITY OF THE OLD BRIDGE IN MOSTAR

M. Kustura, M. Glibić

Faculty of Civil Engineering University of Mostar, Bosnia and Herzegovina

L. Krstevska, L. Tashkov

Institute of Earthquake Engineering and Engineering Seismology, Skopje, Macedonia

ABSTRACT

In order to get cognitions about the seismic stability of the bridge, experimental testing was done by the ambient vibration method to define dynamic characteristics – own frequencies, mode shapes and damping coefficients, at which modern ARTeMIS program package for data processing was used. Numerical analysis of the bridge was done in Tower 3D program package, version 6.0 at which different cases of overloads were taken in consideration. Seismic analysis was conducted for linear-elastic behavior of the bridge, with calculation of seismic forces by Eurocode and by using superposition of mode shapes and acceleration spectra design. Comparing results and dynamical characteristics of the bridge obtained by experimental investigation with performed analysis of the mathematical model of the bridge we can see the compatibility. The obtained results present a qualitative base for performing further non-linear analysis and evaluation of the seismic stability of this respective monument.

Keywords: ambient vibrations, natural frequencies, mode shapes, damping, linear-elastic, acceleration spectra design, masonry.

1. INTRODUCTION

The subject of investigation is the Old Bridge in Mostar, a structure of construction heritage under protection of UNESCO, a monument witnessing connection of people, nations and cultures throughout centuries. During the long period of its existence, the bridge endured all adversities that happened to it, but there was a single moment when it did not withstand. After its destruction, the bridge was reconstructed, and so today it has been serving to its primary purpose again. The goal is to determine the seismic stability of the structure itself. To establish the actual condition, we performed experimental investigations on the bridge using the method of ambient vibrations. For measurement and recording of structure ambient vibrations, a system of seismometers, amplifiers and recorders is applied. Math-

ematical analysis was performed by the modern software Tower 6.0.

In these two manners, dynamic characteristics of the bridge were determined, which we compare with relevant characteristics from the bridge reconstruction project and conclude the level of design and reconstruction of the structure.

2. DESCRIPTION OF THE OLD BRIDGE

2.1. General

The Old Bridge was completed in 1566. is an architectural masterpiece and the most remarkable monument of Mostar and Bosnia and Herzegovina. The bridge existed through centuries and became an UNESCO protected monument of culture and construction heritage, as well as a popular tourist destination.

The destruction of the bridge took place in 1993



Figure 1. The Old Bridge

during the war in Bosnia and Herzegovina. During the reconstruction of the Old Bridge great efforts were made to adhere to original materials and methods. Date of the opening ceremony is 24.07.2004.

2.2. The main structural elements of the Old Bridge and accessories used for bridge assembling

The main structural elements of the bridge are: bearing arch of the bridge, the bracing rib, the bridge abutments and side walls, stone front walls, pedestrian cobbled pathway and stone plates, bridge parapets, upper and lower bridge cornices.

Stone elements of the bridge were reinforced by using a special technological set of manually produced wrought iron and placed over connecting joints following different typological methods of assembling. Basically, there were two types of these iron ties: dogs and bonds, and they were applied on stone elements with intendedly carved slots with slightly wider bottom to avoid making it completely airtight. Metal ties also had wider edges, and after they were fixed, melted lead was poured into slots to finish the closing.

3. EXPERIMENTAL INVESTIGATION OF THE DYNAMIC CHARACTERISTICS OF THE OLD BRIDGE

3.1. General

The Old Bridge in Mostar has been tested by ambient vibration method, measuring the vibra-

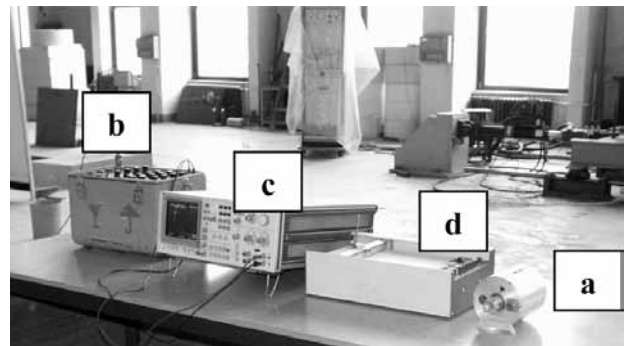


Figure 2. Equipment for measurements by ambient vibrations method

tions in selected points along the bridge and then processing the recorded signals to obtain the dynamic characteristics.

3.2. Equipment used

For structural vibrations recording caused by some ambient excitation a system of seismometers, amplifiers and recorders is used, Fig. 2. The seismometer measures the velocity and it has limitations in frequency and amplitude range. The signal from the seismometer (a) through special cables is transmitted to the signal conditioning system (b) which eliminates the effect of the higher frequencies. Then the filtered and amplified signal is transmitted to the Spectrum analyzer (c) and by Fourier transform the frequency content of the recorded vibration is determinated. The frequency analysis is complete and both amplitude and phase spectra are obtained. Processing of the signals is done in real time and the obtained spectra should be plotted (d) for further analysis and obtaining of damping coefficients.

3.3. Testing performed on the Old Bridge

In the first phase of testing, necessary equipment was taken to the bridge site, and then linked into network and connected into a functional whole. After that, seismometers were placed on the Old Bridge in 22 predefined points.

Seismometers were placed to measure the transversal, longitudinal and vertical vibrations of the bridge at each point.

Eighty eight measurements were performed in-

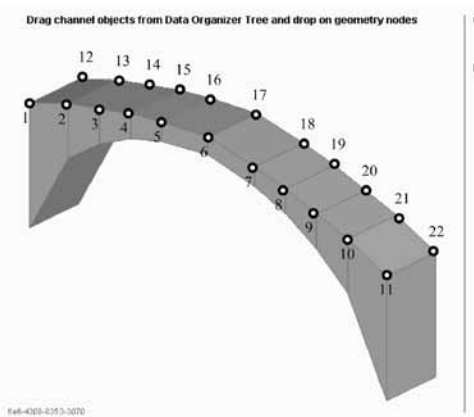


Figure 3. Selected points for installation of seismometers



Figure 4. Tests on the Old Bridge

cluding the dynamic calibration test, while data recording was performed during the time of 100 seconds at the sampling frequency of 200 samples per second.

3.4. Obtained results

Frequency of 7.6 Hz is the resonant frequency for the transversal direction, the dominant frequency for longitudinal axis of the bridge is 11.43 Hz, while the frequency of 13.96 Hz is the resonant frequency in the vertical direction. The coefficients of damping are in the range from 1.5% to 4.3% and they are presented along with the obtained frequencies in Table 3.1.

The obtained mode shapes of vibration are presented in the figures 5-7.

4. NUMERICAL ANALYSIS OF THE STRUCTURE

4.1. Modeling of the structure

The entire calculation was performed in the software suite Tower - version 6.0.

The modeling was performed by plate elements, and their total number was 892, the total number of nodes in the structure was 7230, while the total number of boundary elements was 408.

4.2. Loading conditions and combinations

Loading conditions and their combinations are defined according to Eurocode 1, and for defining of the seismic load, Eurocode 8 was used.

Table 4.1. Load combinations

No.	Combinations	No.	Combinations
1	1.0 g + Sx	5	1.35 g + 1.35 p
2	1.0 g + Sy	6	1.35 g + 1.35 p/2
3	1.0 g + 1.0 p	7	1.0 g + 0.5 p + 1.50 Sx
4	1.0 g + 1.0 p/2	8	1.0 g + 0.5 p + 1.50 Sx

Table 3.1. Obtained values of frequencies and coefficients of damping

Dominant frequency Hz	Coefficients of damping %	Dominant frequency Hz	Coefficients of damping %
7.2	2.3	13.6	2.8
7.60	1.5	13.96	2.4
11.43	2.6	14.6	4.3
13.1	3.1	23.7	3.4

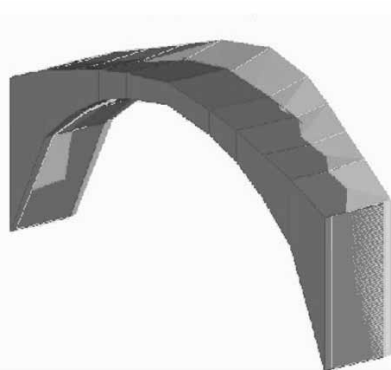


Figure 5. Mode shape in transv. direction, f=7.6Hz

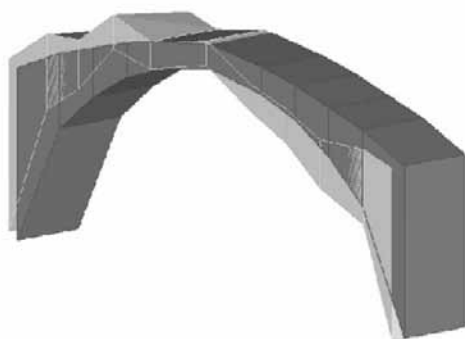


Figure 6. Mode shape in longitud. direction, f=11.43Hz

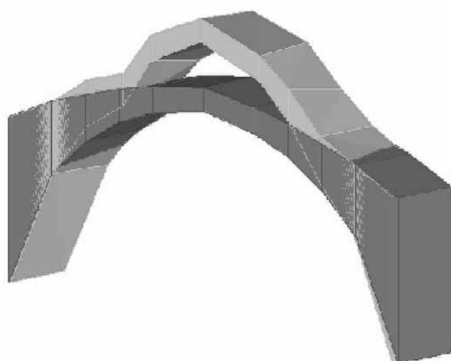


Figure 7. Mode shape in vertical direction, f=13.96Hz



Figure 8. 3D Model of The Old Bridge

4.3. Description of performed seismic analysis

Calculation was performed on the basis of linear-elastic behavior of the structure. Seismic effects are calculated by modal analysis and design acceleration spectrum. The seismic force is determined by the expression:

$$F_B = S_d(T_1) \cdot W$$

where:

$S_d(T)$ - is the ordinate of the design spectrum
 W - is total weight

The bridge is situated in the area where earthquake of VIII degree of seismicity according to MCS scale is expected for the return period of 500 years. The soil design acceleration of $a_g = 0.2$ corresponds to this. The soil is classified into category A. The value of $q = 1.0$ is assumed for behavior factor. The design spectrum in the figure corresponds to such conditions.

4.4. Modal analysis

Obtained values of period and frequency of oscillation are given in Table 4.2.

Table 4.2. Oscillation periods and eigenfrequencies of the bridge

No.	Period (s)	Frequency (Hz)
0,137941	7,249478	
0,109332	9,146441	
0,109332	9,146441	
0,095069	10,518683	
0,087026	11,490859	
0,076211	13,121515	
0,074420	13,437207	

Mode shapes of vibration are given in the figures 10-12.

4.5. Bridge model verification on the basis of obtained experimental results

Analysis of behavior of the Old Bridge, conducted in software suites Tower 6.0 and ANSYS (software used for analysis in reconstruction project of the Old Bridge), both based on the finite element model with assigning of characteristics of materials

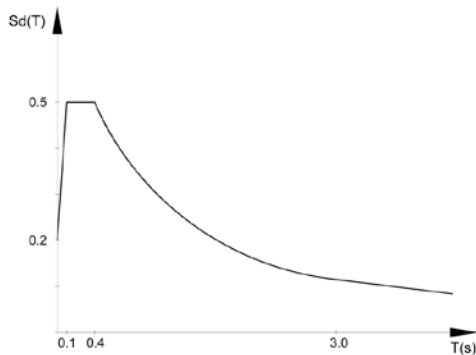


Figure 9. Design spectrum

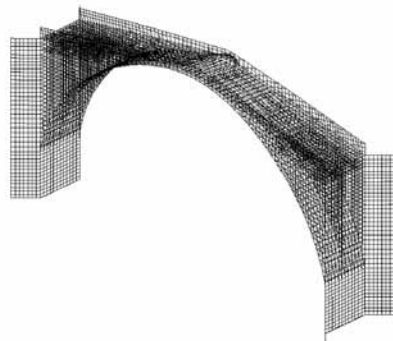


Figure 10. f = 7.25Hz (transversal direction)

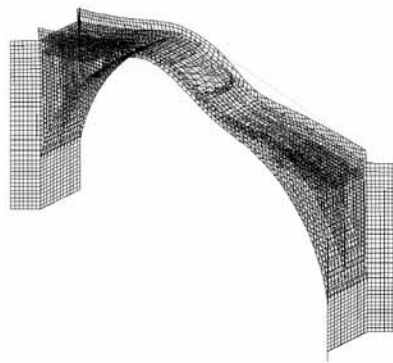


Figure 11. f = 10.52Hz (longitudinal direction)

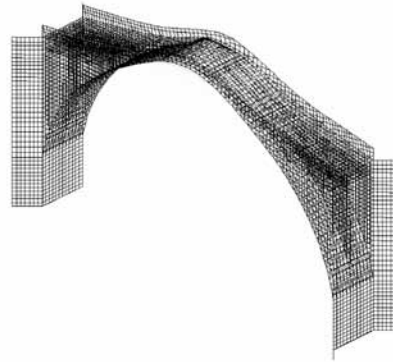


Figure 12. f = 13.12Hz (vertical direction)

obtained for examined samples, gave results that can be said to agree well with results of analysis performed by experimental investigations using the method of ambient vibrations. The values of the natural frequencies are given in Table 4.3.

4.6. Results of performed structure analysis

Stresses and deformations in the bridge and its main structural elements for relevant load combinations are presented in the further part of the thesis.

After the reduction of characteristic strength of stone walls by adopted partial coefficients of safety for material, we can conclude the following:

- obtained compressive stresses in the vault and walls of the bridge presented in Table 4.4. are smaller than mean compressive stresses of stone walls assumed in the Old Bridge reconstruction project, reduced for safety factor;
- obtained tensile stresses presented in Table 4.5. are greater than mean tensile strengths of stone walls assumed in the Old Bridge reconstruction project;
- on occurrence of tensile stresses on the upper side of the arched bridge structure, they will be taken over by bonds and dogs used to connect stone blocks into one monolithic whole, the capacity of bonds should be investigated;
- on occurrence of tensile stresses on the lower side of the arched structure of the bridge, mi-

cro-fractures may appear in mortar. That will result in a shift of the neutral line of stress toward the compressive zone and increase in pressure stress, but will not compromise the bridge stability.

In the Table 4.6 presented are the maximum vertical and horizontal deformations in the highest point of the bridge vault for treated combinations of loads, as well as maximum vertical and horizontal deformations on the entire surface of the bridge vault.

Table 4.3. Comparative presentation of the natural frequencies of the bridge

Natural frequency (Hz)		
Experiment	Tower 6.0 Software	Ansys Software
7.60	7.25	6.88
11.43	10.52	10.48
13.96	13.12	14.68

Table 4.4. Maximum values of obtained compressive stresses in the bridge (MPa)

No.	Combination of loads	Vault	Central rib	Side walls
	1.0 g + Sx	-0,98	-0,44	-0,54
	1.0 g + Sy	-0,81	-0,60	-0,58
	1.0 g + 1.0 p	-0,66	-0,54	-0,77
	1.0 g + 1.0 p/2	-0,67	-0,54	-0,60
	1.35 g + 1.35 p	-0,89	-0,72	-0,81
	1.35 g + 1.35 p/2	-0,90	-0,72	-0,81
	1.0 g + 0.5 p + 1.50 Sx	-1,24	-0,45	-0,62
	1.0 g + 0.5 p + 1.50 Sx	-1,00	-0,76	-0,85

Table 4.5. Maximum values of obtained tensile stresses in the bridge (MPa)

No.	Combination of loads	Vault	Central rib	Side walls
	1.0 g + Sx	0,42	0,25	0,27
	1.0 g + Sy	0,68	0,42	0,66
	1.0 g + 1.0 p	0,16	0,08	0,15
	1.0 g + 1.0 p/2	0,17	0,09	0,16
	1.35 g + 1.35 p	0,21	0,10	0,20
	1.35 g + 1.35 p/2	0,22	0,11	0,21
	1.0 g + 0.5 p + 1.50 Sx	0,70	0,19	0,60
	1.0 g + 0.5 p + 1.50 Sx	0,87	0,13	0,90

Table 4.6. Maximum deformations in the bridge vault (mm)

No.	Combination of loads	Z _{p1}	Y _{p1}	Z _{p2}	Y _{p2}
	1.0 g + Sx	0,55	1,09	1,19	1,09
	1.0 g + Sy	1,83	3,62	1,84	3,62
	1.0 g + 1.0 p	1,73	0,01	1,74	0,02
	1.0 g + 1.0 p/2	1,60	0,01	1,73	0,02
	1.35 g + 1.35 p	2,33	0,02	2,34	0,03
	1.35 g + 1.35 p/2	2,16	0,02	2,34	0,03
	1.0 g + 0.5 p + 1.50 Sx	1,46	2,65	1,46	1,65
	1.0 g + 0.5 p + 1.50 Sx	1,55	5,45	1,56	5,45

Z_{p1} – vertical deformation in the highest point of the bridge vault

Y_{p1} – horizontal deformation in the highest point of the bridge vault

Z_{p2} – vertical deformation in the bridge vault

Y_{p2} – horizontal deformation in the bridge vault

Presented values in Table 4.6 indicate that maximum deformations in the highest point of the bridge vault are mainly also maximum strains in the entire bridge.

5. CONCLUSIONS AND GUIDELINES FOR FURTHER INVESTIGATIONS

5.1. Conclusions

From the performed analyses the following can be concluded:

- minimum differences in bridge shapes of vibration, i.e. somewhat stiffer behavior of the bridge obtained by the method of in situ ambient vibration tests, may be explained by the quality construction with presence of metal elements in the bridge (wrought iron elements, dogs and bonds) affecting the bridge stiffness, and which could not be represented in the numerical model;
- obtained maximum compressive stresses and displacements in the bridge indicate that the bridge structure is the most sensitive in areas near the top of bridge arch as well as in thirds of the bridge span;
- the skill and creativity of old builders, construction method with specifically designed bonds with use of bitches, dogs, and other methods for bonding of stone blocks, un-

questionably provide a unique structural unit that influences structure behavior in all utilization conditions;

- that the bridge's own weight and shape are the dominant factors that influence stability of the entire structure, and hence also for effects of seismic forces.

5.2. Guidelines for further investigations

For the purpose of the best possible understanding of behavior of the Old Bridge as well as its protection and preservation for generations to come, it is necessary to perform constant monitoring of the structure by modern instruments that would register and record every activity of the structure.

The next step should be to test the bridge on a seismic shaking table in order to obtain a more quality picture of the seismic behavior and stability of this monument of culture under protection of UNESCO. One of important objectives will be to investigate and to define the capacity of the bonds and dogs used to connect the stone blocks into one monolithic whole.

REFERENCES

- A Bridge Story, MOSTart, World Banck, UNESCO, PCU, Project Coordination Unit City of Mostar, Mostar, 2004.
- Čolak, I., A Reconstruction of the Site of the Old Bridge in Mostar - A Builders Diary, Deblokada Sarajevo, City of Mostar, UNESCO, Mostar - Sarajevo, 2007.
- The EN Eurocodes, Brussels, 2003.
- General Engineering s.r.l., Reconstruction of The Old Bridge in Mostar, 2000.
- Gotovac, B., Reconstruction of the Old Bridge, Roads and Bridges, Jurnal of the Croatian Road Transport Association, Zagreb, 2004.
- Krstevska, L. & Tashkov, Lj. Ambient Test of Reconstructed Old Bridge in Mostar, ARTeMIS Newsletter 2007.
- Krstevska, L., Experimental in-situ testing of reconstructed Old Bridge in Mostar, Proceedings of The 14th World Conference on Earthquake Engineering, paper ID-12-01-0243, Beijing, China, 2008.
- Krstevska, L., Kustura, M. & Tashkov, Lj., Dynamic testing of the Old Bridge in Mostar, International Scientific Simposium, Mostar 2008.
- Krstevska, L., Kustura, M. & Tashkov, Lj., Dynamic testing of the Old Bridge in Mostar, II GNP, Podgorica, Crna Gora, 2008.
- Official web site: Technical design for the reconstruction of the Old Bridge of Mostar;
- Peković, Ž., Soil Investigation of Mostar bridge fortification, Collection of Papers 2 of the Faculty of Civil Engineering University of Mostar, Mostar, 2002.



STIFFNESS CHARACTERISTICS MODELLING OF RC FRAME STRUCTURES ACCORDING TO EUROCODE 8

Prof. Ljupco Lazarov, Asisst. Koce Todorov

*Faculty of Civil Engineering,
University "Ss. Cyril and Methodius"
Skopje, Macedonia*

ABSTRACT

Eurocodes are contemporary design codes based on the state of the art last decade engineering knowledge and experience. However, some provisions and requirements contained in Eurocode 8 are not sufficiently explained or appropriately defined for practical application. To mention the few of them are: the effective stiffness of structural elements, RC frame masonry infill and soil structure interaction that may have considerable influence in changing the structural response. In order to investigate the influence of different parameters to earthquake structural response, a comparative modal, spectral and nonlinear static push-over analysis of a 5 story 3 bay RC plane frame was analyzed for 6 parameter variations. The presented analysis results show major influence of these parameters in changing the structural vibration period which is reflected consequently in changes of: design seismic force, determined displacements and calculated ductility of the structure under consideration.

Keywords: Eurocode 8, stiffness parameters, linear and nonlinear analysis, RC frame masonry infill, SSI

1. INTRODUCTION

The rapid development of computer science at the hardware and software level, supported by the parallel development and application of numerical methods in structural analysis, in the last ten years has resulted with the development of a number of commercial software packages for modelling and analysis of structures exposed to static and dynamic loads. Professionally designed user interfaces of these software packages, often lead to the emergence of automatism in defining the required characteristics for the mathematical modelling, which in some cases can lead to loss of engineering "sense" and results with occurrence of errors of great magnitude. Therefore, current codes for the design of structures in its provisions and requirements should contain detailed guidelines and recommendations for modelling, analysis

and design, which would largely eliminate possible sources of error which may occur by free interpretation of certain ambiguities in these regulations.

Eurocodes are contemporary design codes based on the state of the art last decade engineering knowledge and experience. However, some provisions and requirements contained in Eurocode 8 are not sufficiently explained or appropriately defined for practical application, which may lead to occurrence at difficulty in defining the required parameters. This can be particularly emphasised among designers in a country, which in its current practice did not have enough experience with the implementation of these or similar requirements. Therefore, a few comments about the impact of certain parameters that can be found in Eurocode

8: Design of structures for earthquake resistance - Part 1: General rules, seismic actions and rules for buildings and especially in section 4.3 Structural Analysis, 4.3.1 Modelling are given below.

Eurocode 8 belongs to the group of seismic provisions based on the concept of reduction of inertial seismic forces that occur in the structure in its linear elastic behavior at the expense of ensuring global ductility consideration. According to this concept, during the strong earthquake it is allowed individual elements of structure to exhibit plastic deformation, dissipating the seismic input energy. Using the approach of equal energy, for the short period structures, and equal displacement for long period structures, the relationship between the reduction of seismic force and the necessary structure ductility is established. This concept of seismic design is known as force based - displacement controlled design concept. The procedure for analysis of structures based on this concept consists of several steps, Fig.1, namely: to determine periods and mode shapes of the analyzed structure (which are a function of stiffness and mass), to define the behaviour factor $-q$ (depending on the structure possibility for providing nonlinear deformation), to obtain the so-called design spectrum by reduction of the elastic response spectrum, to determine and to distribute the seismic design force, to perform the elastic analysis of the structure and to calculate the displacements induced by the design

seismic action and finally to verify structural safety by considering the relevant limit states and specific measures.

From the review of analysis procedure it is evident that structural stiffness is important parameter that can greatly change the structural response for a specific seismic action. Therefore the choice of modelling parameters, in general, can result in reduction or increase of the horizontal stiffness and could be a key factor in determining the reliable structural response. The effective stiffness of structural elements, masonry infill and soil structure interaction are some of the parameters which may have considerable influence in changing the structural response.

2. EFFECTIVE STIFFNESS OF REINFORCED CONCRETE ELEMENTS

The determination of design seismic forces, according to EC 8, is based on linear elastic analysis, which means that structural stiffness is constant during the analysis. The assumptions of constant stiffness is far from real behavior due to the fact that during seismic action in reinforced concrete structural elements subjected to bending, with or without axial force, the first cracks appear for low levels of bending moment compared to the corresponding yield moment. So, a secant stiffness value pointing to yielding would reflect a more realistic behaviour. As stated in EC8, (2004), if a more accurate analysis of

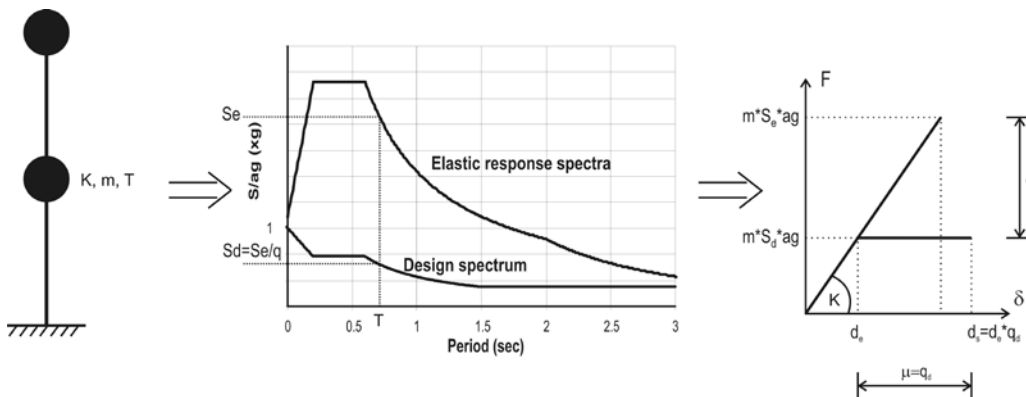


Figure 1. Schematic view of design concept according to EC8

the cracked elements is not performed, the elastic flexural and shear stiffness properties of concrete elements is permitted to be taken as one-half of the corresponding stiffness of uncracked elements. However, in principle, the reduction of stiffness depends on many factors such as: the type of constructive element, the percentage of reinforcement and the level of normal stress caused by the influence of gravity loads. In New Zealand regulations stiffness reduction factors depend from the type of structural element. The values of these factors are equal to 0.35 for beams and are within the limits of 0.4 to 0.7 for columns depending on the level of axial force. Similar values can be found in U.S. recommendations given in the ASCE / SCE 41 from 2007, (2007). In these recommendations the reduction of previous recommended values in FEMA 356, (2000), is given so that the reduction factor for beams is reduced from 0.5 to 0.3, while for columns it is dependent on the level of axial force. For columns in which axial force is less than 0.1 $f_c A_c$, reduction factor from 0.5 is reduced to 0.3, while for columns in which axial

force level is greater than 0.5 $f_c A_c$ effective flexural stiffness is equal to 0.7 of the corresponding stiffness of the uncracked elements. For illustration of these facts the reinforced concrete section analysis with dimensions 40/40cm reinforced with different percentages of reinforcement (0.6%, 1% and 3% of the area of the concrete section) and loaded with varying levels of axial force ($N/f_c A_c = 0, 0.1, 0.3$ and 0.4) is performed, Fig.2, Fig3. From the results of analysis is obvious that the reduction in elastic flexural stiffness is greater in cross-sections loaded with lower axial force. Cross-sections with a smaller percentage of reinforcement have a greater stiffness reduction compared with the cross-sections with the higher reinforcement percentage.

3. INFLUENCE OF MASONRY INFILL

Masonry infill is characterized with significant strength and stiffness and it can greatly alter the response of structures exposed to dynamic loads. On one hand the infill panels contribute to increasing the structural resistance against seismic action. Their presence, increase the

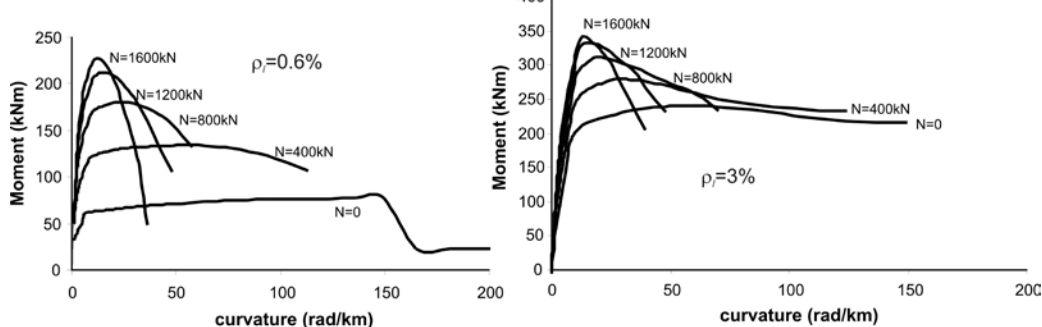


Figure 2. Moment – curvature diagrams for 40/40cm RC section with different reinforcement percentages and variable levels of axial force

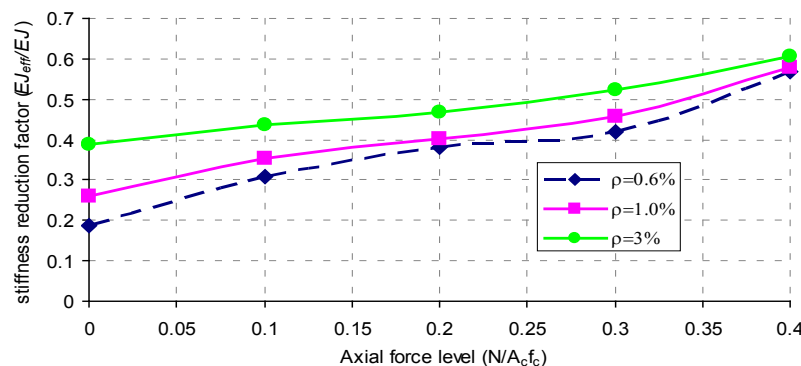


Figure 3. Reduction of elastic stiffness in function of axial force level and reinforcement percentage

structural stiffness, strength and damping and act as a first line of defense in seismic activity reducing the ductility demand and consequent damage of structural elements. On the other hand an irregular distribution of panels in plane and along building height can lead to series of unfavorable effects (torsion effects, dangerous collapse mechanisms, soft or weak storey, variations in the vibration period, etc.). Also, in some cases when the infill panels are regularly distributed in the frame (uniformly infilled frame), the seismic response of the structure can be characterized by a soft storey mechanism developing as a consequence of the brittle failure of masonry panels at a particular level, that produces a sudden reduction of strength and stiffness and an increase in the storey deformation demand. These facts are reason why the scientific and professional community may have different opinions about the impact of infill of the dynamic response of structures.

In the general case, the presences of masonry infill in the reinforced concrete frames change the structural behaviour, by changing the mechanism of lateral force transferring. In this way, predominant frame action whose elements - columns and beams are subjected to bending is transformed into the predominant truss action whose elements are generally subjected to axial forces, Fig.4. While this is indisputable fact, according to the usual practice of design in the past, the interaction between the masonry infill and frame structure was often neglected. This approach can lead to significant errors in determining the stiffness, bearing capacity and ductility of the analyzed structure. This is spe-

cially dangerous in reinforced concrete frames in which there is a discontinuity in the distribution of masonry infill along the height of the building, Fig. 4.1c.

Although in EC8 are not given more precise guidance, in the literature can be found various recommendations on how to include the masonry infill in the mathematical models. Numerical modeling strategies of infilled frames in general are divided into two distinct categories, i.e. micro-modeling and macro-modeling. For micro-modeling of masonry-infilled frames, both the surrounding frame and the infill wall component details are established using a numerical methods such as finite element method (FEM) or discrete element method (DEM). In these methods, the interaction between masonry blocks along the joints as well as the frame-infill interaction is taken into account. Some of the developed nonlinear models, insisting on high accuracy and precision, are so time consuming that can not be used for practical purposes such as the analysis of multistory, multibay framed structures in design offices. This method is usually applicable only in research purposes. In order to analyze the behavior of actual masonry-infilled frames, another methodology, i.e. macro-modeling strategy is usually addressed. In this method, the masonry infill wall is replaced by an equivalent system requiring less computational time and effort. According to this model, an equivalent pin-jointed diagonal strut is a substitute for the infill panel. The equivalent width of the strut depends on the relative infill-frame stiffness. In the literature, a number of macro-models have

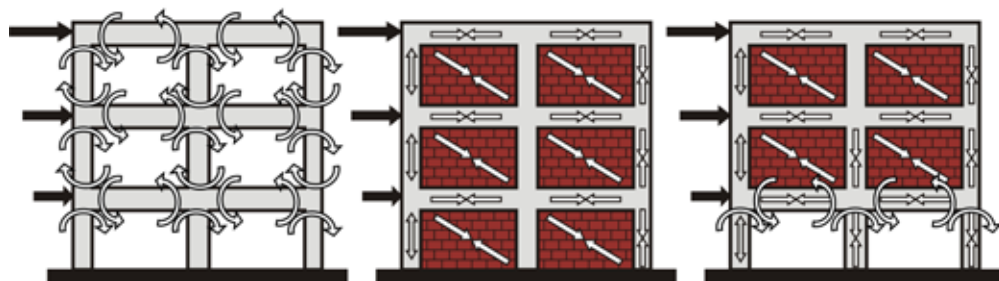


Figure 4. Influence of masonry infill in the change of the lateral load transfer mechanism, a) bare frame, b) fully infill frame, c) masonry infill frame with open first storey

been proposed by other researchers. The disadvantage of these models is that, the properties of each model must be chosen in such a way to match the experimental or numerical findings. In other words, some experimental tests or sophisticated numerical analyses have to be done prior to use of these macro-models.

According to FEMA 356, the calculation of masonry infill in-plane stiffness and strength is based on nonlinear finite element analysis of a composite frame substructure with infill panels that account for the presence of openings and post-yield cracking of masonry. Calculation of stiffness and bearing capacity of masonry infill loaded in plane can be done with the nonlinear model based on finite element method. Alternatively, the elastic in-plane stiffness of a solid unreinforced masonry infill panel prior to cracking can be represented with an equivalent diagonal compression strut with reduced width, and with the same thickness and modulus of elasticity as the infill panel it represents.

4. SOIL-STRUCTURE INTERACTION

Soil-structure interaction can have a significant effect on both structural response and load distribution among structural elements. Soil deformability, represented by appropriate soil springs, can provide significant reduction and/or redistribution of seismic forces in a structure. Vertical soil springs may effectively lengthen the fundamental period of free structural vibration, and could have a beneficial effect for buildings at relatively stiff soil sites. Rotational soil springs at single column footings will tend to relieve the fixed end moment at the column base, and cause redistribution of seismic forces in the structure. Although these effects are recognized in Eurocode 8, like in previous cases, recommendations can not be found for calculation of equivalent spring stiffness characteristics.

Soil spring stiffness or sub-grade reaction modules in vertical direction can be calculated from the condition for equal settlement. This

approach assumes that soil pressure applied at a point of the soil-structure interfaces causes an absolute displacement of that point which is proportional to soil pressure and soil stiffness, $p = k_s \cdot y_s$. In general case spring stiffness depends on several factors such as: modulus of compression of the soil, structural stiffness, the depth of the active area, contact pressure, the type and size of the foundation, etc.

In accordance with the recommendations given in FEMA 356, for shallow bearing footings that are rigid with respect to the supporting soil, single foundation can be modelled explicitly with uncoupled spring model in all six degrees of freedom. In this recommendation it is assumed that foundation soils are not susceptible to significant strength loss due to earthquake loading. In general, soils have considerable ductility unless they degrade significantly in stiffness and strength under cyclic loading. Calculation of stiffness parameters for rigid foundation is adapted with two step calculation process. First, the stiffness terms are calculated for a foundation at the surface. Then, an embedment correction factor is calculated for each stiffness term. The stiffness of the embedded foundation is the product of these two terms. For calculation of the transverse stiffness of the foundation, the influence of three components is taken into account: base friction, side shear resistance and soil passive resistance. In the case of beam on elastic foundation it is known that at the ends of the beam stress concentrations are occurring that, as the order size, can be about 10 times larger than the stresses in the middle of the beam. For these reasons, in modelling of beams on elastic foundation in the literature can be found recommendations where the stiffness of line springs at the both end zones of the beam are about 10 times greater than the stiffness of springs in beam middle zone.

5. COMPARATIVE CASE STUDY

In order to investigate the influence of different parameters to earthquake structural response,

a comparative: modal, spectral and nonlinear static push-over analysis of a 5 story 3 bay RC plane frame was analyzed for 6 parameter variations.

5.1. Description of Models

In the first model (M1), a referent structural model, gross sections for all beam and column elements of a pure RC fixed frame, without masonry infill, were assumed. The second model (M2) differs from the first due to element's reduced stiffness. Reduction coefficients are calculated based on preliminary analysis of nonlinear behaviour of cross sections. Values of 0.3 for all beam and 0.5 for all column elements were adopted for flexural stiffness reduction factor. Shear stiffness was reduced with the factor of reduction equal to 0.4 for all elements. The third structural model (M3) is the referent one with frame infilled with ceramic blocks. Layered shell nonlinear finite elements with constant thickness were assumed for modelling of infill. In this model every infill panel was modelled with one four node shell element connected to beam column joints. For the infill material characteristics values of 3000 MPa for modulus of elasticity and 0.5MPa for compression strength in the diagonal direction (at an angle of 36 degrees to brick mortar joints) were assumed. All masonry infills, included in the model, are with constant thickness of 20 cm. The forth model (M4) is the referent one with elastic supports. Each spring's stiffness is calculated as for an embedment rigid footing according to recommendations given in FEMA 356. Values of 30000 kPa for modulus of deformability and 8500 kPa for shear modulus were assumed. These characteristics are corresponding to soil classified as dense or medium dense sand and gravel, ground type C according to Eurocode 8. For adopted dimensions of rectangular footing 1.5/2.0m, depth of foundation 1.0 m, and height of effective sidewall contact equal to 0.5 m, the independent spring stiffness characteristics for translation along horizontal and

vertical axes $k_x=90000\text{ kN/m}$, $k_z=70000\text{ kN/m}$, and for rotation about y axes $k_{yy}=95000\text{ kN/m}$ were calculated. In the nonlinear analysis all springs behave linear-elastic. The fifth analyzed model (M5) is without masonry infill but with reduced element stiffness and elastically supported, combination of models M2 and M4. Practically, this model is the most flexible of all the models. In the sixth model (M6), all previously mentioned parameters are included: element stiffness reduction, masonry infill and deformability of foundation.

Analyzed structure is 5 storey 3 bays frame with bay span of 4.0 m and storey height of 3.0 m. The total generated mass is 260t, approximately 51.9t per storey. For the modulus of elasticity of concrete is adopted value of 31500MPa. The determination of design seismic force is done according to recommendation of EC8, using a lateral force method of analysis with correction factor $\lambda=0.85$. Design spectrum ordinate is determinate for Type 1 response spectrum, category of soil C, design acceleration of 0.3g and behaviour factor $q=5.85$, calculated as for the structure with high ductility class. Nonlinear characteristics of cross sections are determinate for the reinforcement ratio $p=1\%$ for columns and for required reinforcement according to principals of capacity design in the beams. For pushover analysis all models have the same nonlinear characteristics for all reinforced concrete elements.

5.2. Modal analysis and design spectrum ordinates

Results from modal analysis show significant influence of modelling parameters in changing the structural vibration period which is reflected consequently in changes of design spectrum ordinates, design seismic forces and determined displacements. Vibration periods of the first five mode shapes for all models as well as the ratios T_{M_i}/T_{M_1} are given in table 5.1.

Obtained deviations are most pronounced at fundamental modes and are within the limits

Table 5.1. Modal periods for all analyzed models

	M1	M2	T_{M2}/T_{M1}	M3	T_{M3}/T_{M1}	M4	T_{M4}/T_{M1}	M5	T_{M5}/T_{M1}	M6	T_{M6}/T_{M1}
	Period	Period									
Mode	Sec	Sec									
1	0.538	0.876	1.63	0.178	0.33	0.722	1.34	1.008	1.87	0.502	0.93
2	0.186	0.295	1.59	0.062	0.33	0.219	1.18	0.320	1.73	0.108	0.58
3	0.107	0.163	1.52	0.038	0.35	0.139	1.30	0.175	1.63	0.052	0.48
4	0.071	0.104	1.47	0.033	0.47	0.117	1.65	0.117	1.66	0.040	0.56
5	0.053	0.076	1.44	0.025	0.47	0.070	1.32	0.086	1.64	0.027	0.51

from 0.33 to 1.87 compared to the fundamental period of reference model. According to this, the stiffer model M3 imposes a request for almost twice bigger design spectrum ordinate and seismic design force compared with most flexible model M5, Fig. 5, Table 5.2.

5.3. Displacement analysis

Analysis of calculated displacements from different mathematical models shows large difference of obtained results. The most flexible model M5 has the largest absolute displacements. Its top story displacement is two times bigger than the displacement of reference model M1, or almost 18 times bigger than the displacement of the stiffest model M3. On the other side it has to be mentioned that displacements of the model M5 are calculated for almost 2 times smaller seismic force than the force of the reference model. Similar trend in differences of obtained displacements can be noticed when the relative interstory drifts are compared, Fig.6.

5.4. Pushover analysis

Pushover analysis is a non-linear static analysis taking into consideration constant gravity loads and monotonically increasing horizontal loads. It may be applied to verify or revise the overstrength ratio values or to estimate the expected plastic mechanisms and the distribution of damage along the building. In the current analysis a triangular distribution of lateral loads was applied. Obtained results, Table 5.2, Fig.7, 8, show the differences in the calculated yielding displacement (d_y), ultimate displacement (d_u), force at formation of first plastic hinge (F_y) and force of formation of global plastic mechanism (F_u), even, the structural model have the same designed reinforced concrete sections.

From the presented results it can be concluded that displacement ductility and overstrength factor strongly depend from adopted assumptions in the modelling process. The main reason for this is the redistribution of internal forces

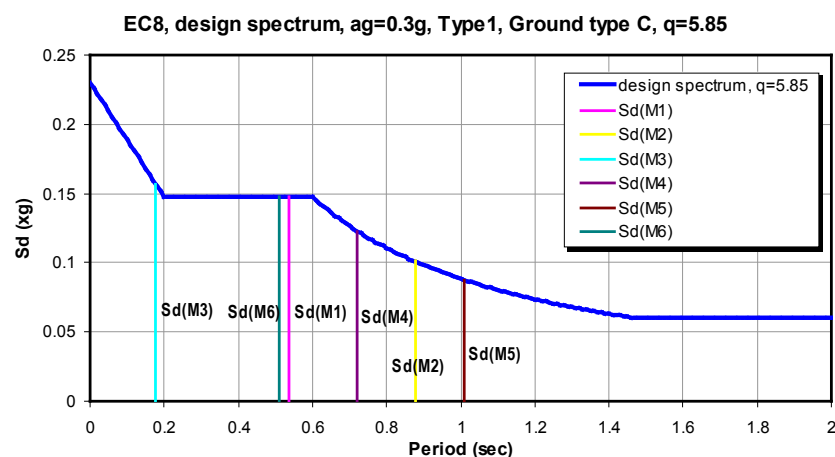


Figure 5. Influence of fundamental period on design spectrum ordinate

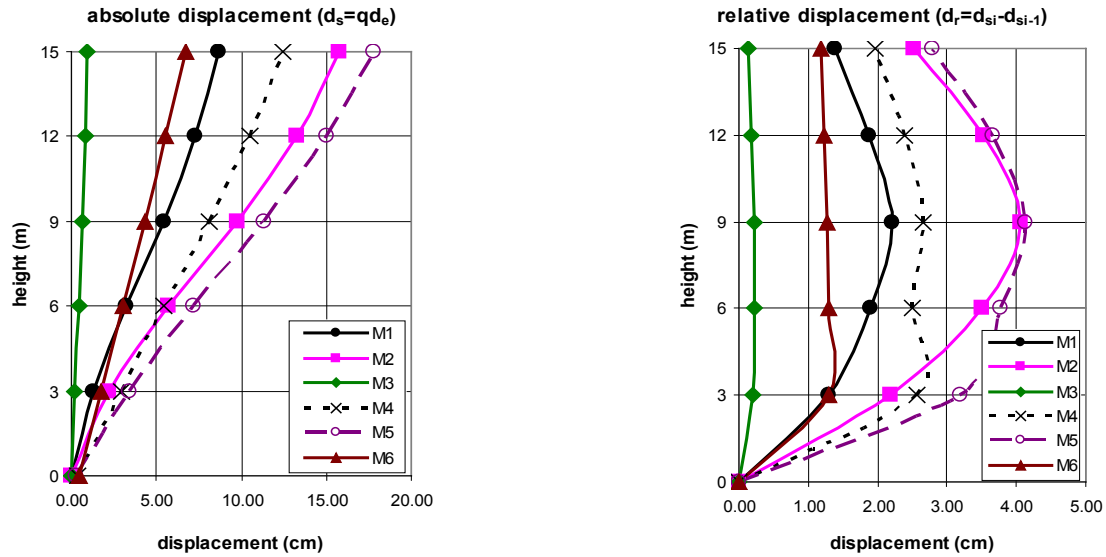


Figure 6. Calculated joint displacements, absolute and relative

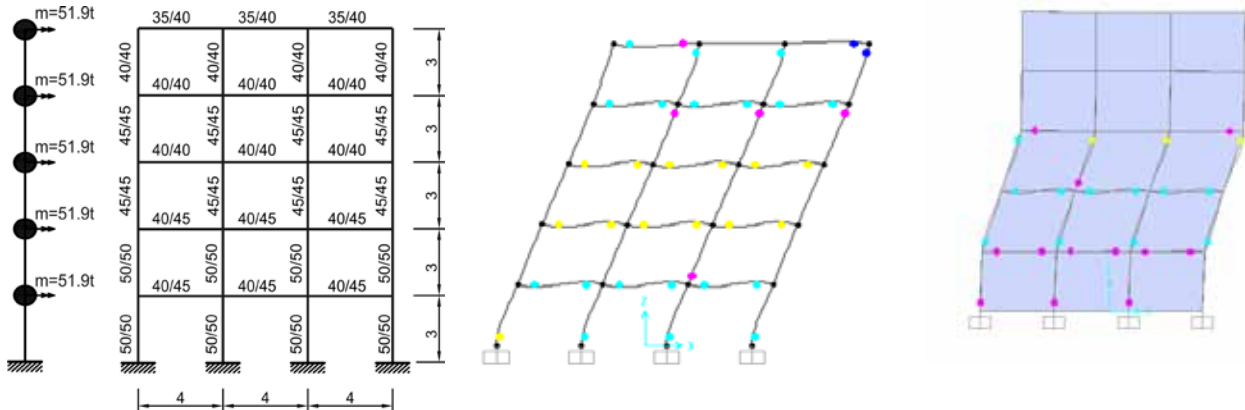


Figure 7. Structure view and global plastic mechanism for models M1 and M3

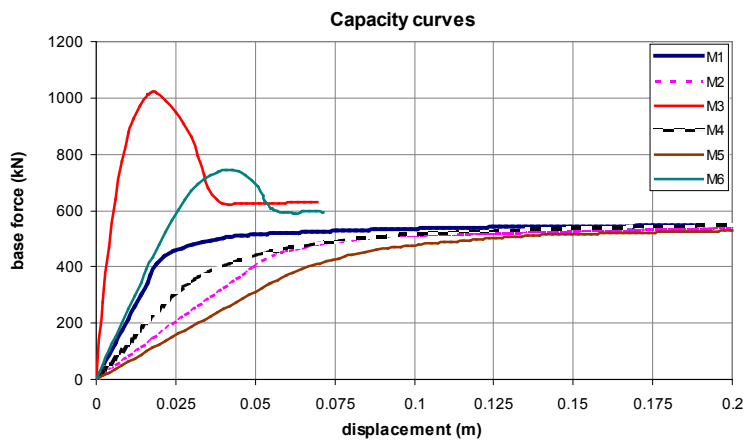


Figure 8. Capacity curves for different models

in structural cross-sections due to changes of the horizontal stiffness. For example, the force at formation of the first plastic hinge in the model with included foundation deformabil-

ity is 1.55 times smaller than the force in the reference model. On the other hand this model shows the largest overstrength factor corresponding to similar force for formation of glo-

Table 5.2. Modal periods, design forces, displacement and pushover analysis results

model	T ₁	Sd (T ₁)	F _b	d _{s_max}	d _{r_max}	d _y	F _y	d _u	F _u	F _y /F _b	F _u /F _b	α_1/α_u	d _u /d _y
	sec	%g	kN	cm	cm	cm	kN	cm	kN	/	/	/	/
M1	0.538	0.147	318.8	8.67	2.20	1.72	370.2	27.62	560.9	1.16	1.76	1.52	16.09
M2	0.876	0.101	218.3	15.80	4.05	4.92	397.7	31.26	553.0	1.82	2.53	1.39	6.36
M3	0.178	0.157	338.4	0.97	0.22	1.17	928.5	3.95	1020.8	2.74	3.02	1.10	3.38
M4	0.722	0.123	264.9	12.45	2.66	1.91	238.3	29.58	558.2	0.90	2.11	2.34	15.50
M5	1.008	0.088	189.8	17.80	4.13	4.99	311.8	32.34	545.5	1.64	2.87	1.75	6.48
M6	0.502	0.147	318.8	6.74	1.29	5.26	651.7	7.24	597.5	2.04	1.87	0.92	1.38

bal plastic mechanisms for these two models. Overstrength factor equal to 0.92 for model M6 means that the force for formation of the first plastic hinge in this model is smaller than the maximum obtained force which occurred before the first concrete element started to yield. Dropping of this force is due to the collapse of masonry infill in the second and third story of the structure.

6. FINAL REMARKS

The presented analysis results show major influence of effective stiffness, masonry infill and

foundation flexibility in changing the structural vibration period which is reflected consequently in changes of: design seismic force, determined displacements and calculated ductility and overstrength factor of the structure under consideration.

Seismic analysis is equation with many unknowns whose elimination can be successfully done with synergy of conceptual design, in-depth analysis of the necessary parameters and properly designed structural details.

REFERENCES

- European Committee of Standardization, (2004) EUROCODE 8: Design of Structures for Earthquake Resistance—Part 1: General Rules, Seismic Actions and Rules for Buildings, EN 1998-1:2004: E.
- Federal Emergency Management Agency (FEMA), (2000) Prestandard and Commentary for the Seismic Rehabilitation of Buildings, FEMA 356., CA, USA.
- American Society of Civil Engineers (ASCE), (2007) Update to ASCE/SEI 41 Concrete Provisions.



HAVE WE FORGOTTEN SKOPJE 1963 EARTHQUAKE?

G. Markovski

*Faculty of Civil Engineering,
Skopje, R. Macedonia*

ABSTRACT

26 th July, year 1963, 5:17 am. Fatal earthquake in Skopje.. Over 1000 casualties. A lot of collapsed and damaged structures.

This natural disaster initiated intensive development in the area of seismology and earthquake engineering. There was investment in education of experts at the USA and Japan respectable centers. The educational programs were changed, new contemporary codes were brought. The quality of the structures became much better. Only thirty years after, with the beginning of the society transition process, we started to forget the 1963 earthquake. The aggressive race for bigger profit has introduced many anomalies which have resulted in worse construction. The so called "urban mafia" has put the process under own control: ordered urbanization, space abuse, speculative design, revision and supervision, trade with poor quality materials.

The Macedonian authorities and especially the experts have to make an effort for elimination of these deviant activities as soon as possible.

Keywords: Skopje earthquake, "urban mafia"

1. THE EARTHQUAKE

26th July 1963 5:17 A catastrophic earthquake struck Skopje, the capital of the Republic of Macedonia. One of the strongest in Europe in the 20th century. The hot summer morning turns into hell. Over 1000 deaths and even more injured. Many collapsed and damaged structures. Family tragedies, destroyed homes, ended dreams. This tragic event was deeply impressed in the minds of the Macedonian citizens and beyond. It grew into a lasting time referent point for time location of events.

Skopje becomes a city of world solidarity. An example of humanitarian breaking of the still not hardened Berlin wall. Under the auspices of UN, the most eminent world city planners, architects and engineers participated in the reconstruction of the ruined city and founded the basis for its future development. The catastro-

phe was a turning point in the mode of design and construction of structures. It initiated intensive development of science in the field of seismology and seismic design. Investments were made in training of professional staff in renowned centres in the USA and Japan. The



Figure 1.1. Railroad Station After Earthquake

curricula of the Civil Engineering faculty were upgraded and the Institute of Earthquake Engineering and Engineering Seismology was established within the SS Cyril and Methodius University. New, modern codes for design of structures were passed. Macedonia became leader in this field not only within the frames of former Yugoslavia but even beyond. The quality of construction became increasingly better. The lesson was learned.

But not for long. Only thirty years after the earthquake, with the beginning of the process of social transition, we started to forget the disasters arising from poor quality construction. Many of the established procedures in the construction process were irretrievably distorted. The unscrupulous aspirations to bigger profits resulted in many anomalies frequently leading to poor quality of construction. The so called urban-construction mafia, led by their own interests, took the procedures in their own hands and as a powerful tsunami, they ruined the painstakingly built system. The wrong and ordered urbanization, violation of space, speculative design and revision, incorporation of materials of questionable quality, construction without professional supervision etc. are only some of the elements of the newly built system. The slow updating of the regulations in the field of design and construction was in favour to these negative phenomena. The quality of construction started to deteriorate.

There is no science in this paper. There are no finite elements, accelerations, periods, push over analyses. This paper contains another kind of analysis, analysis of reality, analysis of the reasons which, in the country with too long social-economic transition, have led to a drop in quality of construction and resulting consequences. Its main goal is to be a kind of an expert "vuvuzela" with a warning loud note that should reach the consciousness of the participants in the process of construction, a humble attempt to point to the importance of the sys-

tem procedures and their observation. Without such an approach, scientific investigations and knowledge, regardless their quality, become senseless, lartpourlartistic and without practical verification.

2. REASONS

The reasons for such a situation are multiple. Most of them are mutually conditioned and interwoven so that they can hardly be addressed according to priority.

2.1. Economic Crisis

Construction was the first to be affected by the economic crisis whose beginnings date back as early as the nineties of the last century. With the closing of several lucrative foreign markets followed by a drastic reduction of domestic investments, there came a merciless devaluation of engineers. A large number of eminent professional staff remained without engagements or with utterly humiliating low income. This caused a vertiginous drop in the valuation of design engineers' labour and falling into the maelstrom of low price leading to low quality product.

2.2. Collapse of Large Design Bureaus

Gradual collapse of high quality, well equipped design firms with long tradition of proper hierarchical order of knowledge took place followed by establishment of many new, small private, or the so called one man-firms, in which there is no team work with transfer and exchange of knowledge. Struggling for subsistence, the engineers have been forced to do different tasks, which left them no time to dedicate themselves to their profession. The young engineers, unprepared, having none to learn from, have cruelly been put into fire, so that instead of turning into design engineers, they have engaged themselves in computation of imposed structural solutions. Powerful, most frequently "pirate" software has been used for computation of structures, but without the necessary previous knowledge, training and critical review of the obtained results.

2.3. System Deconstruction – Reconstruction

The existence of a system and the observation of procedures are the main guarantors for achieving good quality. The greatest loser from the deconstruction of the existing system of realization of structures (from design to technical acceptance), whereat the decomposed constituent elements are chaotically reconstructed into a kind of a "Frankenstein" form, is the quality of the structures. Incomplete projects full of flaws that are sometimes elaborated for quite different structures are handed over, with ordered "false" revisions, construction is carried out without professional supervision, with insufficiently trained workers, with unchecked materials... The procedures are adapted to a greater "flux" but of low quality projects.

2.4. The Belated Legislation

Despite the fact that the changes of the social system and hence the changes in many essential processes in the field of construction started in the distant 1990, it was only fifteen years later that the first law on construction adapted to the new socio-economic conditions was passed in independent Macedonia. We were among the last in Europe that established the Chamber of Architects and Engineers to issue licenses to participants in construction as evidence of their competence for performance of certain activities in the

construction process. The delay of the legislative regulations created a free, unregulated milieu, whose advantages were taken by different kinds of profiteers, through their own lobby groups and for their own benefit. Urbanization became the main focus of interest of many, starting from the authorities to the investors. The quality of construction became marginal, something unimportant, something that went without saying.

2.5. Corruption

The cancer of each society. More or less present in all the spheres. It is for a longer period of time that there has been some latent corruption among part of the administration manifested by "advisory" instructing of the investors to take "the most suitable" design engineer, whose project will enable easier crossing of the labyrinth of complicated administrative procedures (see Fig. 2.1.).

2.6. Education

The education itself is one of the crucial elements of development of society. Good education is the biggest confirmation of the identity of each nation. Accordingly, in this complex process, the education of engineers is perhaps of paramount importance. The problem regarding the education of civil engineers in R. Macedonia can be analyzed from two aspects.

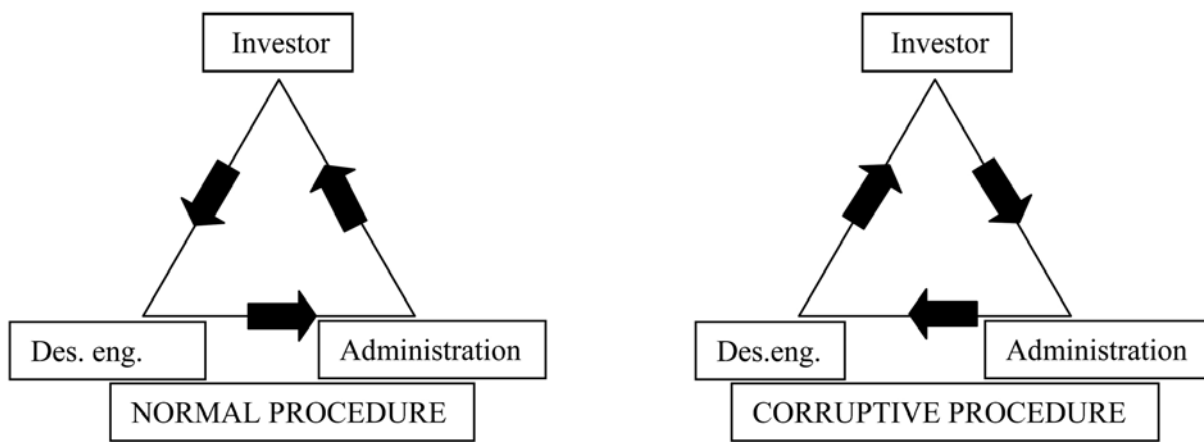


Figure 2.1. Alternative ways in design

First of all, it has been for two decades that we have been having re-direction of young people toward studying at some easier faculties bearing some eminent, exotic names. This has partially been the consequence of the echo that has been reaching these young people from the afore mentioned negative processes and has partially been due to the disturbed system of values in the society. Furthermore, the high education has become a bizarre business category, whereat the easily obtained diplomas have become a dominant indicator of the questionable quality of these faculties.

The second aspect is the life time study. Structural engineering is a serious activity that requires permanent education. There are real-life reasons for the established practice that graduation becomes the end of personal education and training instead of the real beginning. In most of the cases, the low living standard of the engineers does not allow investment in professional literature, latest software, participation in professional and scientific meetings, visit of industrial exhibitions, payment of tuition fees for master and doctoral studies and alike. Fighting for pure survival, the small firms most frequently don't have

Reality



Basic principles for the seismic design of buildings [1]

AVOID SOFT-STOREY GROUND FLOORS

Figure 3.1 Example No.1

Reality



Basic principles for the seismic design of buildings [1]

AVOID ASYMETRIC BRACING

Figure 3.2 Example No.2

Reality



Basic principles for the seismic design of buildings [1]

DISCONTINUITIES IN STIFFNESS AND RESISTANCE CAUSE PROBLEMS

Figure 3.3 Example No.3

the ability to invest in advanced training of their staff whereby acquiring of new knowledge is prevented and hence is prevented keeping pace and competitiveness with the more developed countries.

3. CONSEQUENCES

One of the consequences with potential catastrophic effects is the low quality structure. High quality structures are certainly the only guarantee for successful protection against effects, among which are those of earthquakes that have taken place and will certainly take place in Macedonia, but unfortunately, we have lately been witnesses of frequent architectonic-engineering adventures upon existing and new structures. Structures are designed and constructed with flaws in genetic code. In addition to materials of doubtful quality, incorporated in these structures are ignorance, amateurism, speculations and corruption.....

Preoccupied only with the urban aspect of construction providing big profit, we have allowed the "appearance" of a large number of the so called "unlawfully constructed engineering structures" whose existence and use represents an immediate threat for the security of the citizens. Within a short period, we have succeeded



Figure 3.4 Example No.4



Figure 3.5 Example No.5



Figure 3.6 Example No.6

to endanger the established quality of design and construction. We have allowed the domination of chaos over order, ignorance over knowledge, poor quality over high quality, profit over responsibility

Presented further will be some examples of structures constructed with "classical" structural engineering errors.

4. SOLUTION

The solution of the problem is complex and, in the long run, requires corresponding activities of a large number of actors. A concept, a strategy, knowledge and persistence is necessary. Actions should be taken simultaneously in a number of directions, being at the same time aware of the fact that the results will not show immediately. Some of the possible solutions are:

4.1. New Legislative Regulations

It is urgently necessary to pass legislative regulations with prescribed far more strict criteria on obtaining and extending personal licenses for the performance of corresponding professional activities. Such stricter criteria are particularly important to be passed for the Reviewer category by which the supervision of projects will truly make sense. Such a solution will also directly lead to correction



Figure 3.7 Example No.7

Basic principles for the seismic design of buildings [1]

AVOID PARTIALLY INFILLED FRAMES



Figure 3.8 Example No.8

Basic principles for the seismic design of buildings [1]

SEPARATE ADJACENT BUILDINGS BY JOINTS



Figure 3.9 Example No.9

Basic principles for the seismic design of buildings [1]

FAVOUR COMPACT PLAN CONFIGURATIONS

of the destructively low prices of design. At the same time, in cooperation with the insurance companies, insurance against damage done to third persons should be introduced and practiced whereby the attitude of all the participants in construction will come far more responsible.

4.2. Regulated Minimal Prices

Considering the fact that a regulated profession with extraordinarily high social responsibility is at stake, it is necessary that the Chamber passes a Schedule of Rates by which it will define the minimal prices of engineering services and will find out ways for its observation. In this way, the continuous reduction of quality through the endless spiral of poor quality will be prevented..

4.3. Professional Administration

The central and local administration should employ structural engineers in the corresponding administration organs. This will enable control over the design documentation from structural engineering aspect, as well, preventing thus its further trivialization in respect to the urban and architectonic aspects of design.

REFERENCES

Hugo Bachman. (2003), Seismic Conceptual Design of Buildings – Basic principles for engineers, architects, building owners and authorities, Swiss Federal Office for Water and Geology; Swiss Agency for Development and Cooperation

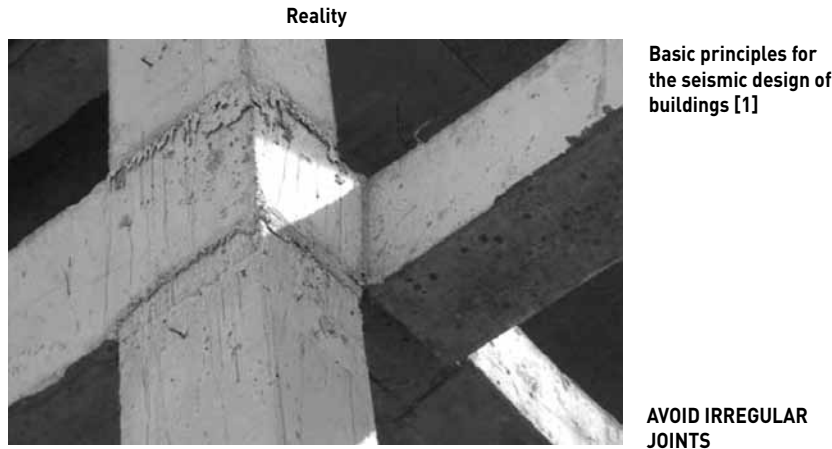


Figure 3.10 Example No.10

4.4. Life time learning

It is necessary to build a system of life time learning that will enable permanent advanced training of professional staff, keeping pace with the latest professional and scientific achievements, education in respect to the new technical regulations (as for example the Eurocodes) and alike. To this end, the main role should be played by the Chamber, the University and the professional associations. Such a system of permanent education will also represent a kind of a filter to distinguish between quality and poor quality.

However, quality cannot be achieved overnight. This particularly refers to a qualified structural engineer. This is a long term process in which each discontinuity, particularly in acquiring new knowledge, may have an utterly unfavourable effect.

5. LESSON LEARNT

Structural engineering is a studious activity. One of the most studious. It is an activity that requires permanent education, high responsibility, wide spectrum of profound knowledge and, first of all, well built system that will guarantee proper application of acquired knowledge in practice, i.e., in real life. In this activity, the improvisations and flaws in the procedures, whatever the level, are not allowed and could lead to unforeseeable consequences.

The errors made in the past must not be done again. Therefore, we must not forget the Skopje earthquake.



EARTHQUAKE-INDUCED LANDSLIDES - GIS METHODOLOGY FOR ZONATION

J. Cvetanovska & V. Sesov

*Institute of Earthquake Engineering
and Engineering Seismology,
Macedonia*

ABSTRACT

The numerous historic data and results from investigations on the earthquake effects during the last decades show that site conditions play the major role in establishing the earthquake damage potential. Landslides and liquefaction, as direct seismic effects, are causing some pattern of soil failure, often found as the most destructive one. In fact, damage from triggered landslides has sometimes exceeded damage directly related to strong shaking and fault rupture [Jibson et al., 2000]. The subject of this research study is analysis and zoning of the geographical distribution of landslide hazards, as one of the most characteristic forms of geotechnical instabilities occurring during earthquakes. For this purpose, a detailed GIS procedure for analysis and zoning of the landslide potential in seismic conditions has been carried out. The investigation has been focused for the selected area of sub-urban parts of Skopje, capital city of Macedonia. The documentation on the selected area necessary for analysis of the landslide hazard have been digitized, geo-referenced and analyzed in GIS environment. The final product is represented by digital maps of expected permanent displacements for a defined earthquake scenario, in different water-saturation conditions of the unstable soil layer. Results from this study, such as the potentially affected population and infrastructure, can be used as a data base for preventive mitigation activities for reducing the consequences of the geotechnical seismic associated hazards in urban areas.

Keywords: microzonation, landslide, earthquakes, GIS

1. INTRODUCTION

The consequences of increased urbanization of inhabited places are quite evident worldwide. With their expansive development, mega cities,

although being a central point of national and regional economic development, are becoming increasingly susceptible to risks pertaining to natural catastrophes. This is due to the spatial expansion of the populated places in hazardous areas, Fig. 1.

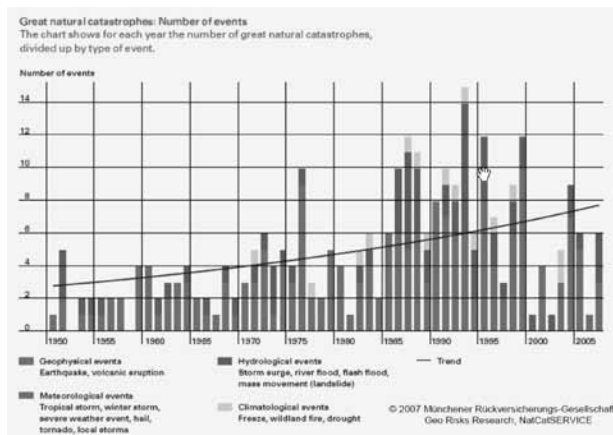


Figure 1. Increasing trend of occurrence of natural hazards

(Munich Re Group-Geo Risk Research, 2007)

In the course of the 1990-ties, almost two billion people were struck by natural catastrophes as are earthquakes, floods, forest fires, tropical storms, landslides and volcanic eruptions (UNCHR, 2001). A major part of loss of human lives and material loss was due to landslides. For example, in the last century in Italy, 180000 landslides were recorded. Out of these, several hundreds are potentially active and around 5000

urban regions are struck by local instabilities of slopes (CNR - National Group for Geo-hydrological Disaster Prevention). The most frequent causes of slope disturbance are other initial factors: climatic changes, earthquakes, volcanic eruptions as well as the human factor. Given the above, it is not surprising that landslides as geo-hazards are becoming the main focus of investigation of a number of investigators, engineers and urban planners worldwide.

Thanks to the recently developed technology, first of all, the "remote sensing" techniques (fast acquisition of data on given areas via satellite) and geographic-information systems (efficient collection, systematization, elaboration and analysis of georeferenced data), high quality management of geo-hazards and risks pertaining to landslides becomes feasible. Geographic Information Systems are becoming a standard tool in management and dealing with risk related to natural phenomena. Burrough(1986) and Aronoff (1989) give introduction to the principals of GIS and its opportunities. With the development of several powerful set of tools such as Arc/Info (Enviromental Systems Research Institute 1992), Integraph Corporation's MGE (Integraph Corporation 1993), IDRISI (Eastman 1992a, 1992b), ILWIS (ITC-Netherlands), application of GIS into management of natural and technological risks, significantly has increased. When it comes to geotechnical instabilities, particulary landslides, Carrara(1978), C.J. Van Westen (1993) , Brass(1989), Murphy and Vita-Finzi (1991) applied different approaches and criteria for analysis and zonation of landslide hazard and risk usingGIS methodology.

The occurrence of slope instability generally depends on the complex interactions among a number of interrelated factors. Therefore, an interactive and integrated procedure – methodology for assessment of potential terrain instabilities is necessary. The practical and fast updating of different parameters of a given model, the combination of functions of data from a

number of maps among which there is also a digital model of the terrain, the possibilities for visualization of data by means of graphic characteristics are only part of the possibilities offered by the geographic-information systems in managing the risks pertaining to natural phenomena.

2. OBJECTIVES OF STUDY

This study focus on advantages of geographic-informational systems in the process of definition of the potential geotechnical instabilities, more precisely landslides as secondary seismic hazard in earthquake prone regions. In literature, as well in practice, exist and are applied methodologies and approaches for zoning of potential landslides. Some of these have already been incorporated in the national regulations, positive example is Switzerland, ("Management of Risk Pertaining to Landslides in Switzerland")

The main objective of the investigations performed within this research is analysis, distribution and zoning of potential landslides and instable slopes in earthquake conditions in order to define the risk related to occurrence of this type of hazards for the population and the infrastructure. According to the general GIS-based procedure for zoning of landslide potential in earthquake conditions after Jibson 1998 , a modulus for computation of the safety factor based on pixels, critical acceleration and permanent displacements according to Newmark has been incorporated in GIS. The final product is presented by digital maps of expected permanent displacements for a defined earthquake scenario combined with different water-saturation conditions of the instable soil layer. Detailed deterministic zoning of expected permanent displacements in earthquake conditions has been performed. Keefer (1985) has applied this methodology for the city of Berkeley, California.

The GIS methodology approach introduced by Jibson, elaborated and explained in further text, has been applied on a selected region



Figure 2. Damage to the Skopje – Sopishte local road due to landslide a) and b); Landslide at Sava Kovacevic Str., Pripor resulting in failure of retaining wall preventing the normal functioning of the street c).

on the south-east sub-urban parts of Skopje, where local soil instabilities have been registered lately. The working area is square proportioned 5 km x 5 km within the coordinates 7533000 to 7538000 metres, from west to east. In order to make a deterministic zoning of the landslide hazard, i.e., to create the necessary data base and documentation in GIS, there have been collected data from a number of reports, geotechnical reports, main and working designs on repair of already occurred instabilities in this area elaborated by IZIIS and other companies dealing with geotechnical field investigations and measurements. All the documentation on the selected area necessary for analysis of the landslide hazard have been digitized, georeferenced and analyzed by use of the GIS software Arcview 9.3.

Skopje, as the capital of the Republic of Macedonia covering 1,854 km², with a population of 700 000 citizens (density of population of 273 citizens/km²), represents a central point of concentration of the most important material and human resources.

The intensive development of the city of Skopje, especially after the 1963 earthquake, as the main centre of human and material resources in Republic of Macedonia is one of the key prerequisites for the increase of the risk related to natural disasters. Namely, the built structures on steep terrains and the concentration of population and material property on potentially unstable locations considerably

increases the risk pertaining to geotechnical hazards. In addition to the seismic activity of the territory of Macedonia which can be one of the main triggering factors of loss of stability of slopes are: uncontrolled creation of landfills (that have lately created steep slopes that are potentially unstable), construction activities that don't follow technical regulations and standards (cuttings, vertical excavation, etc.), intensive cutting and destruction of the forests and the vegetation on the terrain (contributing to occurrence of erosion and instability of the surface soil layers), improper management of outflows, channels (increase of the underground water table that causes reduction of the effective strength of soil materials), etc.

The geological structures have changed through the years due to the seismic tectonic activity, particularly after the catastrophic Skopje earthquake of 1963. Generally, the city of Skopje is susceptible to processes of desertification. The climatic changes contribute to the aggravation of the situation, ie.:

- Prolongation of draught periods;
- Decrease of the vegetation cover;
- Increase of torrential rains;
- Increase of the risk of occurrence of wild fires;
- Increase of soil erosion;
- Increase of occurrence of floods.

Presented below are some of recent registered instabilities caused by the above stated factors, which were the main reason for this research, Fig. 2:



a)



b)

Figure 3. Occurrence of large deformations in the lower part of the landslide in municipality of Rakotintsi a); Occurrence of a vertical crack in a wall of an individual house b)

Among the recent recorded landslides is the landslide in the municipality of Rakotinci village that took place in 2005 causing serious damage to 45 family houses, Fig.3.

3. METHODOLOGY

The sequential steps of seismic landslides hazard zonation, involved in the GIS based procedure introduced by Jibson and others (1998) applied on a study area of suburban parts of Skopje, is presented on figure 4. To develop the model for deterministic zoning of landslides triggered by earthquakes, Jibson used the large set of available data on the Northridge 1994 earthquake. By combining this data based on analysis of permanent displacement according to the Newmark model (1965), the potential landslide was modeled as a block placed on an inclined plane under an angle α . Wilson and Keefer (1983) showed that using Newmark's method to model the dynamic behavior of landslides on natural slopes yields reasonable and useful results. Wieczorek and others (1985) subsequently produced an experimental map showing seismic landslide susceptibility in San Mateo County, California, using classification criteria based on Newmark's method. Wilson and Keefer (1985) also used Newmark's method as a basis for a broad regional assessment of seismic slope stability in the Los Angeles, California, area.

The block has its own critical acceleration, which needs to exceed the sliding resistance of the material in order to cause motion of the soil mass – the block. The result is displacement of the terrain at each pixel caused by the Northridge earthquake. Being already calibrated with the Northridge earthquake, this model can be used in any other earthquake scenario. Digital maps can be easily upgraded, revised, amended by newly acquired data and used for analysis of other scenarios of concern.

Following this procedure, deterministic zoning has been applied for part of the study area of Skopje, on the southeast side of Vodno, with a focus on the region along the road from Kisela Voda municipality to Rakotintsi village and the surrounding populated areas. The steps introduced in the zoning model are presented, as follows:

A) Computation of the static safety factor

From the digital terrain model the slope map of the terrain, (Fig. 5) was created at first. Next, using data from geotechnical in-situ and laboratory investigations, from the geology map (Fig. 6) the raster maps of effective cohesion c' , material unit weight γ and effective internal friction angle ϕ' are created. 'Raster calculator' is one of the crucial tools

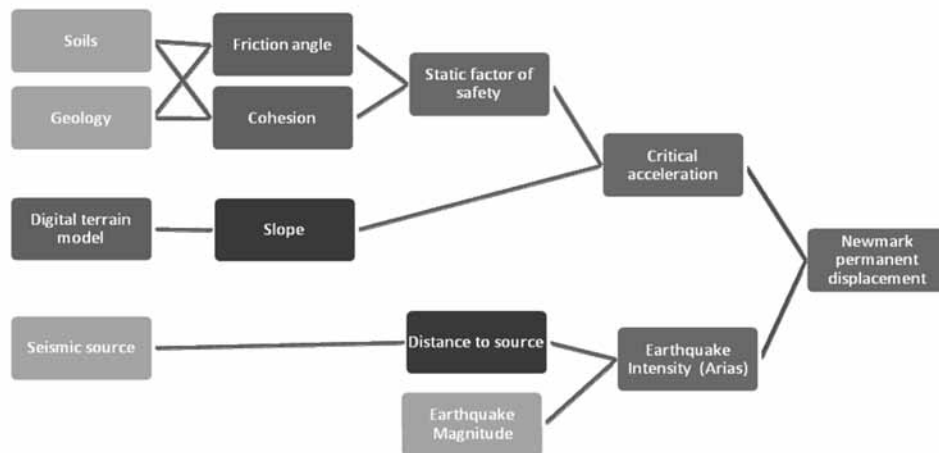


Figure 4. Flow chart of the procedure for landslides zoning

for spatial analysis in Arcview 9.3. It provides pixel based calculation, and creation of digital maps which contain information in raster format, a value of parameter in every single pixel.

Pixel based computation of the safety factor (Fig. 8), for 3 different scenarios of ground water saturation, with incorporation of the already defined raster maps in the module – formula in GIS (3.1) is done. The following scenarios have been defined:

Period with relatively low intensity of rains, i.e., natural dry conditions ($m = 0$);

Period of moderate intensity of rains or snow melting i.e., conditions of relatively intensive precipitation ($m = 0.5$);

Period of complete water saturation ($m = 1$) of the unstable soil layer, scenario with the greatest potential for occurrence of instabilities.

$$F = \frac{c' + (\gamma - m \gamma_w) z \cos^2 \beta \tan \phi}{\gamma z \sin \beta \cos \beta} \quad (3.1)$$

Table 1 presents the psychical meaning of the parameters and their implementation in digitalized maps in GIS.

B) Computation of the critical acceleration

Critical acceleration in fact, represents susceptibility of the geological formations to landslides triggered by earthquakes (Fig. 9). With incorporating the module for computation of critical acceleration, maps have been created with the value of critical acceleration necessary for motion of the potentially unstable soil mass for the three scenarios of water saturation. Figure 9 describes, in fact,

Table 1: Parameters incorporated as maps in GIS

Parameters	Values incorporated in GIS
c' = effective cohesion ($\text{kPa} = \text{kN/m}^2$)	map of effective cohesion
γ = material unit weight (kN/m^3).	map of material unit weight
γ_{water} = unit weight of water (kN/m^3).	10
m = (proportion of the slab thickness that is saturated).	zw/z (0-dry conditions, 0.5 -50% water saturation, 1- full saturation)
zw = height of ground water above the failure slab (m).	0; 0.5z and z
z = slope-normal thickness of the failure slab (m).	map of slope normal thickness
β = slope of terrain ($^\circ$).	map of slope developed by the DTM
ϕ' = effective internal friction angle ($^\circ$).	map of effective internal friction angle

the level of susceptibility of the terrain to landslides in earthquake conditions for 50 % water ground saturation. To obtain results, for activation of the potential landslides under a given earthquake scenario, it is needed to compare these maps with the expected accelerations for the particular study area.

$$a_c = (FS - 1)g \sin \alpha \quad (3.2)$$

Where: FS – safety factor, g = ground acceleration (m/sec^2); b - slope of terrain ($^\circ$)

C) Computation of permanent displacements - Newmark method

Using the Jibson's regression formula calibrated from twice integrated time histories of accelerations from California and amended with 555 records of 13 earthquakes, there have been created maps of permanent displacements of the study area under the three scenarios of water saturation (Fig. 11). Although the Newmark displacement represents an empirical criterion for the behavior of the slopes, still is considered as appropriate relative index of slope-performance for regional analysis (Jibson and others, 1998). It should be noted that this final map should not be used as a basis to determine the absolute risk from seismically triggered landslides at any locality, as the sole justification for zoning or rezoning any parcel, for detailed design of any lifeline, for site-specific hazard-reduction planning, or for setting or modifying insurance rates (Keefer).

$$\text{Log}D_n = 1.521\log I_a - 1.993\log a_c - 1.546 \quad (3.3)$$

Where: la – Aries intensity (m/sec); ac – critical acceleration (m/sec^2)

Arias Intensity is selected as parameter for defining the critical values that causes landslides in earthquake conditions. Jibson and Keefer (1992) used the Arias Intensity as a parameter representing the seismic poten-

tial in order to define the Newmark permanent displacement caused during the New Madrid earthquakes 1811 and 1812. For the research purposes of this study, to define the spatial distribution of Arias Intensity, the attenuation law based on historical earthquake data from California (Wilson and Keefer 1985) is used:

$$\text{Log}_{10}I_a = -4.1 + M_w - 2\text{Log}_{10}(d^2 + h^2)^{0.5} - 0.5P \quad (3.4)$$

Where: la – Arias Intensity (m/sec); Mw – Moment magnitude; d- shortest distance to hypocenter or fault source (km); h- focal depth of earthquake source (km); P- probability of exceedence

Fig. 7 represents map with registered faults so far , located near the study area , while table 2 presents the characteristics of the seismic potential of this faults The "Vodnjanski" fault is crossing directly below the study area so it is chosen as source of seismic potential in the further analysis. For that purpose, a map representing the spatial Arias Intensity of possible earthquake scenario with source in the Vodnjaski fault is created in GIS (Fig. 10).

The main limitations of the model are found in the aspect of quantity of data on earthquakes, geology, and geotechnical parameters and alike. It can be freely concluded that the applied method represents a useful tool for simple, systematic and extremely useful zoning of the hazard related to landslides in earthquake conditions. The possibility for computation of failure probability in predicting models for given locations opens many possibilities for research in the direction of establishment of new improved methodologies that can easily be incorporated in the GIS platform.

4. OUTPUTS - CREATED MAPS IN GIS PLATFORM

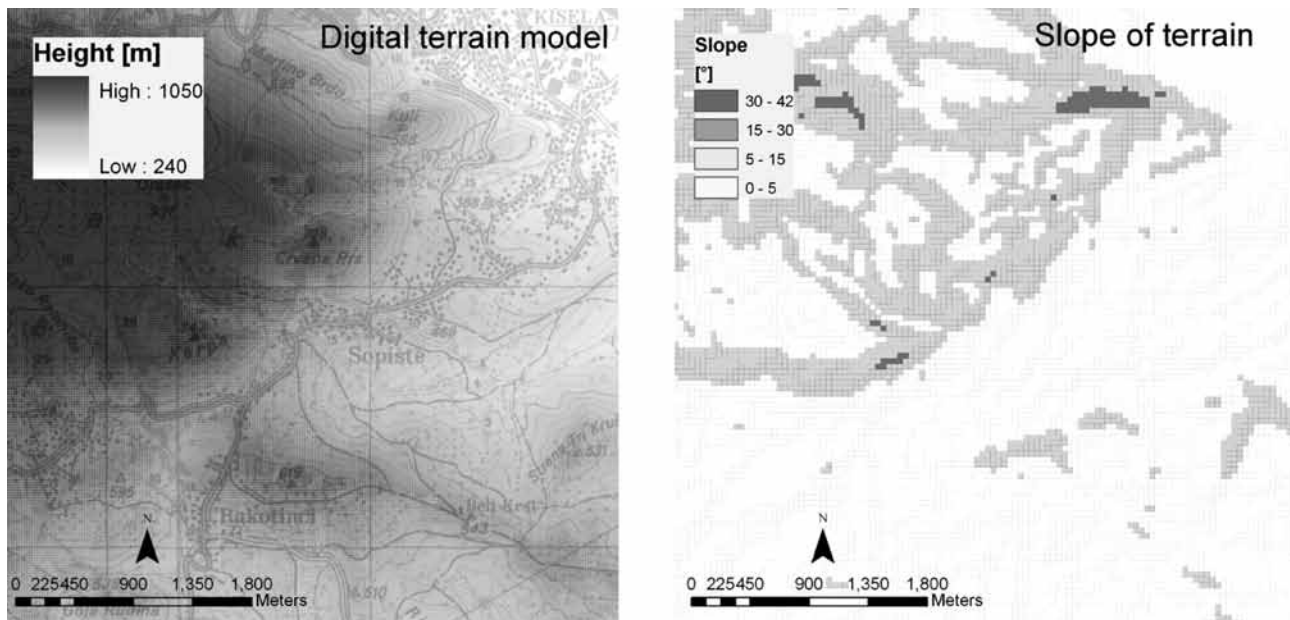


Figure 5. Digital terrain model (left) and slope map (right)

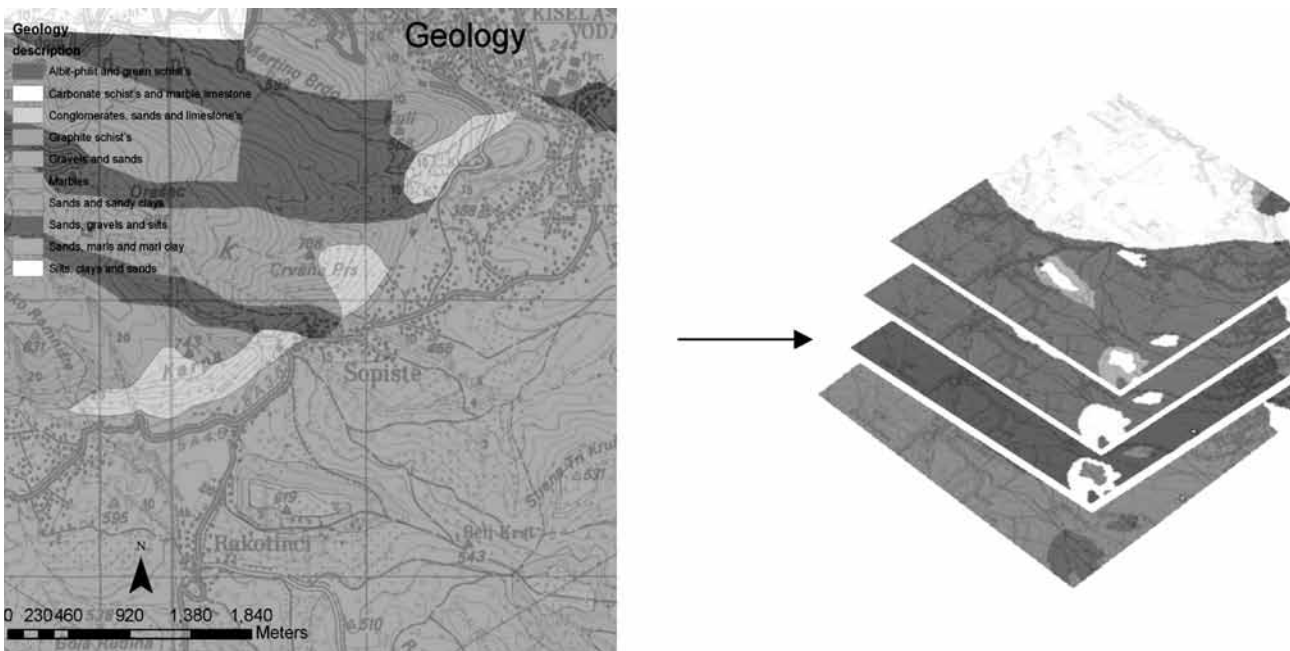


Figure 6. From the geological attribute table raster maps of soil parameters have been created (internal friction angle, material unit weight, cohesion and depth of unstable soil layer)

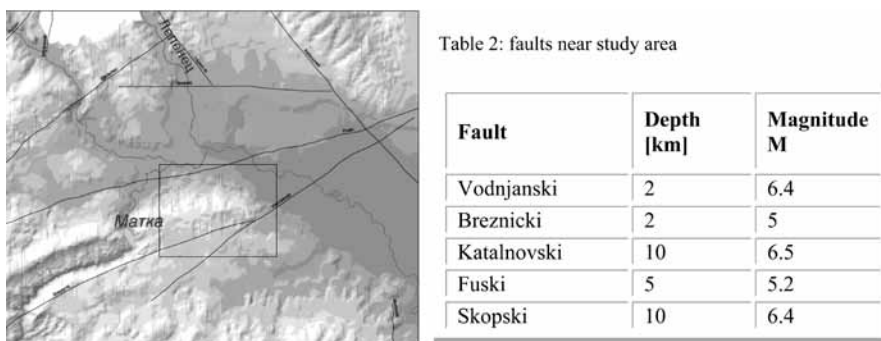


Figure 7. Fault near study area

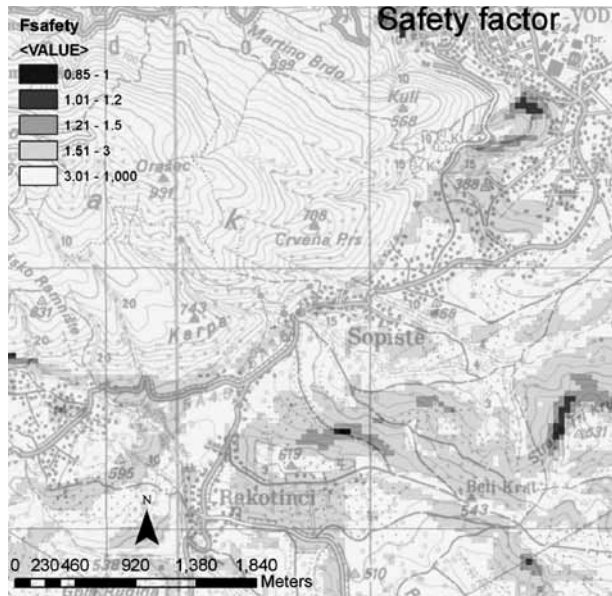


Figure 8. Computation of the safety factor for each pixel by incorporation of the already defined raster maps in the module formula in GIS for 50 % ground water saturation

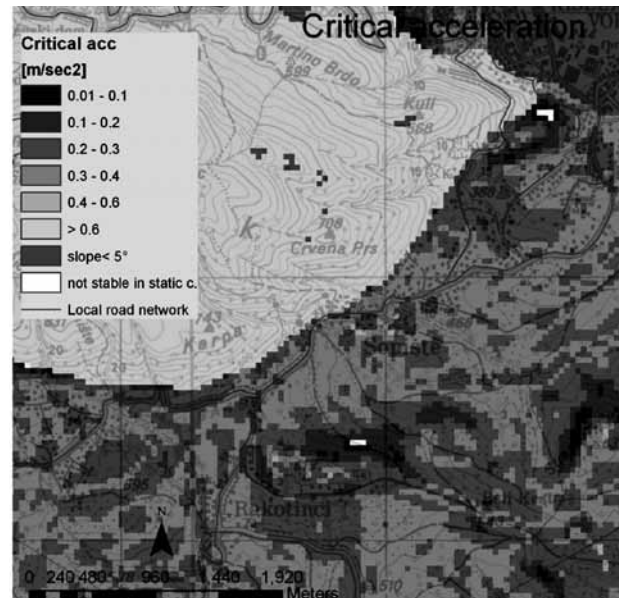


Figure 9. Critical acceleration of geological formations, susceptibility to landslides in earthquake conditions

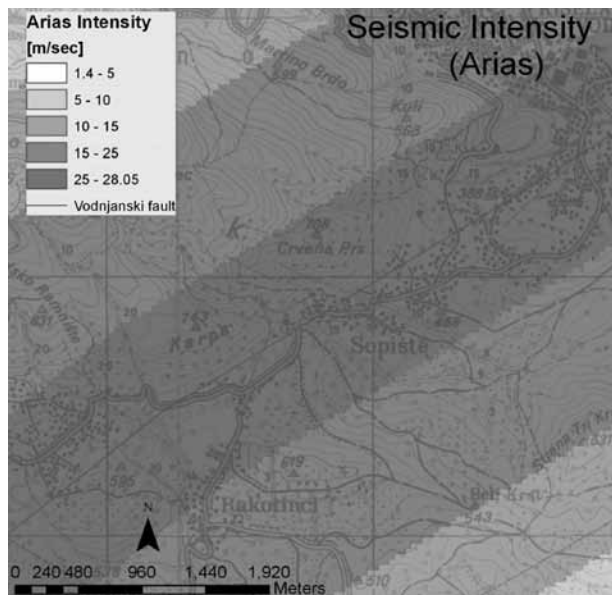


Figure 10. Seismic Arias Intensity for an earthquake scenario with source of event at Vodnjanski fault

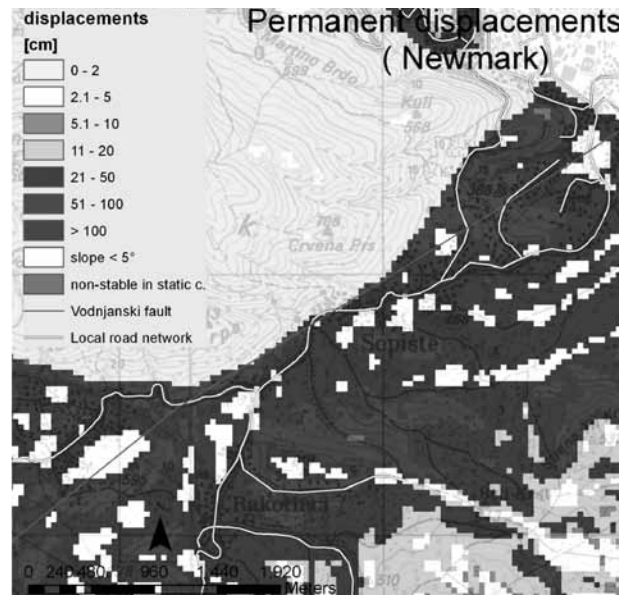


Figure 11. Permanent Newmark displacements of terrain in case of 50 % water saturation of instable soil layer and earthquake with source at Vodnjanski fault

5. CONCLUSIONS AND RECOMMENDATIONS

The elaborated approach in GIS environment was applied on a selected region for the purpose of microzoning of potential hazards related to landslides triggered by earthquakes. The selected region encompasses the southeast part of the city of Skopje including part of the slopes and the foothill of Vodno mountain. For the se-

lected target area, analysis and zoning of landslide potential in earthquake conditions was performed. The zoning of the landslide hazard was done according to two criteria as follows: regional zoning (Keefer) and detailed deterministic zoning (Jibson). Based on the results from the investigations realized within this master thesis, the following conclusions are drawn: With its universal application in analysis of spa-

tially distributed phenomena, GIS represents an excellent tool for multidisciplinary cooperation of researchers in different fields. By possessing as many as possible data from different fields and consideration of possible scenarios for given situations, a realistic insight in the situation on the stability of the terrain is obtained.

The GIS analyses have resulted with geo-referenced digital maps of the selected area showing the spatial distribution of landslide phenomena in earthquake conditions. Two criteria and pre-defined scenarios of water saturation and ground acceleration – seismic effects have been analyzed.

For the target area, it can be concluded that it has the potential for instability that, in certain scenarios, can possibly result in occurrence of economic and social losses: the individual houses located in potentially unstable zones are directly exposed to increased risk related to the destructive effects of landslides caused by earthquakes. There is one road connecting the inhabited places with the main resources in the center of the Skopje city whose burial in the case of crisis can prevent access or providing of any help to the cut area, since it is the only road connection.

It is particularly important to note that the created database for the analysis of potential instabilities of the selected target area represents an “open source” database that can be upgraded, developed and amended permanently with new additional data on: geological, geophysical field and laboratory investigations, data on intensity of precipitation (mm water column, mm snow cover), number of inhabitants, traffic load on roads, drainage channels, etc. in a fast and simple way that will enable better quality of passed decisions. Implemented methodology is very easy applicable for any other spatial analysis of hazard and risk and gives satisfactory results with relatively low cost of financial and in short time period.

ACKNOWLEDGEMENT

This research study is made in the frames of the postgraduate studies of earthquake engineering at the Institute of Earthquake Engineering and Engineering Seismology, Skopje, Macedonia. The authors are grateful to all geotechnical companies and research institutions which have contributed with sharing the geotechnical parameters database for the study area.

REFERENCES

- Randall W. Jibson, Edwin L. Harp, & John A. Michael. (1998). A Method for Producing Digital Probabilistic Seismic Landslide Hazard Maps: An Example from the Los Angeles, California, Area. *Open-File Report 98-113*
- C.L. van Westen. (1993). Application of Geographic Information systems to landslide hazard zonation.
- Transportation Research Board . Landslides Investigation and Mitigation. (1998) *Special report 247*
- Christophe Bonnard , Olivier Lateltin, Christoph Haemmig, Hugo Raetzo. (2005). Landslide risk management in Switzerland. *Landslides 2 : 313-320*, Springer-Verlag.
- Arsovski M.& Petkovski R. (1975). Neotectonics of republic of Macedonia. *IZIIS report 75-49*
- Scott B. Miles & David K. Keefer. (1985). Seismic landslide hazard for the city of Berkeley, California.



ANALYTICAL INVESTIGATIONS OF SEISMIC BEHAVIOUR OF RC FRAME BUILDINGS WITH MASONRY INFILL

R. Apostolska, G. Necevska-Cvetanovska & J. Cvetanovska

*Institute of Earthquake Engineering and Engineering Seismology (IZIIS),
"Ss.Cyril and Methodius" University, Skopje, Republic of Macedonia*

ABSTRACT

The experience from the occurred earthquakes and performed investigations show that the effect of the infill can be different – favorable (when the structural system has low resistance) and unfavorable (short column effect, shear failure of joints, global instability of the system – “soft” storey mechanism etc.). Taking into account the fact that it is a common engineering practice to neglect the infill effect in the design of structures, it is obvious that investigations for definition of the actual seismic resistance of frame RC buildings with masonry infill are currently of a high concern. This paper deals with selected results from analytical investigations and comparison of the seismic resistance of a five- and a seven- storey RC frame structure with and without a masonry infill. The results from the analyses show that the infill essentially affects the seismic resistance of RC buildings.

Keywords: masonry infill, seismic performance, resistance, linear and nonlinear analysis

1. INTRODUCTION

Design and construction of RC structures with masonry infill are common in European engineering practice especially in its seismic active southern part. The effects of infill on seismic performance of integral structure are very important, (figure 1). Field experience from recent earthquakes and analytical/experimental research show that the effects of masonry infill could be (Fardis. 2006):

- Positive-in case that the bare structural system has little seismic resistance
- Negative-if the contribution of masonry infill to lateral strength and/or stiffness is large relative to that of the frame itself. In such a case the infill may override the seismic design and render ineffective the efforts of the designer to control the inelastic re-



Figure 1. Damages on infill

sponse by spreading inelastic deformation demands throughout the structure.

The unfavorable effects can be representing throughout:

- Loss of the integrity of the infill in the ground storey that may produce “soft storey” and trigger global collapse, (figure 2)
- If infill are non-uniformly distributed in plan or in the elevation, inelastic deformation demands will concentrate in part of the building which have more sparse infill
- Local effects of infill may cause brittle failure of frame member, notably columns, (figure 3)

The masonry infill significantly increase structural strength and stiffness until seismic demands become greater than infill strength. After this moment deterioration of global strength and stiffness is registered. Experience from the recent experimental investigations show that



Figure 2. Negative effect of infill on seismic performance of structure – “soft” storey mechanism



Figure 3. Negative effect of infill on seismic performance of structure

infill can change damage distribution in structure, (Dolsek, Fajfar. 2006).

In the new buildings design according to Eurocode 8, (EN 1998: Eurocode 8.2004) the masonry infill are threat as a source of structural additional strength and so called “second line defense”. So the reduction of input seismic action as a result of favorable infill effects is not allowed. Considering this, design of RC buildings with masonry infill according to EC8 is on safety side but it is not rational because leads to significant increase of reinforcement in the structural element in comparison with the bare frame. Having in mind that the design EC8 method for RC frames with infill are too conservative it is necessary to quantify the effects of the infill on seismic performance of the structure properly, which means:

- The infill should be explicitly incorporate in the structural model for analysis and design
- Performance of the infill should be verified against seismic demands as a results of the nonlinear analysis and design of structures

The problem is even more complex in the case of seismic performance evaluation of the existing RC buildings with masonry infill. It was previously stated that the influence of the infill is most significant when the structural system itself doesn't posses adequate seismic resistance, which is often case in large number of substandard RC buildings constructed before implementation of seismic codes, as well as in the case on newly design building without respecting capacity design approach. In such buildings the explicitly consideration of infill in analytical model and their verification are necessary and beneficial not only for the designer but also for the investors and society as whole. Nevertheless Part 3 of Eurocode 8 which is use for seismic assessment and strengthening of the existing structures doesn't give any opportunity to the designer to incorporate the (positive) influence of the infill in the process of seismic assessment of existing structure.

2. SEISMIC PERFORMANCE OF RC BUILDINGS WITH MASONRY INFILL

Having in mind the necessity for quantitative definition of influence of infill on seismic performance of RC building structures, selected results obtain from analytical investigations of two buildings modeled without and with masonry infill (Apostolska, Necevska-Cvetanovska et al. 2010.) are presented within the frame of the paper.

2.1. Linear Elastic Analysis of Five Storey RC Frame Building

The analysis of the structural system was carried out under vertical loads and seismic action defined according to the Rulebook for construction of building structures in seismic areas, (PIOVS, 1981) for intensity of IX after MCS. A seismic effect on the structure was defined according to the lateral force method of analysis. Two different analysis have been performed i.e. structural system without, (figure 4) and with masonry infill.

Comparison between fundamental period of vibration of structure, relative story displacements, as well as stiffness, for both of the models, without and with infill is presented in table 1. Distribution of maximum absolute story displacements as well as force-displacement relationship for both of the models is given in the figures 5 and 6.

The effect of the infill is obvious and it is reflect through reduction of total displacements and increase of stiffness.

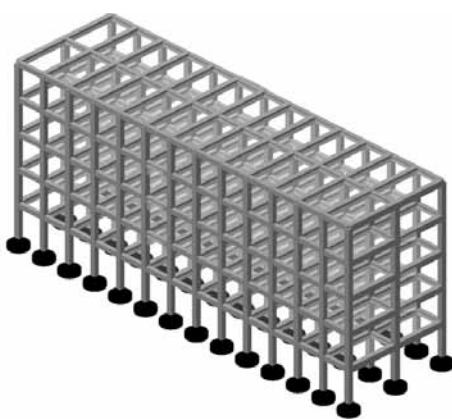


Figure 4. 3D model of five storey RC building without infill

2.2. Linear Elastic Analysis of Seven Storey RC Frame Building

The analysis of the seven storey RC building structure without and with masonry infill (figures 7 and 8) has been performed under vertical and seismic loads. The seismic loading are defined in three different ways: as equivalent static lateral forces for intensity IX after MCS, (PIOVS, 1981.); EC8 design spectra (EN1998-1:2004) and real earthquake registration - El Centro for two levels of acceleration - 0.25g and 0.35g. The analysis of the structural system was performed by finite element method using SAP2000v10.0.0 Advanced software (Wilson & Habibullah, 2006).

Table 1. Relative story displacements and stiffness

Story	Without infill, T1=0.52sec		With infill, T1=0.47sec		Difference, ΔT=9.5%	
	δrel. (cm)	K (kN/cm)	δrel. (cm)	K (kN/cm)	δrel (%)	K (%)
5	0.16	8984	0.14	10461	14.1	16.4
4	0.30	9700	0.25	11671	16.9	20.3
3	0.41	9815	0.33	12144	19.2	23.7
2	0.47	10198	0.34	14080	27.6	38.1
1	0.32	16276	0.24	21146	23.0	29.9

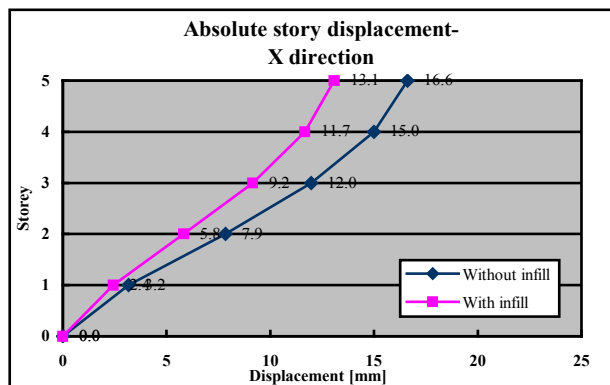


Figure 5. Absolute story displacement

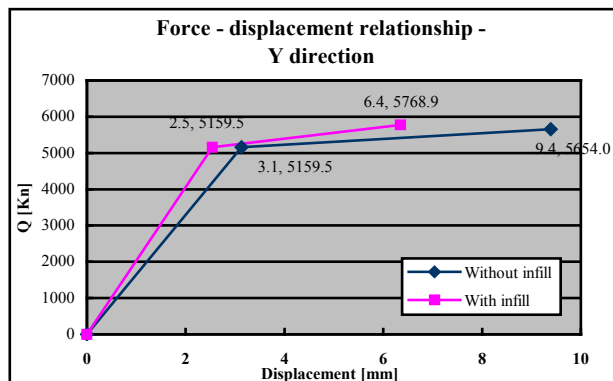


Figure 6. Force-displacement relationship

Relative storey displacements, transversal forces and elastic stiffness for structural model without and with masonry infill, calculated for equivalent static loads and EC8-design spectra are presented in table 3 and table 4.

Distribution of the absolute maximum storey displacements for both models (without and with infill) under equivalent seismic forces and EC8 design spectra with input acceleration of $a_{\max} = 0.25g$ are presented in figure 9.

In the table 5, calculated relative story displacements and elastic stiffness for structural model without and with masonry infill are presented.

2.3. Nonlinear “Push-over” Analysis of Seven Storey RC Frame Building

In order to make assessment of the seismic performance of the building structural system considering the influence of the masonry infill, nonlinear “push-over” analysis has been carried out. As a result of the analysis the most probably mechanism of damage distribution is elaborated also (figure 10).

Infill is modeled as equivalent diagonals. Nonlinearity is concentrated in those diagonals and with increase of the level of input horizontal displacements plastic hinges entry even in the collapse prevention zone (point “E” in figure 11).

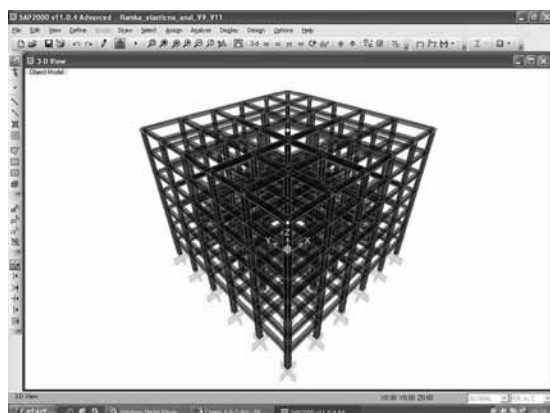


Figure 7. 3D mathematical model of seven storeys RC building without infill

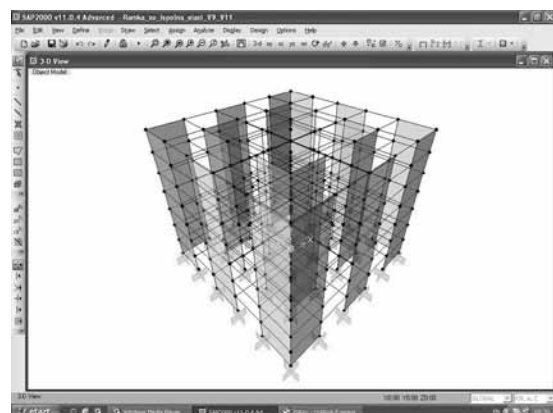


Figure 8. 3D mathematical model of seven storeys RC building with infill

Table 2. Fundamental period of vibration of structure

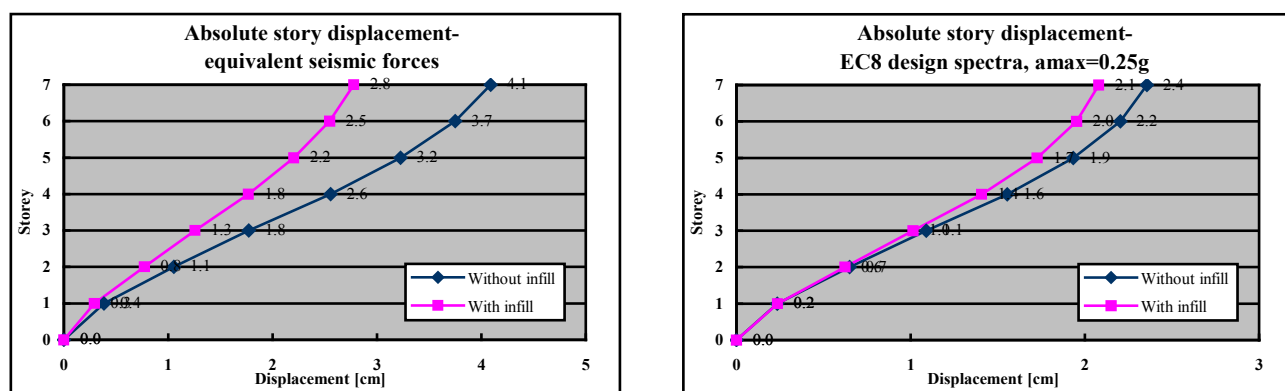
Fundamental period of vibration of structure									
Without infill			With infill			Difference [%]			
T ₁	T ₂	T rot	T ₁	T ₂	T rot	T ₁	T ₂	T rot	
0.964	0.964	0.869	0.849	0.849	0.708	11.9	11.9	18.4	

Table 3. Relative displacement, transversal forces and stiffness

Story	Equivalent static loads							Ux	Kx		
	Without infill			With infill			Diference				
	Ux	Qx	Kx	Ux	Qx	Kx	[%]				
	cm	kN	kN/cm	cm	kN	kN/cm					
VII	0.342	1539.	4500.	0.232	1536.6	6623.	32.16		47.18		
VI	0.522	2339.	4481.	0.343	2334.9	6807.	34.29		48.91		
V	0.670	3006.	4487.	0.436	3000.9	6883.	34.93		49.40		
IV	0.783	3539.	4848.	0.509	3532.8	6941.	34.99		43.17		
III	0.720	3939.	5471.	0.488	3935.6	8066.	32.22		47.43		
II	0.678	4206.	6204.	0.479	4201.9	8722.	29.35		40.59		
I	0.383	4340.	11332.	0.291	4334.1	14893.	24.02		31.42		

Table 4. Relative displacement, transversal forces and stiffness

Story	EC8 – design spectra, 0.25g							
	Without infill			With infill			Diference	
	Ux	Qx	Kx	Ux	Qx	Kx	Ux	Kx
	cm	kN	kN/cm	cm	kN	kN/cm	[%]	
VII	0.153	611.3	3995.	0.128	750.	5859.	16.34	46.66
VI	0.269	1194.3	4440.	0.226	1518.4	6719.	15.99	48.33
V	0.380	1706.1	4490.	0.318	2198.1	6912.	16.32	49.94
IV	0.465	2117.5	4554.	0.395	2752.4	6968.	15.05	49.01
III	0.439	2412.7	5497.	0.390	3162.5	8109.	11.16	47.52
II	0.416	2593.2	6234.	0.387	3418.2	8833.	6.97	41.69
I	0.234	2658.3	11360.	0.236	3513.8	14889.	0.85	31.07

**Figure 9.** Distribution of the displacements at the storey levels

The beams are in the initial range of nonlinearity, mainly in transition from elastic to post-elastic state (point "B" in fig. 11) and in immediate occupancy range (point "IO" in fig. 11).

Distribution of the plastic hinges in two characteristics frames of analyzed RC building structure at selected steps of "push-over" analysis are presented in figures 11.

3. CONCLUSION

In order to define seismic performance of RC building structures with masonry infill and to

evaluate the influence of the infill on structural behaviour ample analytical investigation of two structures with different stories and without/with infill have been realized.

Generally can be concluded that the effect of the infill on the seismic performance of the structure is significant. The presence of infill increases initial structural stiffness and strength and decrease fundamental period of vibration as well as absolute and relative storey displacements. As a result large elastic stiffness

Table 5. Relative story displacements and stiffness

Story	Without infill		With infill		Difference	
	$\delta_{rel.}$ (cm)	K (kN/cm)	$\delta_{rel.}$ (cm)	K (kN/cm)	$\delta_{rel.}$ (%)	K (%)
7	0.34	4500.	0.23	6623.	32.2	47.2
6	0.52	4481.	0.34	6807.	34.3	48.5
5	0.67	4487.	0.44	6883.	34.9	49.1
4	0.78	4848.	0.51	6941.	35.0	43.2
3	0.72	5471.	0.49	8066.	32.2	47.4
2	0.68	6204.	0.48	8722.	29.4	40.6
1	0.38	11332.	0.29	14893.	24.0	31.4

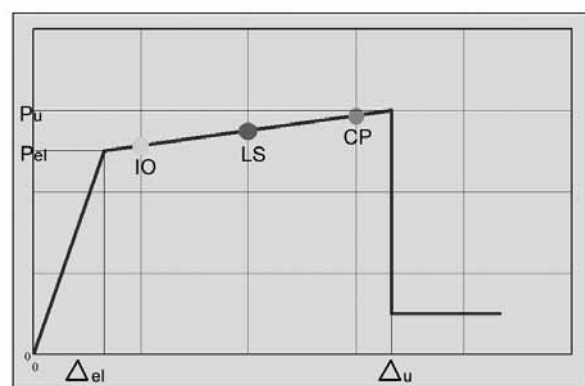
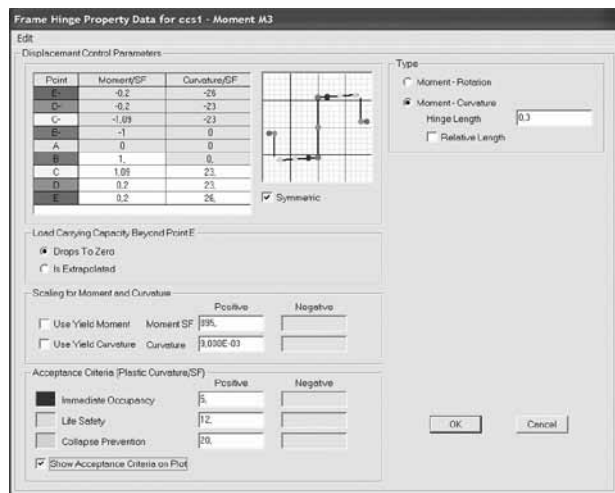


Figure 10. Moment-curvature relationship with characteristic points

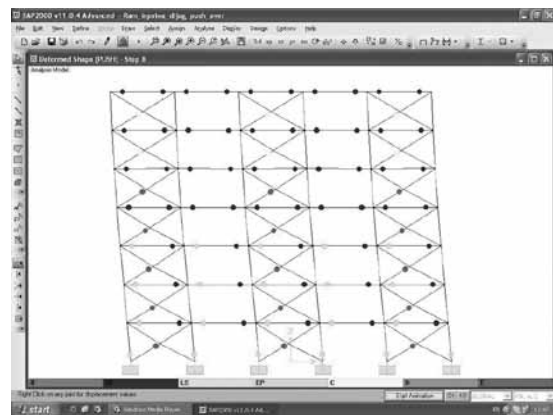
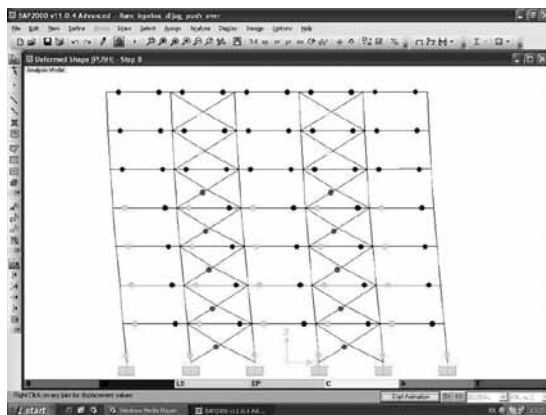


Figure 11. Distribution of plastic hinges in the characteristics frames

and small deformability, immediately after appearance of first cracks nonlinearity increase rapidly up to failure of infill. One can conclude that in the elastic range and in the beginning of nonlinear range masonry infill increase seismic resistance of RC building structural systems and has significant influence on the nonlinear dynamics response of structural systems.

Having in mind fact that in common engineering practice the influence of infill is not considered, further research for definition of appropriate mathematical models for nonlinear behaviour of infill is necessary. The main goal of such research investigations should be as much as possible realistic definition of seismic performance of RC building structures with masonry infill. In line with this as one of the several

identified research needs to achieve improved design guidelines for seismic protection in the EU is seismic assessment and retrofitting with emphasis to masonry-infilled frame buildings, (Pinto et al., 2007).

REFERENCES

- Jankovska, B. (2009). Seismic performance of RC frame buildings with masonry infill. *Master thesis*
- Apostolska R., Necevska-Cvetanovska G., Cvetanovska J., Jankovska B. (2010). Analytical investigations of seismic behaviour of RC building structures with masonry infill, *Proc.of the GNP, February, Zabljak, Montenegro, 2010.*
- Dolsek M., Fajfar P. (2006). Simplified Seismic Assesment of Infilled Reinforced Concrete Frames, *Proc. of the 13ECEE, Geneva.*
- EN 1998: (2004). Eurocode 8: Design of structures for earthquake resistance. Part 1: General rules, seismic actions and rules for buildings, 2004.
- Fardis M. (2006). Seismic Design Issues for Masonry – infilled RC Frames, *Proc. of the 13ECEE, Geneva.*
- Pinto A., Taucer F., Dimova S. (2007). Pre-normative research needs to achieve improved design guidelines for seismic protection in the EU - *EUR 22858 EN.*



ALL FOR PAPERS

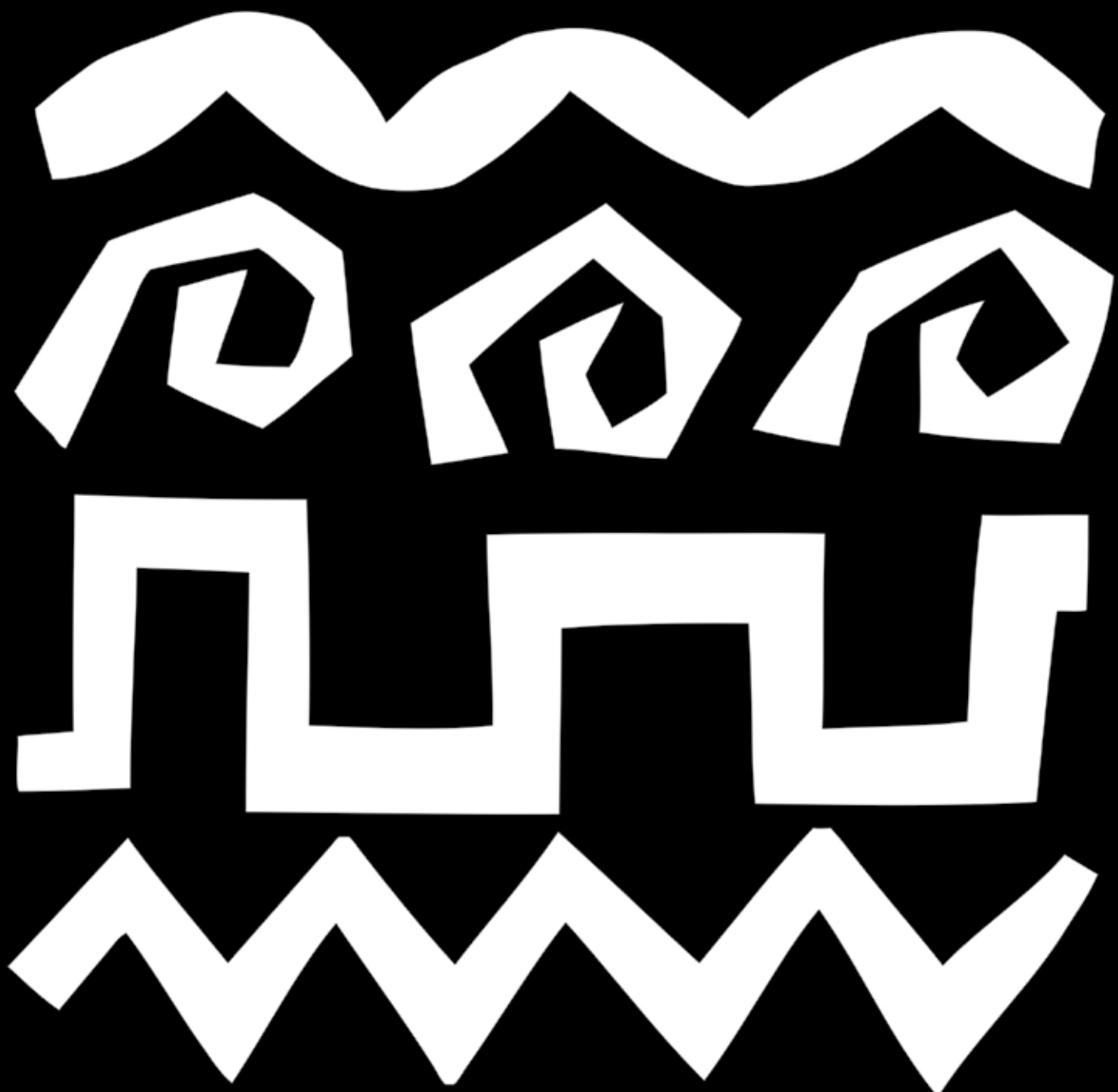
We invite you to submit high quality papers for review and possible publication in area of structural engineering. The manuscript should not exceed 15 pages in double spaced format and must be submitted in Microsoft word and pdf file format, in English. All authors must agree on the content of the manuscript and its submission for publication in this journal before it is submitted to us. Manuscripts should be submitted via email to

golubka@pluto.iziis.ukim.edu.mk

Paper Submission Deadline for the next issue is: July15, 2011



infraSTRUCTURE



ДГКМ

ДРУШТВО НА
ГРАДЕЖНИ
КОНСТРУКТОРИ НА
МАКЕДОНИЈА

MASE

MACEDONIAN
ASSOCIATION OF
STRUCTURAL
ENGINEERS

14

МЕЃУНАРОДЕН СИМПОЗИУМ
INTERNATIONAL SYMPOSIUM

СТРУГА, МАКЕДОНИЈА
STRUGA, MACEDONIA
28. 09 - 01.10, 2011

STRUCTURAL ENGINEER

ГРАДЕЖЕН КОНСТРУКТОР

FOREWORD BY THE EDITOR

- 567 **IN-PLANE SHEAR BEHAVIOUR OF UNREINFORCED MASONRY WALLS**
Sergej CURILOV, Elena DUMOVA-JOVANOSKA
- 576 **CONTRIBUTION OF SEISMIC STRENGTHENING OF MONUMENTS TO THEIR BLAST RESISTANCE**
Goran JEKIC, Veronika SENDOVA, Ljubomir TASKOV
- 584 **PERFECTLY MATCHED LAYERS - AN ABSORBING BOUNDARY CONDITION FOR ELASTIC WAVE PROPAGATION**
Josif JOSIFOVSKI, Vasil VITANOV, Oto von ESTORFF
- 592 **SEISMIC STABILITY OF THE OLD BRIDGE IN MOSTAR**
Mladen KUSTURA, Lidija KRSTEVSKA, Mladen GLIBIC, Ljubomir TASKOV
- 599 **STIFFNESS CHARACTERISTICS MODELLING OF RC FRAME STRUCTURES ACCORDING TO EUROCODE 8**
Ljupco LAZAROV, Koce TODOROV
- 608 **HAVE WE FORGOTTEN SKOPJE 1963 EARTHQUAKE?**
Goran MARKOVSKI
- 615 **EARTHQUAKE-INDUCED LANDSLIDES - GIS METHODOLOGY FOR ZONATION**
Julijana CVETANOVSKA, Vlatko SESOV
- 624 **ANALYTICAL INVESTIGATIONS OF SEISMIC BEHAVIOUR OF RC FRAME BUILDINGS WITH MASONRY INFILL**
Roberta APOSTOLSKA, Golubka NECEVSKA CVETANOVSKA, Julijana CVETANOVSKA